

THE STABILITY OF AMORPHOUS SOLIDS:  
THE ROLE OF FAST SURFACE CRYSTALLIZATION

By

Mariko Hasebe

A dissertation submitted in partial fulfillment of  
the requirements for the degree of

Doctor of Philosophy  
(Pharmaceutical Science)

at the

UNIVERSITY OF WISCONSIN-MADISON

2015

Date of final oral examination: 6/30/2015

This dissertation is approved by the following members of the Final Oral Committee:

Lian Yu, Professor, School of Pharmacy and Department of Chemistry

Mark D. Ediger, Professor, Department of Chemistry

Glen Kwon, Professor, School of Pharmacy

Sandro Mecozzi, Associate Professor, School of Pharmacy and Department of Chemistry

Melgardt M. de Villiers, Professor, School of Pharmacy

## **Acknowledgements**

Foremost, I would like to thank my advisors, Professor Lian Yu for supporting me during these past six years. You have become more than a mentor. You have taught me not only a body of knowledge and skills, but also has helped me understand how my ambitions fit into graduate education and my long-term career choices. I am very grateful that I received such a wonderful training to be a scientist under you, who never give up on students and coach their maturation until they can perform independently as scientist. It has been wonderful experiences to work under you.

I want to thank to present and past members of the Yu group. All of you have been very supportive, and I feel we became a work family after spending a lot of time in the lab and outside of the lab. Ye and Lei, thank you for sharing your knowledge with me. I remember that I was quite impressive by the scientific discussions at the group meeting between you. I was hoping to be like you when I became a senior student. Thanks to Ting for encouraging me not to give up on the projects, and proving a good environment in the lab. Erica, thank you for guiding me the projects. Special thanks to Dani for helping to finish up projects. I am also grateful for our friendship after all. Thanks to Caleb for being a good friend even after you left the lab to check on me. Siwei, thanks for being a great classmate and friend. Watching you being positive always lifted me up when I struggled. Travis, you have encouraged me to do better science. Your questions and suggestions for my projects were always helpful. Wei and Men, I always enjoyed talking with you about a various topics. To M, Shigang, Yinshen, and Chengbin, thank you for being a great coworker.

A good support system is significant to surviving and keeping me calm in graduate school. Noriko and Khadija, you have been amazing friends. We shared so many happy and sad moments together. I never forget that you have been there for me when I felt down. Thanks to Heidi, Ty,

Kenton, Sue and Richard for being a good friend over 10 years. I admire you always have positive energy. Matt, you are the best gym trainer. You taught me that fitness is a way of living. No matter how much life knocks me down, your place always helps me keep going. You have trained me to be a strong woman. Abhiram, it was always fun to work out with you. Thank you for your help to practice with me over and over for my job interviews. Rika and Ranga, you always remind me what is most important in my life. I always value your opinions. Yuchuan, I do not know how many times you gave me positive insights not to give up on trying for job search.

I especially thank my mom. I would not have made it this far without your support. When you became sick, you showed me how to fight for hope. You are the strongest woman I have known. When I was young, you used to say “Fall down seven times, stand up eight”. You have shown me what it really means. You have taught me the ways of life, given me the strength to face my challenges. Thank you for your unconditional supports all the time.

Finally, the best outcome from these past six years is finding my best friend Aditya. It has not been an easy ride for me last and this year, but I truly thank you for sticking by my side all the time, even when I felt depressed. I feel all of the hardships made us stronger together. I am excited to grow older with you because the best is yet to be.

## Table of Contents

<b>Abstract</b> .....	vi
-----------------------	----

### Chapter 1: Introduction

1.1 Overview of this thesis.....	1
1.2 Amorphous pharmaceutical solids: definition and importance.....	2
1.3 Surface mobility and surface-enhanced physical and chemical transformations.....	3
1.4 Inhibition of surface crystallization.....	11
1.5 Contributions of this thesis.....	13
References.....	18

### Chapter 2: Fast Surface Crystal Growth on Molecular Glasses and Its Termination by the Onset of

<b>Fluidity</b> .....	21
2.1 Abstract.....	22
2.2 Introduction.....	22
2.3 Materials and methods.....	25
2.4 Results.....	26
2.4.1 Indomethacin (IMC).....	26
2.4.2 Nifedipine (NIF).....	32
2.4.3 <i>o</i> -Terphenyl (OTP).....	33
2.5 Discussion.....	39
2.5.1 Mechanism of surface crystal growth on organic glasses.....	39
2.5.2 Disruption of surface crystal growth on organic glasses by the onset of fluidity.....	42
2.5.3 Comparison of the effects of fluidity on surface and bulk crystal growth in organic glasses	47
2.6 Conclusions.....	48
References.....	50

<b>Chapter 3: Fast Surface Crystallization of Molecular Glasses: Creation of Depletion Zones by Surface Diffusion and Crystallization Flux</b> .....	54
<b>3.1 Abstract</b> .....	55
<b>3.2 Introduction</b> .....	55
<b>3.3 Materials and methods</b> .....	57
<b>3.4 Results</b> .....	59
<b>3.4.1 <math>\alpha</math> IMC</b> .....	59
<b>3.4.2 <math>\gamma</math> IMC</b> .....	64
<b>3.5 Discussion</b> .....	67
<b>3.5.1 Depletion zones along slow-advancing flanks of <math>\alpha</math> IMC needles</b> .....	67
<b>3.5.2 Depletion zones near <math>\gamma</math> IMC surface crystals</b> .....	71
<b>3.5.3 Depletion zones around the fast-growing tips of <math>\gamma</math> IMC needles</b> .....	74
<b>3.6 Conclusions</b> .....	76
References.....	79
<b>Chapter 4: Fast Surface Growth on Molecular Glasses: The Effect of Spatial Confinement</b> .....	82
<b>4.1 Abstract</b> .....	83
<b>4.2 Introduction</b> .....	83
<b>4.3 Materials and methods</b> .....	86
<b>4.4 Results</b> .....	87
<b>4.4.1 Effect of glass width on surface crystal growth</b> .....	87
<b>4.4.2 Effects of glass thickness and substrate materials on surface crystal growth</b> .....	89
<b>4.5 Discussion</b> .....	94
<b>4.5.1. Critical width and depth for disrupting surface crystal growth on molecular glasses</b> .....	96
<b>4.5.2. Slowdown of surface crystal growth over time</b> .....	98
<b>4.6 Conclusions</b> .....	100
References.....	101

<b>Chapter 5: Future Work</b> .....	104
<b>5.1</b> The effect of heating above $T_g$ on growth of surface crystal.....	104
<b>5.2</b> Creation of depletion zones.....	107
<b>5.3</b> Confinement effect on surface crystal growth.....	110
<b>5.3.1</b> Critical width on inhibition of surface crystallization in molecular glasses.....	110
<b>5.3.2</b> The effect of glass thickness on surface crystal growth.....	114
<b>5.4</b> Conclusion.....	116
References.....	117

## Abstract

The amorphous solids can be used in a number of applications such as food, bio-preservation, organic electronics, and drugs. In pharmaceutical systems, amorphous drugs have greater solubility and bioavailability than their crystalline counterparts, giving them an important function in drug delivery formulation.

Recent studies have compared surface-enhanced crystallization to bulk crystal growth. The surface crystal growth rate can be orders of magnitude faster than growth rate in the bulk. It has been shown that surface-enhanced crystallization is a common phenomenon on molecular glasses. Thus, it is significant to understand the mechanism of fast surface crystallization on molecular glasses.

We report that the onset of fluidity generally disrupts fast surface crystal growth in indomethacin ( $\alpha$  IMC), nifedipine (NIF), and *o*-terphenyl (OTP). The severity of this inhibition depends on crystal morphology. Segregated needles are more susceptible to the liquid flow than crystals that grow in compact domains. With scanning electron microscopy (SEM) and atomic force microscopy (AFM), we characterize the surface evolution of depletion zones around growing a crystal. We find that the observed depletion zones are well reproduced by the known coefficients of surface diffusion and crystal growth rate. Finally, the effect of special confinement on surface crystal growth was performed. Surface crystal growth was disrupted if the width is reduced to below several micrometers or if the glass film is thinner than the depth of depletion zones. Similarly, surface crystallization kinetics is affected by glass thickness or substrate. Surface crystal growth is initially fast, but slows over time if the glass film is thinner than approximately 10  $\mu\text{m}$ . All these effects reflect the environmental perturbation of surface crystal growth. The slowdown

of surface crystal growth in microns-thick films may be caused by the propagation of cracks created by a fracture in the bulk.

These results are relevant to understand the stability of amorphous solids against surface crystallization in formulations and product development.

# Chapter 1

## Introduction

When I think of “glasses”, the first thing that comes to mind is window glass. However, glasses or amorphous solids have many more applications. Amorphous materials can be used in food, bio-preservations, organic electronics, and drugs. In pharmaceutical systems, amorphous drugs have greater solubility and bioavailability than their crystalline counterparts, giving them an important function in drug delivery formulation.

A major issue in the development of amorphous materials is their stability against crystallization because crystallization negates their advantages. Recent work has shown that molecular glasses can have high surface mobility and this mobility is responsible for fast surface transformations. For example, the velocity of crystal growth can be much faster on the free surface than in the bulk. This thesis addresses the mechanisms behind fast surface crystallization on molecular glasses.

### 1.1 Overview of this thesis

This introductory chapter (Chapter 1) will review the definition of glasses or amorphous solids and their impact, chemical and physical reaction at surfaces, surface diffusivity, and inhibition of reactions at surfaces. Chapter 2 details the study of the termination of surface crystal growth on molecular glasses by the onset of fluidity. In Chapter 3, the evolution of the glass surface around surface crystals is examined. Chapter 4 presents observations of the spatial confinement effect on surface crystal growth on molecular glasses. Critical dimensions on inhibition of surface crystal growth will be presented. In Chapter 5, future studies will be proposed to achieve greater

understanding of the mechanism of surface crystallization on molecular glasses.

## **1.2 Amorphous pharmaceutical solids: definition and importance**

Solids can be categorized into two groups: amorphous solids and crystalline solids. Crystalline solids show a long-range order of molecular packing, while amorphous solids lack this trait. Amorphous solids have many applications. Organic glasses are used in electronics such as organic light-emitting diodes (OLEDs).<sup>1</sup> Amorphous solids can be used in food and polymers. In pharmaceutical science, amorphous drugs can be useful for drug delivery because they usually have higher solubility, dissolution rate and bioavailability.<sup>2</sup> Dissolution in the gastrointestinal tract is often the rate-limiting step to absorption for many drugs. Thus, improvement in the dissolution rate may enhance the bioavailability of that drug. However, amorphous drugs can be thermodynamically unstable and have a high tendency to crystallize. Crystallization negates the advantages of amorphous drugs for drug delivery. Thus, it is critical to understand the stabilization of amorphous drugs to avoid crystallization during drug development and formulation.

There are a number of ways to prepare amorphous solids. Cooling liquids is one of the most common methods. Crystallization can be avoided by cooling a liquid below the melting point  $T_m$  quickly enough that it becomes super-cooled liquid.<sup>3</sup> With cooling molecules of a super-cooled liquid move more and more slowly. The temperature at which an amorphous solid forms is called the glass transition temperature  $T_g$ . At the glass transition temperature, the molecular rotation time is on the order of one hundred seconds, viscosity is approximately  $10^{12}$  pa s,<sup>4</sup> and the diffusion coefficient is approximately  $10^{-16}$  cm<sup>2</sup>/s.<sup>5,6</sup>

Other methods to create amorphous solids include the mechanical activation (milling, grinding)

of crystals, rapid precipitation from solution, and continuous concentration processes such as lyophilization (freeze drying).<sup>2,7</sup> Dehydration of crystalline hydrates is another method to make an amorphous solid<sup>8</sup>. Yet another technique, vapor deposition, can provide amorphous solids<sup>9</sup>.

### **1.3 Surface mobility and surface-enhanced physical and chemical transformations**

In this section, I review the relevant information on surface diffusion on molecular glasses and three processes that are enhanced by surface mobility: crystallization, formation of stable glasses by vapor deposition, and protein degradation.

#### **1.3.1 Surface diffusion**

The surface mobility of amorphous solids can affect their physical and chemical stability. Surface mobility plays a significant role in crystal growth, catalysis, lubrication, and stability of coatings. Surface diffusion is a major property for evaluating surface mobility.<sup>10,11</sup> Many studies have measured surface self-diffusion of metals, inorganic and semiconductors. However, little data exist on the surface diffusion of organic materials. Understanding surface diffusion in molecular glasses is critical for developing soft materials and electronic applications including fast surface crystallization.

At present the surface diffusion coefficient  $D_s$  on molecular glasses have been for 3 molecular glasses: indomethacin (IMC), nifedipine (NIF), and *o*-terphenyl (OTP). Figure 1 summarizes the data on these systems. Zhu et al. made the first measurement for IMC and showed that surface diffusion is one million times faster than bulk diffusion.<sup>12</sup> Subsequent studies measured the surface diffusion coefficients of NIF and OTP glasses.<sup>13,14</sup>

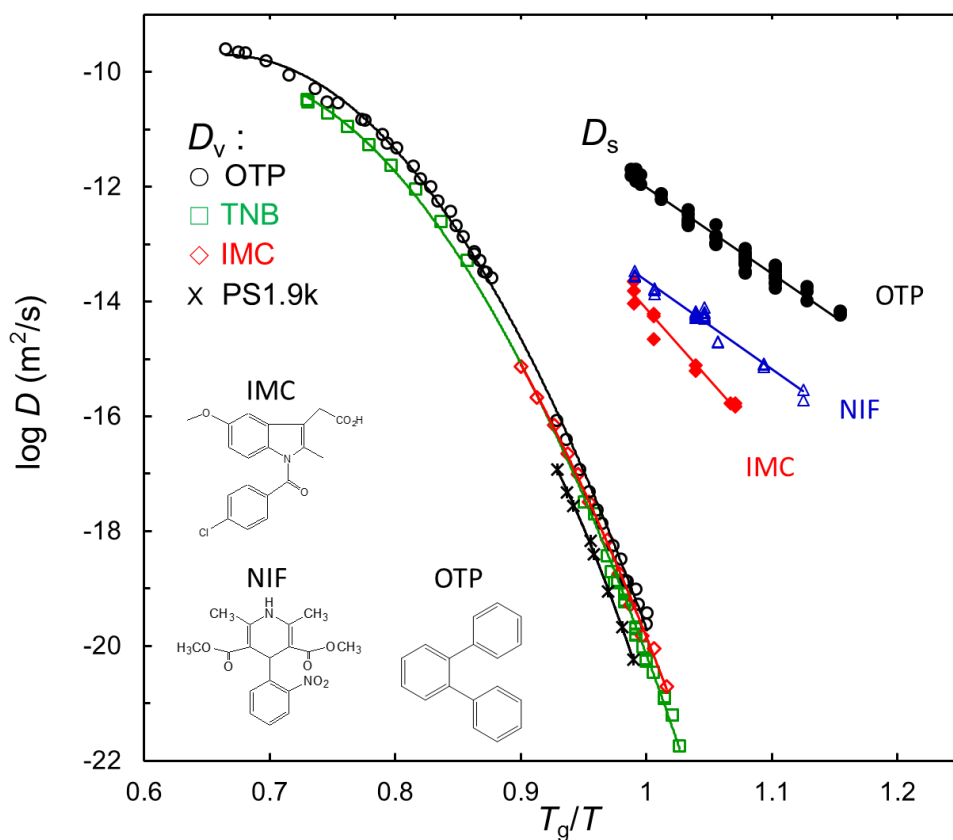


**Figure 1.** Surface and bulk diffusion coefficients,  $D_s$  and  $D_v$ , of amorphous OTP, NIF and IMC as a function of  $T_g$  scaled temperature<sup>14</sup> ( $T_g = 246$  K for OTP, 315 K for IMC and NIF, and 347 K for TNB). All bulk diffusion coefficients were measured by Ediger and coworkers (see Ref. 13 for references). The inset shows the structure of IMC, NIF and OTP.

Surface diffusion in the three systems is much faster than bulk diffusion, with  $D_s/D_v = 10^6$ - $10^8$  at  $T_g$ .

Zhang et al. report that the order of surface diffusivity is OTP (fastest), followed by NIF and then IMC (slowest).<sup>14</sup> This order correlates with the relative strengths of intermolecular forces in the three systems. Zhang et al. also report a correlation between surface diffusion and surface crystal growth the three systems (see later).

### 1.3.2 Surface-enhanced crystal nucleation

The process of crystallization consists of nucleation and growth. In this section, examples of surface-enhanced crystal nucleation will be introduced. Surface-enhanced crystal nucleation was observed in sodium metaphosphate ( $\alpha$  -  $\text{NaPO}_3$ ). In the vicinity of  $T_g$ , crystallization is faster at the surface than in the bulk.<sup>15,16</sup> The morphology is needle-like (Figure 2a).  $\text{Co}_{72}\text{Si}_{12}\text{B}_{26}$  glass also shows surface induced nucleation in Figure 2b.<sup>17</sup> The cross-sectional view of the micrograph shows that crystals grow from the surface into the bulk. Nucleation in the bulk is not observed. This implies that crystal nucleation at surfaces should be faster than in the bulk.

### 1.3.3 Fast surface crystal growth on molecular glasses

In glassy materials such as silicates and metallic alloys, crystal growth has similar velocities on the surface and in the bulk.<sup>18,19,20,21,22</sup> However, it was found that surface crystal growth can be much faster than bulk crystal growth for molecular glasses.<sup>23,24,25,26,27,28</sup>

Recent studies have established several features of surface crystallization on molecular glasses. Sun et al. reported that surface crystals rise upward by as much as hundreds of nanometers as they grow laterally. Wu et al. demonstrated that the surface crystal growth can be

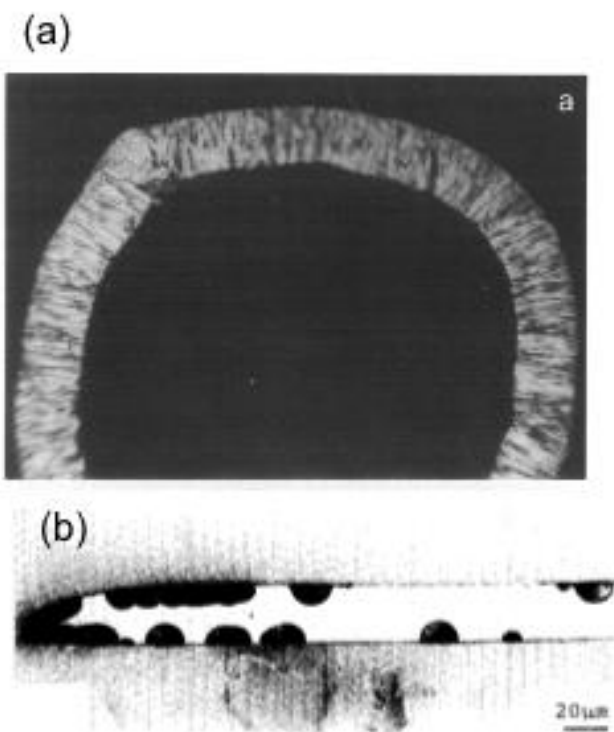


**Figure 2.** (a) The cross sectional view of devitrified  $\text{NaPO}_3$  glass.<sup>15</sup> Crystalline layer at the surface indicates fast surface nucleation. (b) The cross-sectional view of crystallized  $\text{Co}_{72}\text{Si}_{12}\text{B}_{26}$  glass. All crystals grow from the free surface, which indicates surface induced nucleation<sup>17</sup>.

inhibited by an ultra-thin coating of gold (10 nm) or polymer (3-20 nm).<sup>29</sup> It was also found that fast surface crystal growth correlates with fast surface diffusion:  $u_s = D_s / (3 \mu\text{m})$  (Figure 3).<sup>14</sup>

This relation is observed for OTP, IMC, NIF and amorphous silicon, and demonstrates that surface diffusion and surface crystal growth have similar kinetic barriers. Together, these observations argue that fast surface crystal growth on molecular glasses is supported by fast surface diffusion.

Amorphous silicon is a good model system to understand the relationship between surface diffusion and hemispherical grain growth.<sup>30,31,32</sup> Sakai et al. studied this process in ultra-high vacuum. They observed that hemispherical grains grow on the surface of amorphous silicon and the process creates depletion zones on the amorphous surface.<sup>30</sup> Subsequently, Sallese et al. developed an analytical model to describe the evolution of depletion zones using surface diffusion and crystallization flux.<sup>31</sup>

#### **1.3.4 Stability of vapor deposited glasses related to surface mobility**

Glasses can be prepared by condensing vapors on a substrate. Although glasses prepared by vapor deposition can be less stable than glasses formed by cooling liquids, Swallen et al. recently demonstrated that organic glasses prepared by physical vapor deposition can in fact be extremely stable compared to organic glasses formed by cooling liquids<sup>9</sup>. They reported that the glasses of *tris*-naphthylbenzene (TNB) and IMC prepared by vapor deposition showed higher thermodynamic stability, lower enthalpy, and higher density than ordinary glasses. Many pharmaceutical materials such as IMC, NIF, felodipine, and phenobarbital form stable glasses by vapor deposition (Figure 4).<sup>33</sup>

The stability of vapor deposited glasses is attributed to enhanced mobility at the surface of

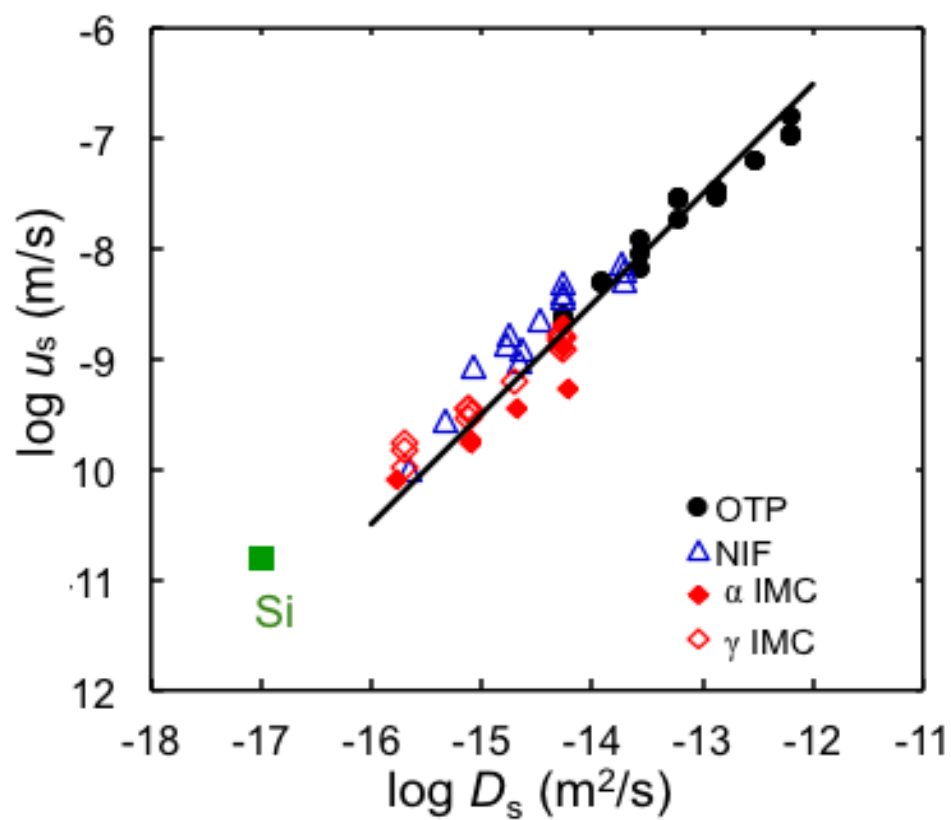


**Figure 3.** Correlation between the surface crystal growth rate  $u_s$  and surface diffusion  $D_s$ .<sup>14</sup>

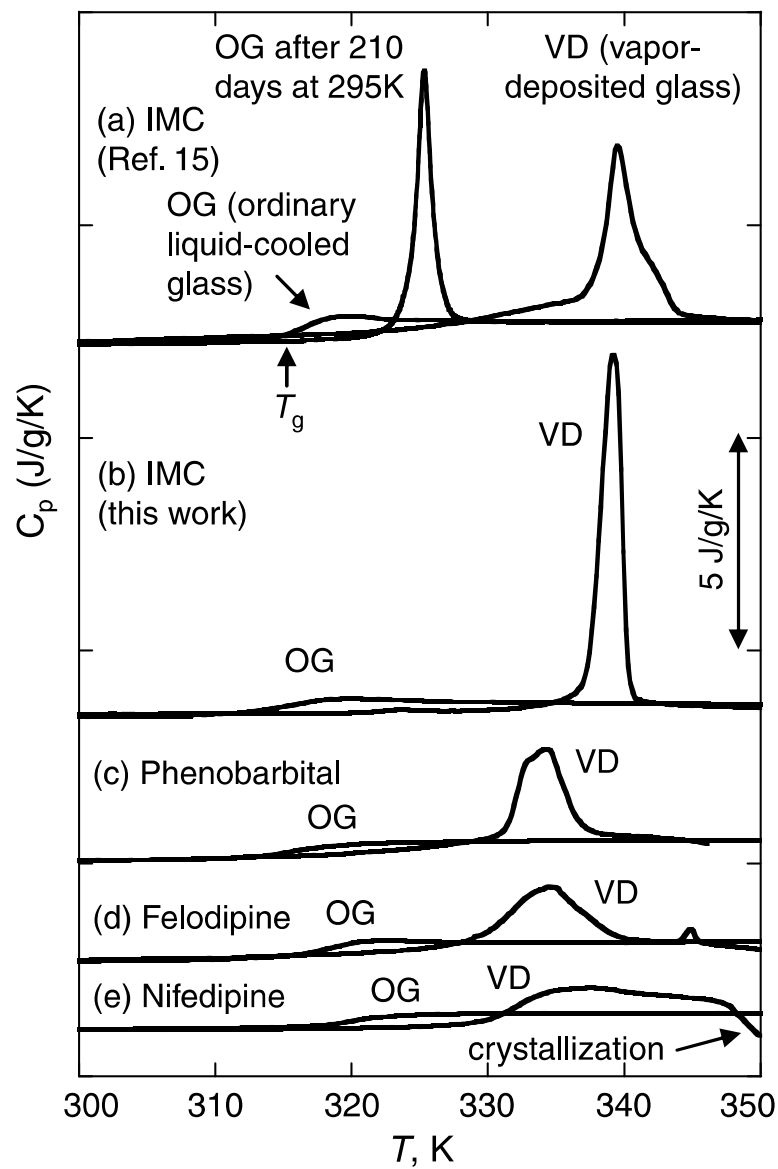


**Figure 4.** Heat capacities of vapor-deposited (VD) and liquid-cooled (OG) glasses of various materials.<sup>33</sup>

the glass.<sup>12,13,14</sup> Surface mobility is so fast that molecules at the surfaces can rearrange to find a stable packing configuration before the next molecules arrive from the vapor phase, allowing molecules at the surfaces to equilibrate leads to stable glasses. The formation of ultra-stable glasses by vapor deposition may be a useful technique to produce amorphous drugs that resist crystallization and have improved solubility and bioavailability.

### **1.3.5 Protein degradation at surfaces**

Protein therapeutics are receiving increasing attention by the pharmaceutical industry. Since there are many concerns over the liquid-state stability of proteins in long-term storage, the solid-state dosage is preferred. However, even in the solid state and during the preparation of solid dosage forms, chemical degradations can occur; for example, oxidation, deamination, and aggregation. Protein formulations prepared by spray drying or freeze-drying tend to have very high Specific Surface Area (SSA), potentially leading to surface-induced degradation.<sup>34,35</sup> Abudal-Fattah et al. evaluated dried protein products of IgG (1) prepared by lyophilization, foam drying, and spray drying.<sup>36</sup> They concluded that the total protein accumulation at the surface plays an important role in accelerating the process of degradation. The surface coverage of the protein was decreased by adding surfactant, which increases the stability of protein kinetics. Costantino et al. reported a linear relationship between spray-dried powder surface area and monomer loss (an indicator of degradation) for Bovine Serum Albumin (BSA).<sup>37</sup>

Pikal and co-workers reported that recombinant human growth hormone (rhGH) molecules have significantly faster degradation rates at the surface than in the bulk during the process of lyophilization.<sup>38</sup> They demonstrated that the amount of protein found at the solid-interface controls the rate of protein degradation during storage of lyophilized formulations. They formulated different glass-forming stabilizer to examine how SSA of the glass and concentration

of the protein in the surface layer were affected. The first order degradation rate constant including oxidation, deamination, and aggregation was measured.

Their observations suggest that the reason for the majority of degradation found on the solid surface is that residual stress may be easily generated at the surface by the process of drying, which results in the loss of native protein secondary structure. Furthermore, they speculate that mobility of protein molecules at the surface may be much faster than that of in the bulk, leading to faster degradation. This is analogous to surface-enhanced crystallization observed in organic glasses.

#### **1.4 Inhibition of surface crystallization**

Amorphous drugs can be very useful for drug delivery because of enhanced solubility, dissolution rate and bioavailability. However, they can be chemically and physically unstable. Thus, it is necessary to stabilize them against physicochemical changes. The conventional thinking for stabilizing amorphous drugs focuses on the processes in the bulk. Recent observations of fast surface crystallization demonstrate the importance of inhibiting surface processes for stability. In this section, we will discuss attempts to prevent the surface crystallization of amorphous drugs.

Wu and Yu reported that layers of polymer and gold nanocoating a few nm thick on the surface of amorphous indomethacin inhibited the overall surface crystallization (Figure 5).<sup>29</sup> Surface crystal growth was inhibited by 10 nm gold coating deposited by sputtering. A 3-20 nm polymer coating is applied to the IMC surface crystal using layer-by-layer (LbL) deposition. This technique could be useful for controlled drug delivery.<sup>39,40,41</sup> Surface crystallization kinetics is reduced by thin surface coatings, which supports the view that fast surface crystal

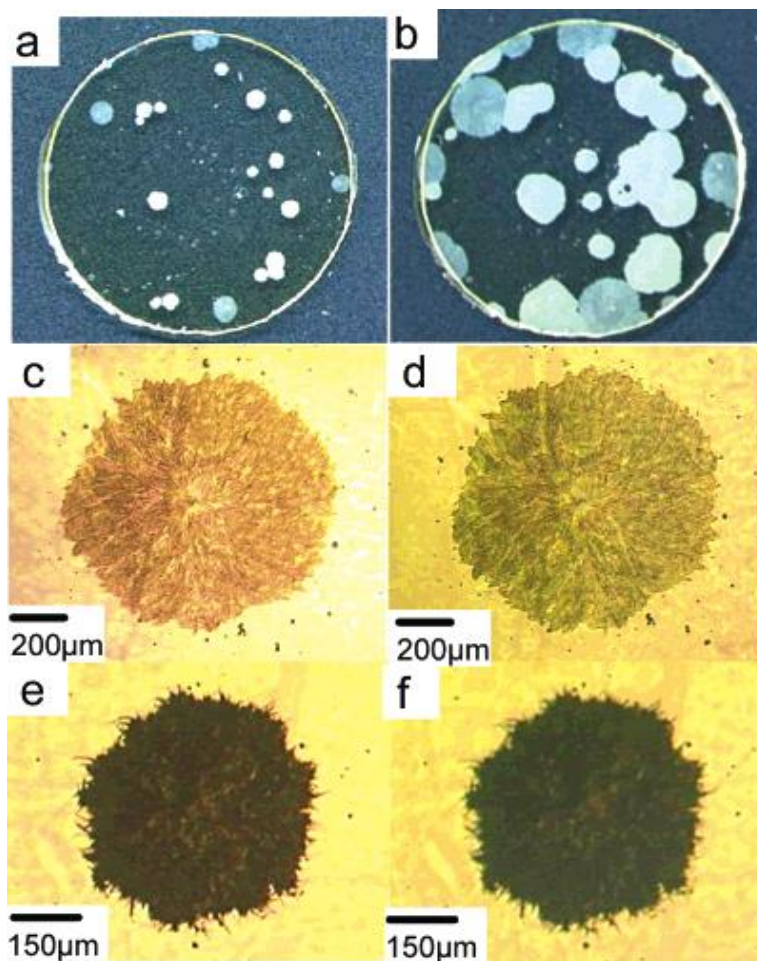


**Figure 5.** Nano-coating can inhibit surface crystallization on IMC glass at 313 K.<sup>29</sup>

- (a) Uncoated amorphous IMC after 90 hours at 313 K;
- (b) Same as (a) after 7 days;
- (c) Surface crystals of  $\gamma$  IMC as in (a) coated with gold;
- (d) Same as (c) after 7 days at 313 K;
- (e) Surface crystals of  $\alpha$  IMC as in (a) coated with gold;
- (f) Same as (c) after 7 days at 313 K.

growth is enabled by surface mobility. It would be more attractive to make use of bio-comparable or eco-friendly materials for coating such as chitosan, gelatin, and alginate on microcrystalline cellulose are biocompatible and degradable.<sup>42</sup>

Polymer additives are often used to stabilize amorphous drugs. The effect of polymer additives on the crystallization of amorphous drugs has been studied.<sup>28, 43, 44, 45</sup> Cai et al. report that 1% poly (vinylpyrrolidone) (PVP) additives on NIF can strongly inhibit bulk crystal growth<sup>43</sup> (Figure 6). In contrast, the effect of polymer additives on surface crystal growth is weaker.

Similarly, Kestur and Taylor observed that 3 % PVP slows bulk crystal growth kinetics in amorphous felodipine by a factor of 10, but surface crystal growth only a factor of 2.<sup>28,45</sup> Thus, the polymer additive has a stronger inhibitory effect on bulk crystal growth than surface crystal growth in felodipine, as in NIF.

## 1.5 Contributions of this thesis

The research goal of this thesis is to understand the mechanism of fast surface crystal growth on molecular glasses. Three projects will be presented. Chapter 2 presents fast surface crystal growth on molecular glasses in four different systems: OTP, NIF and IMC in two polymorphs. This work was published in the *Journal of Physical Chemistry B* with myself, Daniele Musumeci, Travis Powell, Ting Cai, Erica Gunn, Lei Zhu, and Lian Yu as authors.<sup>27</sup> Organic glasses can grow crystals much faster on the free surface than in the interior, a phenomenon important for fabricating stable amorphous materials. This surface process differs from and is faster than the glass-to-crystal (GC) growth mode existing in the bulk of molecular glasses. We report that similar to GC growth, surface crystal growth terminates if glasses are heated to gain fluidity. In their steady growth below the glass transition temperature  $T_g$ , surface

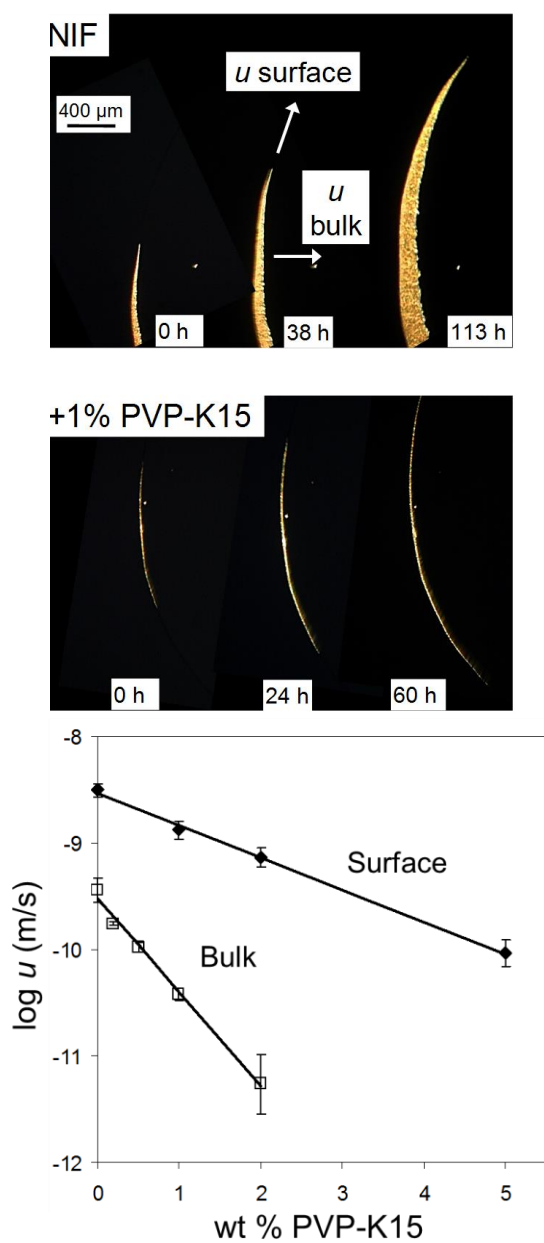


**Figure 6.** The images by optical microscopy show the effect of 1% PVP K15 additives in NIF glass at 303 K.<sup>43</sup> Perimeter surface experiments show the observation of surface and bulk crystallization. The plot (right) shows crystal growth kinetics of polymer additives (PVP) in NIF at 303 K. The polymer additive inhibits bulk crystal growth more strongly than surface crystal growth.

crystals rise above the amorphous surface while spreading laterally and are surrounded by depressed grooves. Above  $T_g$ , the growth becomes slower, sometimes unstable. This damage is stronger on segregated needles ( $\alpha$  IMC, NIF, and OTP) than on crystals growing in compact domains ( $\gamma$  IMC). This effect arises because the onset of liquid flow causes the wetting and embedding of upward-growing surface crystals. Segregated needles are at greater risk because their slow-growing flanks appear stationary relative to liquid flow at a low temperature. The disruption of surface crystal growth by fluidity supports the view that the process occurs by surface diffusion, not viscous flow. Compared to the bulk GC mode, surface crystal growth is disrupted less abruptly by fluidity. Nevertheless, to the extent that fluidity damages them, both processes are solid-state phenomena terminated in the liquid state.

Chapter 3 discusses a signature of fast surface crystal growth on molecular glasses depressed grooves around surface crystals. This work was published in the *Journal of Physical Chemistry* with myself, Daniele Musumeci, and Lian Yu as authors.<sup>46</sup> Molecular glasses can grow crystals much faster at the free surface than in the interior. A property of this process is the creation of depressed grooves or depletion zones around the crystals on the initially flat amorphous surface. With scanning electron microscopy and atomic force microscopy, we studied this phenomenon in IMC, which crystallizes in two polymorphs ( $\alpha$  and  $\gamma$ ) of different morphologies. The observed depletion zones are well reproduced by the known coefficients of surface diffusion and the velocities of crystal growth. At the slow-growing flanks of needle-like  $\alpha$  IMC crystals, depletion zones widen and deepen over time according to the expected kinetics for surface diffusion responding to a crystallization flux. Before fast-advancing growth fronts, depletion zones have less time to develop; their steady-state dimensions agree with the same model revised for a moving phase boundary. These results support the view that surface diffusion enables fast

surface crystal growth on molecular glasses. Our finding helps understand crystal growth in thin films in which the formation of deep depletion zones can cause de-wetting and alter growth kinetics.

Chapter 4 reports a preliminary study on the effect of spatial confinement on surface crystal growth in molecular glasses. Recent studies have shown that organic glasses can grow crystals substantially faster at the free surface than in the interior. Previous studies were performed with glass films essentially infinitely thick and wide. This study examines the effect of spatial confinement on the process using glass films whose width and thickness were systematically reduced and whose supporting substrates were more to less adhesive. The major finding is that surface crystal growth on molecular glasses can be disrupted by spatial confinement on length scales that greatly exceed several molecular layers – the length scale envisioned for surface diffusion. For a thick glass film of NIF or OTP, the process is disrupted if the width is reduced to below several micrometers. This critical width is approximately the lateral “footprint” for surface crystal growth, composed of the single-crystal domain and the distance over which the amorphous surface is perturbed. Similarly, the process in IMC is disrupted if the glass film is thinner than the vertical “footprint”, which is defined by the depth of the depletion zones around a growing crystal. We also report a more subtle confinement effect observed with glass films approximately 10  $\mu\text{m}$  thick on strongly adhesive substrates. Surface crystal growth in these films has the expected initial velocity, but the velocity decreases over time, approximately on the timescale at which the surface crystal layer grows to the bottom of the substrate. All these effects reflect the environmental perturbation of the growth of surface crystals. These effects are significant because organic glasses of technological importance have finite dimensions, may be attached to substrates, and the resulting confinement can affect the process of surface

crystallization.

Chapter 5 proposes future studies that would be beneficial to understand fast surface crystal growth based on ideas that have arisen from the reported studies.

**References:**

---

1. Han, E.; Do, L.; Niidome, Y.; Fujairah, M. Observation of Crystallization of Vapor-Deposited TPD Films by AFM and FFM. *Chem. Lett.* **1994**, 969-972.
2. Yu, L. Amorphous Pharmaceutical Solids: Preparation, Characterization and Stabilization. *Adv. Drug Delivery Rev.* **2001**, 48, 27-42.
3. Ediger, M.D.; Harrowell, P. Perspective: Supercooled Liquids and Glasses. *J. Chem. Phys.* **2012**, 137, 080901.
4. Angell, C.A. Structural Instability and Relaxation in Liquid and Glassy Phases near the Fragile Liquid Limit. *J. Non-Cryst. Solids* **1988**, 102, 205-221.
5. Maps, M.K.; Swallen, S.F.; Ediger, M.D. Self-diffusion of Supercooled *o*-Terphenyl near the Glass Transition Temperature. *J. Phys. Chem. B* **2006**, 110, 507-511.
6. Swallen, S.F.; Ediger, M.D. Self-diffusion of the Amorphous Pharmaceutical Indomethacin near  $T_g$ . *Soft Matter* **2011**, 7, 10339-10344.
7. Hancock, B.C.; Zografi, G. Characteristic and Significance of the Amorphous State in Pharmaceutical Systems. *J. Pharm. Sci.* **1997**, 86, 1-12.
8. Saleki-Gerhardt, A.; Stowell, J.G.; Byrn, S.R.; Zografi, G. Hydration and Dehydration of Crystalline and Amorphous Forms of Raffinose *J. Pharm. Sci.*, **1995**, 84, 318-323.
9. Swallen, S.F.; Kearns, K.L.; Maps, M.K.; McMahon, R.J.; Kim, Y.S.; Ediger, M.D.; Yu, L.; Wu, T.; Satija, S. Organic Glasses with Exceptional Thermodynamic and Kinetic Stability. *Science*, **2007**, 315, 353-356.
10. Ehrlich, G.; Stolt, K. Surface Diffusion. *Annu. Rev. Phys. Chem.* **1981**, 31, 603-637.
11. Seebauer, E.G.; Allen, C.E. Estimating Surface Diffusion Coefficients. *Prog. Surf. Sci.* **1995**, 49, 265-330.
12. Zhu, L.; Brian, C.; Swallen, S. F.; Straus, P. T.; Ediger, M. D.; Yu, L. Surface Diffusion of an Organic Glass. *Phys. Rev. Lett.* **2011**, 106, 256103.
13. Brian, C. B.; Yu, L. Surface Self-Diffusion of Organic Glasses. *J. Phys. Chem. A* **2013**, 117, 13303-13309.
14. Zhang, W.; Brian, C.; Yu, L. Fast Surface Diffusion of Amorphous *o*-Terphenyl and Its Competition with Viscous Flow in Surface Evolution. *J. Phys. Chem. B* **2015**, 119, 5071-5078.

- 
15. Schmelzer, J.; Pascova, R.; Müller, J.; Gutzow, I. Surface-Induced Devitrification of Glasses: the Influence of Elastic Strains. *J. Non-Cryst. Solids*. **1993**, *162*, 23-29.
  16. Avramov, I.; Grantcharova, E.; Gutzow, I. Crystallization and Rheological Behaviour of Alkali Metaphosphate Glass-Forming Melts. *J. Cryst. Growth*. **1981**, *52*, 111-114.
  17. Koster, U. Surface Crystallization of Metallic Glasses. *Mater. Sci. Eng.* **1988**, *97*, 233-239.
  18. Diaz-Mora, N.; Zanutto, E. D.; Hergt, R.; Müller, R. Surface Crystallization and Texture in Cordierite Glasses. *J. Non-Crystalline Solids* **2000**, *273*, 81-93.
  19. Fokin, V. M.; Zanutto, E. D. Surface and Volume Nucleation and Growth in TiO<sub>2</sub>-Cordierite Glasses. *J. Non-Crystalline Solids* **1999**, *246*, 115-127.
  20. Wittman, E.; Zanutto, E. D. Surface Nucleation and Growth in Anorthite Glass. *J. Non-Crystalline Solids* **2000**, *271*, 94-99.
  21. Yuritsyn, N. S. Crystal growth on the surface and in the bulk of Na<sub>2</sub>O·2CaO·3SiO<sub>2</sub>-glass // Nucleation Theory and Applications, Editors: J.W.R.Schmelzer, G.Roepke, V.B.Priezzhev. Dubna, JINR, **2005**, p.22-42.
  22. Wisniewski, W.; Bocker, C.; Kouli M.; Nagel M.; Rüssel, C. Surface Crystallization of Fresnoite from a Glass Studied by Hot Stage Scanning Electron Microscopy and Electron Backscatter Diffraction. *Cryst. Growth Des.* **2013**, *13*, 3794-3800.
  23. Sun, Y.; Zhu, L.; Kearns, K.L.; Ediger, M. D.; Yu, L. Glasses Crystallize Rapidly at Free Surfaces by Growing Crystals Upward. *Proc. Natl. Acad. Sci U.S. A.* **2011**, *108*, 5990-5995.
  24. Wu, T.; Yu, L. Surface Crystallization of Indomethacin below  $T_g$ . *Pharm Res.* **2006**, *23*, 2350-2355.
  25. Zhu, L.; Wong, L.; Yu, L. Surface-Enhanced Crystallisation of Amorphous Nifedipine. *Mol. Pharm.* **2008**, *5*, 921-926.
  26. Gunn, E.; Guzei, I. A.; Yu, L. Does Crystal Density Control Fast Surface Crystal Growth in Glasses? A Study with Polymorphs. *Cryst. Growth Des.* **2011**, *11*, 3979-3984.
  27. Hasebe, M.; Musumeci, D.; Powell, C. T.; Cai, T.; Gunn, E.; Zhu, L.; Yu, L. Fast Surface Crystal Growth on Molecular Glasses and Its Termination by the Onset of Fluidity. *J. Phys. Chem. B* **2014**, *118*, 7638-7646.
  28. Kestur, U.S.; Taylor, L.S. Evaluation of the Crystal Growth Rate of Felodipine Polymorphs in the Presence and Absence of Additives as a Function of Temperature. *Cryst. Growth Des.* **2013**, *13*, 4349-4354.

- 
29. Wu, T.; Sun, Y.; Li, N.; de Villiers, M.; Yu, L. Inhibiting Surface Crystallization of Amorphous Indomethacin by Nanocoating. *Langmuir* **2007**, *23*, 5148-5153.
30. Sakai, A.; Tatsumi, T.; Ishida, K. Growth Kinetics of Si Hemispherical Grains on Clean Amorphous Si Surfaces. *J. Vac. Sci. Tech. A*. **1993**, *11*, 2950-2953.
31. Sallese, J. M.; Ills, A.; Bouvet, D.; Fazan, P.; Merritt, C. Modeling of the Depletion of the Amorphous-Silicon Surface during Hemispherical Grained Silicon Formation. *J. App. Phys.* **2000**, *88*, 5751-5755.
32. Dalton, A. S.; Llera-Hurburt, D.; Seebauer, E.G. Surface Diffusion Kinetics on Amorphous Silicon. *Surf. Sci. Lett.* **2001**, *494*, 761-766.
33. Zhu, L.; Yu, L. Generality of Forming Stable Organic Glasses by Vapor Deposition. *Chem.Phys. Lett.* **2010**, *499*, 62-65.
34. Cicerone, M.T.; Pikal, M. J.; Qian, K.K. Stabilization of Proteins in Solid Form. *Adv. Drug Delivery Rev.* **2015**, *in press*.
35. Ameri, M.; Maa, Y, F.; Spray Drying of Biopharmaceuticals: Stability and Process Considerations. *Dry. Technol.* **2006**, *24*, 763-768.
36. Abdul-Fattah, A.M. ; Truong-Lei-V.; Yee, L.; Nguyen, D.S.; Kalonia, M.T.; Cicerone, Pikal, M.J. Drying-Induced Variations in Physico-Chemical properties of Amorphous Pharmaceuticals and Their Impact on Stability (I): Stability of a Monoclonal Antibody. *J.Pharm.Sci.* **2007**, *96*, 1983-2008.
37. Costantino, H.R.; Firouzabadian, L.; Wu, C.; Carrasquillo, K.G.; Griebenow, K.; Zale, S.E.; Tracy, M.A. Protein Spray Freeze Drying. 2. Effect of Formulation Variables on Particle Size and Stability. *J.Pharm.Sci.* **2002**, *92*, 388-395.
38. Xu, Y.; Grobelny, P.; Von Allmen, A.; Knudson, K.; Pikal, M.; Carpenter, J.F.; Randolph, T.W. Protein Quantity on the Air-Solid Interface Determines Degradation Rates of Human Growth Hormone in Lyophilized Samples. *J.Pharm.Sci.* **2014**, *103*, 1356-1366.
39. Ai, H.; Jones, S.; de Villiers, M. M.; Lvov, Y. M. Nano-Encapsulation of Furosemide Microcrystals for Controlled Drug Release. *J. Controlled Release* **2003**, *86*, 59-68.
40. Pargaonkar, N.; Lvov, Y. M.; Li, N.; Steenekamp, J. H.; de Villiers, M.M. Controlled Release of Dexamethasone from Microcapsules Produced by Polyelectrolyte Layer-by-Layer Nanoassembly. *Pharm. Res.* **2005**, *22*, 826-835.

- 
41. Zahr, A. S.; de Villiers, M. M.; Pishko, M. V. Encapsulation of Drug Nanoparticles in Self-Assembled Macromolecular Nanoshells. *Langmuir* **2005**, *21*, 403-410.
42. Strydom, S.J.; Otto, D.P.; Leibenberg, W.; Lvov, M.; de Villiers, M.M.; Preparation and Characterization of Directly Compactible Layer-by-Layer Nanocoated Cellulose. *Int.J.Pharm.* **2011**, *404*, 57-66.
43. Cai, T.; Zhu, L.; Yu, L.; Crystallization of Organic Glasses: Effects of Polymer Additives on Bulk and Surface Crystal Growth in Amorphous Nifedipine. *Pharm Res.* **2011**, *28*, 2458-2466.
44. Powell, C.T.; Cai, T.; Hasebe, M.; Gunn, E.M.; Gao, P.; Zhang, G. Yu, L. Low-Concentration Polymers Inhibit and Accelerate Crystal Growth in Organic Glasses in Correlation with Segmental mobility. *J Phys Chem B.* **2013**, *117*, 10334-10341.
45. Kestur, U.S.; Lee, H.; Santiago, D. Rinaldi, C.; Won, Y-Y.; Taylor, L.S. Effects of the Molecular Weight and Concentration of Polymer Additives, and Temperature on the Melt Crystallization Kinetics of a Small Drug Molecule. *Cryst Growth Des.* **2010**, *10*, 3585-3595.
46. Hasebe, M.; Musumeci, D.; Yu, L. Fast Surface Crystallization of Molecular Glasses: Creation of Depletion Zones by Surface Diffusion and Crystallization Flux. *J. Phys. Chem. B* **2015**, *119*, 3304-3311.

## Chapter 2

### **Fast Surface Crystal Growth on Molecular Glasses and its Termination by the Onset of Fluidity**

Mariko Hasebe, Daniele Musumeci, C. Travis Powell, Ting Cai, Erica Gunn, Lei Zhu and Lian  
Yu

Department of Chemistry and School of Pharmacy  
University of Wisconsin – Madison, Madison, WI, 53705

As published in  
Journal of Physical Chemistry B, Volume 118 (27), Pages 7638–7646, 2014

## 2.1 Abstract

Organic glasses can grow crystals much faster on the free surface than in the interior, a phenomenon important for fabricating stable amorphous materials. This surface process differs from and is faster than the glass-to-crystal (GC) growth mode existing in the bulk of molecular glasses. We report that similar to GC growth, surface crystal growth terminates if glasses are heated to gain fluidity. In their steady growth below the glass transition temperature  $T_g$ , surface crystals rise above the amorphous surface while spreading laterally and are surrounded by depressed grooves. Above  $T_g$ , the growth becomes slower, sometimes unstable. This damage is stronger on segregated needles ( $\alpha$  indomethacin, nifedipine, and *o*-terphenyl) than on crystals growing in compact domains ( $\gamma$  indomethacin). This effect arises because the onset of liquid flow causes the wetting and embedding of upward-growing surface crystals. Segregated needles are at greater risk because their slow-growing flanks appear stationary relative to liquid flow at a low temperature. The disruption of surface crystal growth by fluidity supports the view that the process occurs by surface diffusion, not viscous flow. Compared to the bulk GC mode, surface crystal growth is disrupted less abruptly by fluidity. Nevertheless, to the extent that fluidity damages them, both processes are solid-state phenomena terminated in the liquid state.

## 2.2 Introduction

Glasses are amorphous solids that have crystal-like mechanical strength and liquid-like spatial uniformity,<sup>1,2</sup> making them ideal for many applications. While traditional glasses are inorganic and polymeric, organic glasses of lower molecular weights are being explored for applications ranging from electronics to bio-preservation to pharmaceuticals.<sup>3,4,5</sup> Amorphous materials must be stable against crystallization and in this context, a relevant recent finding is that organic glasses

can grow crystals much faster at the free surface than in the interior.<sup>6</sup> Surface crystals have been observed to rise above the glass surface by hundreds of nanometers as they grow laterally. It is noteworthy that fast surface crystal growth is common among molecular glasses,<sup>7,8,9,10,11</sup> but apparently less so for glasses of other compositions;<sup>12,13</sup> it is considered non-existent in metallic<sup>14</sup> and silicate<sup>15,16,17</sup> glasses. Because crystallization consists of nucleation and growth, we stress that the phenomenon studied here concerns the *growth* of existing crystals, not the nucleation of a new crystalline phase. In the just-cited studies of metallic and silicate glasses, the free surface was observed to facilitate nucleation but not crystal growth. Understanding fast surface crystal growth helps advance the science of amorphous solids, crystallization, and surface mobility.

There have been different explanations for fast crystal growth on amorphous surfaces.<sup>6,18</sup> One model attributes the process to high surface mobility,<sup>6</sup> envisioning that molecules leave the glass surface layer-by-layer to join upward-growing crystals. This view is consistent with the inhibitory effect of thin coatings on surface crystal growth<sup>19</sup> and the correlation between the rates of surface crystal growth and diffusion.<sup>20,21</sup> On the glasses of indomethacin (IMC) and nifedipine (NIF), the velocity of surface crystal growth scales with the surface diffusion coefficient:  $u_s = D_s/(10 \mu\text{m})$ . In another model, surface crystallization is attributed to the efficient release of crystallization-induced tension at surfaces.<sup>18</sup>

To avoid confusion, we note that the phenomenon studied here concerns crystal growth *on the free surface* of molecular glasses. This process is distinct from and faster than the so-called glass-to-crystal or GC mode,<sup>22,23,24</sup> which exists *in the interior* of glasses. For systems showing the GC growth phenomenon, the velocity of bulk crystal growth is diffusion-limited at high temperatures, but abruptly rises near the glass transition temperature  $T_g$ , becoming too fast to be

controlled by bulk diffusion. At present, the mechanism of GC growth remains mysterious.<sup>23,24,25,26,27,28</sup>

Glasses become flowing liquids upon heating. Previous studies have found that the onset of fluidity can terminate the bulk GC growth in molecular glasses.<sup>23,24,25,28</sup> The goal of this study is to determine whether an analogous effect exists for the process of surface crystal growth. Independently, the existence of such an effect is suggested the observation that heating above  $T_g$  can change the mechanism of surface evolution from surface diffusion to viscous flow.<sup>20,21</sup> (In this context, surface diffusion is the lateral translation of molecules on the surface, and viscous flow is the collective movement of the liquid responding to a pressure imbalance.) Such a change is expected to perturb the process of crystal growth supported by surface diffusion; for example, at high fluidity, surface crystals would appear stationary to a flowing liquid and be wetted and engulfed, preventing their upward growth. From its response to the onset of fluidity, we hope to better understand the molecular mechanism of surface crystal growth.

We studied three organic glasses: IMC (crystallizing in  $\alpha$  and  $\gamma$  polymorphs), NIF, and *o*-terphenyl (OTP). These molecules have different structures (see Figures 1, 4, and 6), physical properties (Table 1), and rates of crystal growth. IMC and NIF glasses are known to exhibit fast surface crystal growth,<sup>6,7,8,19</sup> and we report the phenomenon for OTP here for the first time. Together these systems enable a broad survey of surface crystal growth on organic glasses.

We report that the onset of fluidity generally disrupts fast surface crystal growth on molecular glasses. The severity of this disruption depends on crystal morphology: segregated needles are more vulnerable than crystals that grow in compact domains. These results are well explained by the activation of liquid flow on the timescale of crystal growth, which allows the liquid to wet and embed upward-growing surface crystals. Segregated needles are at greater risk because their

slow-advancing fronts appear stationary to the flowing liquid at a relatively low temperature. The termination of surface crystal growth by fluidity argues that the process is not sustained by viscous flow, but by surface diffusion. Compared to the bulk GC growth, surface crystal growth is disrupted less strongly by fluidity. Nevertheless, to the extent that fluidity damages them, both processes are inherently solid-state processes that are terminated in the liquid state.

### 2.3 Materials and methods

Indomethacin (1-(*p*-chlorobenzoyl)-5-methoxy-2-methylindole-3-acetic acid, 99+%,  $\gamma$  polymorph), nifedipine (1,4-dihydro-2,6-dimethyl-4-(2-nitophenyl)-3,5-pyridinedicarboxylate; NIF), and *o*-terphenyl (OTP) were purchased from Sigma-Aldrich. To prepare a sample for crystal growth measurement, the crystalline substance was melted on a clean square coverslip at 15 K above the melting point and covered with a smaller round coverslip (typically 15 mm in diameter). The assembly was cooled to below  $T_g$  by contact with a metal block, pre-equilibrated at room temperature for IMC and NIF and with dry ice for OTP. The sample was confirmed to be free of crystals by polarized light microscopy. The square cover slip was detached by bending its edges away from the organic glass, creating a glass film with a free surface. The films were 10 – 100  $\mu\text{m}$  thick. In the case of IMC and NIF, surface crystallization was initiated at 313 K ( $T_g$  – 2 K) spontaneously and the sample was transferred to a desired temperature for further measurement. Crystal growth was measured under  $\text{N}_2$  purge through a light microscope (Olympus BH2-UMA). The time of observation was sufficient for the growth to reach several hundred micrometers, during which the growth rates were relatively constant. Growth at 303 – 338 K for IMC and 303 – 328 K for NIF was observed real-time on a temperature-controlled stage (Linkam THMS 600) under  $\text{N}_2$  purge. For slower growth at 296 K, the sample was stored.

in a plastic bag with purged with N<sub>2</sub> in the air-conditioned laboratory ( $296 \pm 1$  K) and observed only at the beginning and the end of storage. Because of its slow nucleation, an OTP glass was initiated to grow surface crystals by placing a seed on its surface and the sample was transferred to the Linkam stage waiting at a crystallization temperature.

Polymorphs were identified by x-ray powder diffraction (Bruker D8 Advance diffractometer with Cu K $\alpha$  radiation) and with a Raman microscope (Thermo DXR). A 780 nm laser was used for NIF and 532 nm laser for IMC to record the Raman spectra. Surface crystal growth was observed real time with an Atomic Force Microscope (AFM; Veeco Multimode IV Scanning Probe Microscope) in the tapping mode under N<sub>2</sub> purge. An AFM hostage was used for temperature control and calibrated against the melting point of OTP (329 K). The AFM tips (300Al-G10, BudgetSensors) are specified as follows: tip radius 10 nm, half-cone angle 20-25° (10° at apex).

## 2.4 Results

### 2.4.1 Indomethacin (IMC).

IMC glasses grow crystals much faster on the free surface than in the interior.<sup>6,7,19</sup> The process has been observed for two polymorphs ( $\alpha$  and  $\gamma$ ), with  $\alpha$  IMC forming segregated needles and  $\gamma$  IMC compact domains (see the AFM images in Figure 1). These different morphologies are expected from the structures of the polymorphs:  $\alpha$  IMC has a compressed unit cell along the  $a$  axis and  $\gamma$  IMC a nearly cubic unit cell (Table 1); according to the Bravais-Friedel-Donnay-Harker model,  $\alpha$  IMC crystals grow elongated along  $a$  and  $\gamma$  IMC crystals are more equal-dimensional.

**Table 1.** Physical properties of the systems studied

Substance	IMC		NIF	OTP
Formula	C <sub>19</sub> H <sub>16</sub> ClNO <sub>4</sub>		C <sub>17</sub> H <sub>18</sub> N <sub>2</sub> O <sub>6</sub>	C <sub>18</sub> H <sub>14</sub>
MW, g/mol	357.79		346.34	230.30
$T_{g,DSC}$ , K	315		315	246
Surface crystal str.	$\alpha$ IMC <sup>29</sup>	$\gamma$ IMC <sup>30</sup>	$\beta$ NIF <sup>31</sup>	OTP <sup>32</sup>
$a$ , Å	5.462	9.295	9.840	18.583
$b$ , Å	25.310	10.969	13.807	6.024
$c$ , Å	18.152	9.742	14.206	11.728
$\alpha$ , deg.	90	69.38	61.39	90
$\beta$ , deg.	94.38	110.79	79.76	90
$\gamma$ , deg.	90	92.78	81.99	90
$Z$	6	2	4	4
Sp. grp.	$P2_1$	$P-1$	$P-1$	$P2_12_12_1$
$\rho$ , g/cm <sup>3</sup>	1.42	1.37	1.382	1.165
$T$ , K	203	296	296	296

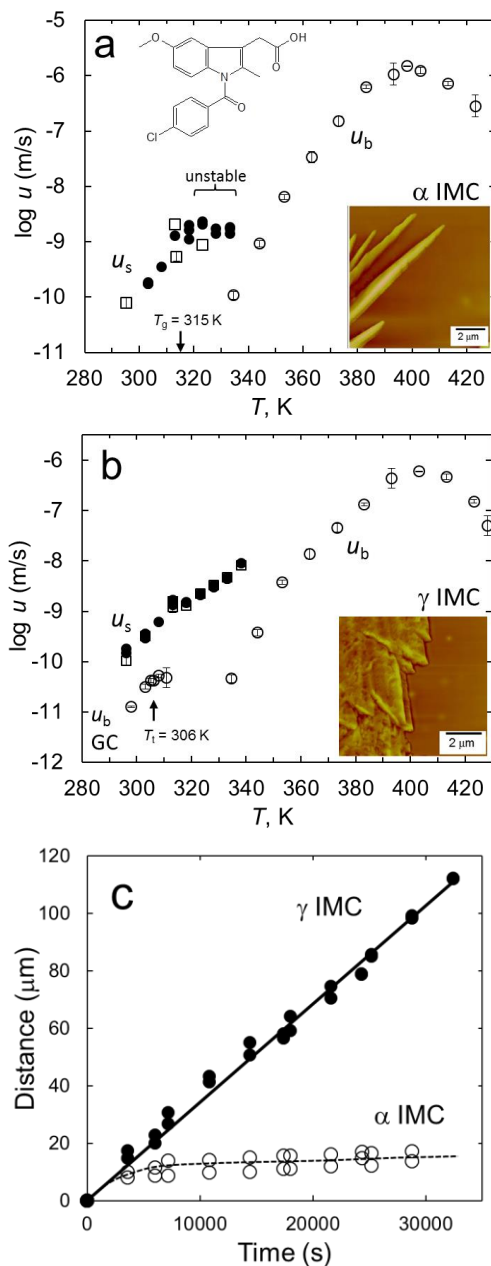


**Figure 1.** Crystal growth rates of  $\alpha$  IMC (a) and  $\gamma$  IMC (b) at the free surface ( $u_s$ ) and in the bulk ( $u_b$ ). The AFM images show the morphologies of surface crystals. Color scale = 1500 nm for  $\alpha$  IMC and 400 nm for  $\gamma$  IMC. The structure of IMC is given in (a). Above 318 K, the surface growth of  $\alpha$  IMC is unstable and slows over time, but  $\gamma$  IMC surface crystals continue to grow steadily. This difference is shown in (c) for  $T = 328$  K. In (a), the region labeled “unstable” shows the early growth rates of  $\alpha$  IMC.

Figure 1 shows the velocities of surface crystal growth  $u_s$  in amorphous IMC as functions of temperature. These velocities well exceed those of bulk crystal growth  $u_b$  (also shown). For  $\gamma$  IMC, we display  $u_b$  in both the diffusion-limited regime<sup>33</sup> and the glass-to-crystal or GC growth regime (labeled “ $u_b$  GC”).<sup>28</sup> The latter terminates at 306 K. For  $\alpha$  IMC, only  $u_b$  in the diffusion-limited regime is shown. (While this polymorph can grow in the glassy state, its growth is much slower and the present data are incomplete.<sup>28</sup>) The  $u_s$  data from previous studies are shown with open symbols<sup>7,6</sup> and those from this work in solid ones; where comparison is possible, the agreement is reasonably good.

In the glassy state ( $T < T_g$ ), heating speeds up the surface growth of both polymorphs, but their responses differ above  $T_g$ . For  $\alpha$  IMC (Figure 1a), the growth rate  $u_s$  levels off and eventually decreases with increasing temperature, whereas the effect is weaker for  $\gamma$  IMC (Figure 1b). Above 318 K, the surface growth of  $\alpha$  IMC becomes unstable: some crystals grow, while others lie dormant; eventually the growing crystals stop advancing also. This instability is partly responsible for the scatter in the growth rates of  $\alpha$  IMC. In contrast, the compact domains of  $\gamma$  IMC expand steadily at a constant rate. This difference between the two polymorphs is illustrated in Figure 1c for  $T = 328$  K. In the first few hours, the two polymorphs grow at similar rates; over time, the growth of  $\alpha$  IMC slows, but  $\gamma$  IMC keeps growing at the same velocity. Because of its time dependence, the  $u_s$  of  $\alpha$  IMC above 318 K is the average velocity over the first 2 hours; the value will be substantially lower if a longer period is chosen.

It is noteworthy that the surface and bulk growth of  $\gamma$  IMC responds differently to heating (Figure 1b). The bulk growth of  $\gamma$  IMC (GC mode) is active below 306 K, yielding compact spherulites expanding at constant velocities, but is disrupted above 306 K.<sup>28</sup> In the disrupted state,  $\gamma$  IMC grows loose fibers at velocities that decrease over time. In contrast, the surface growth of

$\gamma$  IMC persists in a steady state up to higher temperatures. As a result, it is possible to grow a thin surface crystal layer over a bulk liquid in which GC growth is halted. These data argue that fluidity influences surface and bulk crystal growth differently, a subject we return to in the Discussion.

To understand why the two IMC polymorphs respond differently to the onset of fluidity, we examined their growth in real time by AFM. Figure 2a shows two consecutive images during the growth of a needle-like  $\alpha$  IMC crystal. These images were recorded 25 min apart at 317 K, approximately the highest temperature at which steady surface growth is observable. As expected from the needle morphology, axial growth is much faster than lateral growth,  $u_{sz} \gg u_{sx}$ , with  $u_{sz}/u_{sx}$  estimated to be 100 or greater. The height of the crystal is well above the glass surface ( $y_c > y_g$ ) by hundreds of nanometers. AFM reports the width of an  $\alpha$  IMC needle  $x_c$  to be hundreds of nanometers;  $x_c \approx 400$  nm at 3  $\mu\text{m}$  from the tip. In estimating this width, the broadening effect has been corrected to account for the finite width of the AFM tip and its conical shape. This correction is illustrated with the vertical lines in Figure 2a and is especially important for tall objects rising sharply above the surface.

An important feature of surface crystal growth is that the crystals are surrounded by depressed grooves or depletion zones on the glass surface. This feature is labeled DZ in Figure 2. For an  $\alpha$  IMC needle, the depletion zone widens and deepens with increasing distance to the tip; at a distance of 3  $\mu\text{m}$ , the width is ca. 500 nm and the depth ca. 200 nm. In estimating these dimensions, we accounted for the fact that AFM overestimates the width of a tall crystal and consequently underestimates the width of the adjacent depletion zones; this correction is illustrated in Figure 2a. Note also that the width given here is approximate, since the depletion zone gradually transitions to flatness; we take the “onset” of a depletion zone to be the location

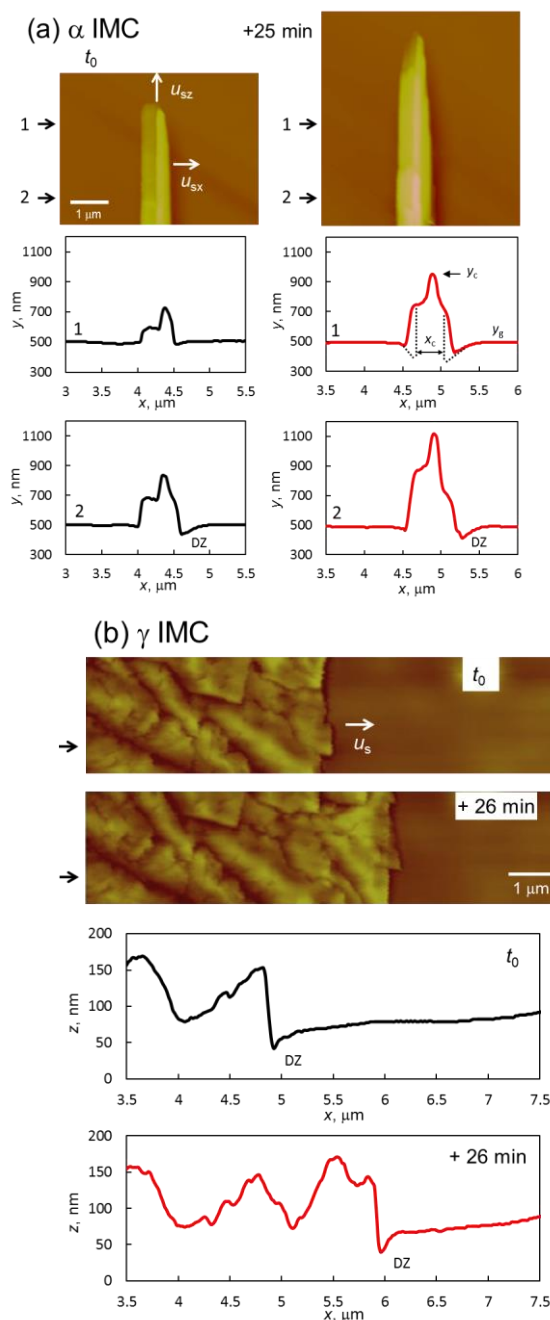


**Figure 2.** Real-time AFM images of the surface growth of  $\alpha$  IMC (a) and  $\gamma$  IMC (b) at 317 K. Black arrows show where height profiles are plotted.  $u_s$ : velocity of surface crystal growth. For  $\alpha$  IMC,  $u_{sz}$  is the axial growth velocity and  $u_{sx}$  the slower lateral growth velocity. DZ: depletion zone. The dotted lines in (a) show the actual contours of the crystal/glass interface, to correct the AFM error in measuring high objects.

where the glass surface curves down significantly. The depletion zones can be asymmetric, and measurements at different temperatures found that their dimensions are insensitive to temperature change below  $T_g$ . As we discuss later, the depletion zone is a consequence of mass transport by surface diffusion in support of crystal growth

In the case of  $\gamma$  IMC, AFM showed compact, steadily advancing surface crystals (Figure 2b). The growth front also rose above the glass surface, but to a lower height relative to  $\alpha$  IMC. A depletion zone is detectable on the glass surface before the growth front, with the width being ca. 200 nm and the depth ca. 100 nm. The principal difference between the IMC polymorphs is that the growth front of  $\gamma$  IMC advances nearly uniformly, whereas  $\alpha$  IMC has fast axial growth but slow lateral growth. We argue later that this difference accounts for the different responses of the two polymorphs to the onset of fluidity.

#### 2.4.2 Nifedipine (NIF).

Fast surface crystal growth has been observed on NIF glasses<sup>8,11</sup> and the present study focused on the effect of increasing fluidity on this process. Figure 3a shows the velocities of crystal growth at the free surface ( $u_s$ ) and in the bulk ( $u_b$ ) of amorphous NIF; the solid symbols indicate the data from this work. Although NIF is polymorphic, only the growth of the  $\beta$  polymorph was observed in these studies.<sup>31</sup> As in the case of  $\alpha$  IMC, heating within the glassy state ( $T < T_g$ ) steadily raises the  $u_s$ , but with further heating above  $T_g$ ,  $u_s$  plateaus and eventually decreases. Thus, the surface crystal growth of NIF is similarly disrupted as that of  $\alpha$  IMC. In contrast to  $\alpha$  IMC, however, the instability of surface crystal growth above  $T_g$  was not as pronounced for NIF; its growth rate was reduced but remained approximately constant during observation.

Similar to  $\alpha$  IMC, NIF grew needle-like crystals on the glass surface (Figure 3b). The crystal structure of NIF (Table 1) suggests that the needles are elongated along the short  $a$  axis of the

unit cell. As in the case of  $\alpha$  IMC, NIF surface crystals are surrounded by depletion zones on the glass surface flanking the elongated crystals. Because of their fast growth, precise measurement of the depletion zones was difficult. Our best data show that the depletion zones are typically 100 nm deep and 400 nm wide at a distance of several micrometers from the tip.

For reference, Figure 3 also displays the velocities of crystal growth *in the interior* of NIF glasses,<sup>34</sup> in the glass-to-crystal (GC) mode. Note that this bulk growth mode exhibits a similar disruption upon heating above  $T_g$ . This disruption is more abrupt than that of the surface crystal growth. We will comment later on the similarity and differences between the terminations of surface and bulk crystal growth in organic glasses by fluidity.

### 2.4.3 *o*-Terphenyl (OTP).

OTP is a model for studying glass-forming liquids<sup>35,36</sup> and their crystal growth.<sup>22,23,37,38,39,40,41</sup> Liquid OTP can develop in the bulk a fast mode of crystal growth (the GC mode) as it is cooled to near  $T_g$ .<sup>22,23</sup> GC growth persists deep in the glassy state of OTP and terminates as the system is heated to above  $T_g$ . We report here that at the free surface of OTP glasses, even faster crystal growth occurs and this process also terminates upon heating above  $T_g$ .

After seeding the surface of an OTP glass with a crystal, new growth soon becomes evident (Figure 4). Needle-like crystals grow rapidly from the seed. Through a light microscope, the crystals appear transparent and thin, and their growth rate  $u_s$  is 10 times faster than the known bulk growth rate  $u_b$ .<sup>23,41</sup> Figure 5 summarizes the rates of crystal growth, with the data from this work shown in solid symbols. It is noteworthy that among the systems known to exhibit fast surface crystal growth,<sup>6,7,8,19</sup> the process in OTP is the fastest. After the surface of an OTP glass is covered with a layer of crystals (Figure 5), additional crystallization can still occur because of

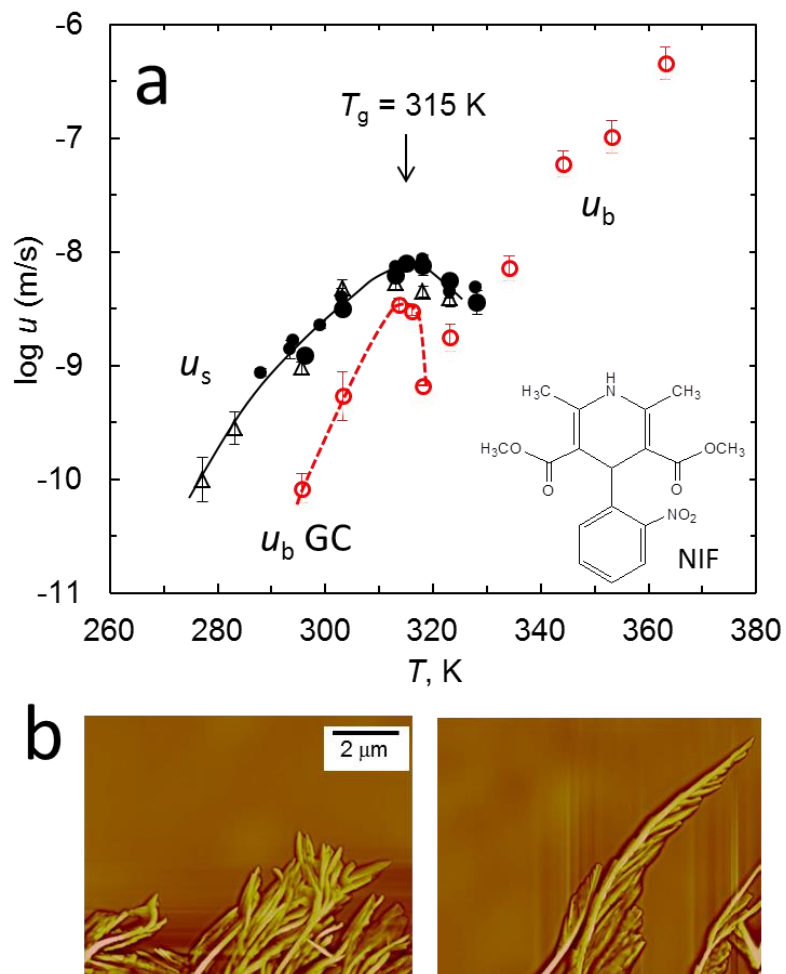


**Figure 3.** (a) Crystal growth rates at the surface  $u_s$  and in the bulk  $u_b$  of amorphous NIF. The inset shows the structure of NIF. (b) AFM images of needle-like NIF surface crystals.

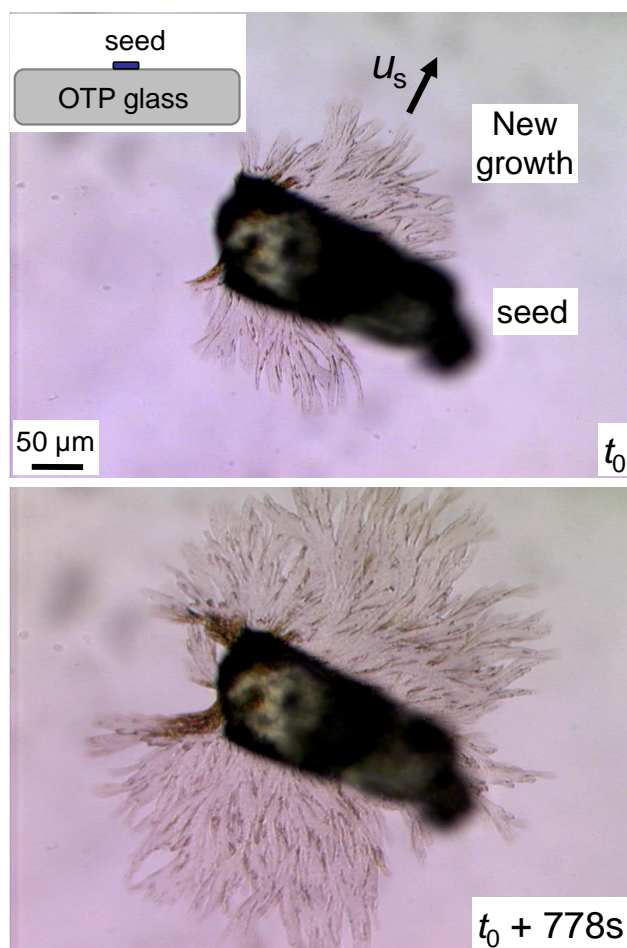


**Figure 4.** Crystals growing at the free surface of an OTP glass from a seed at 243 K.  $u_s$  is the growth velocity.

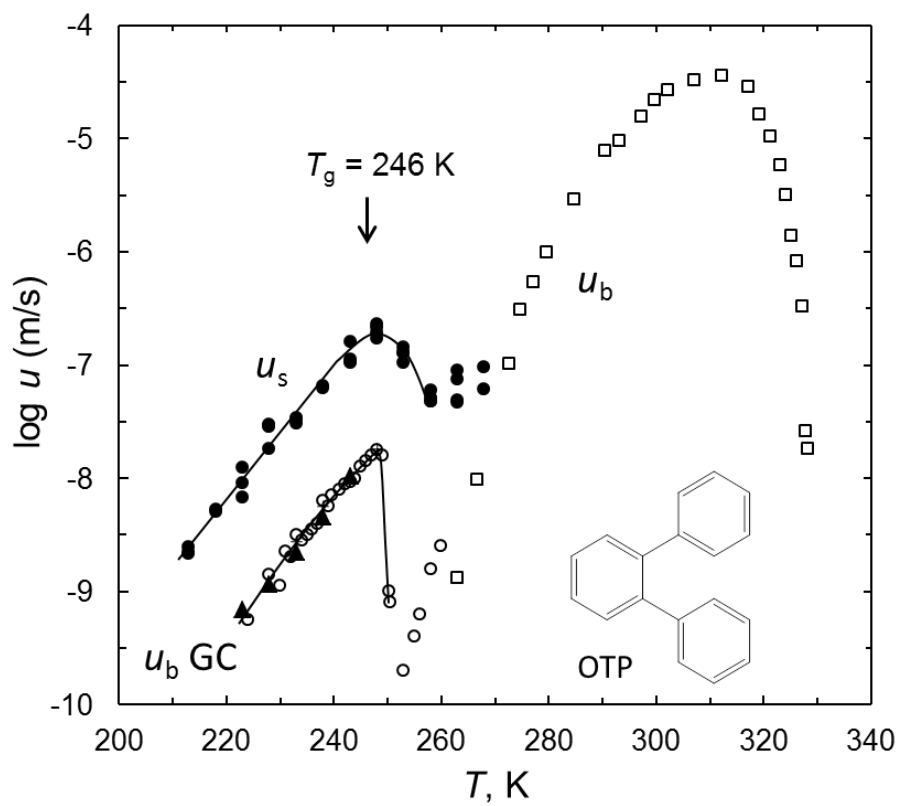


**Figure 5.** Crystal growth rates at the surface ( $u_s$ ) and in the bulk ( $u_b$ ) of amorphous OTP.  $u_b$  is from Ref. 37 (open squares), Ref. 23 (open circles), and this work (solid triangles). The inset shows the structure of OTP.

bulk crystal growth. Circular domains appear and expand over time (Figure 6), at the known bulk growth rates.<sup>23,41</sup> These domains are more opaque and birefringent than the over-layer of surface crystals, indicating greater thickness. X-ray diffraction showed that the resulting product has the same unit cell as the known OTP crystal structure.<sup>32</sup> These results show that the second-stage crystallization corresponds to bulk crystal growth beneath a thin layer of surface crystals. The fact that OTP surface crystals are nucleated by a seed of the known crystal structure (Figure 4) and in turn nucleate the same (Figure 6) argues that the same crystalline phase grows on the surface and in the bulk of OTP glasses (i.e., no polymorphic change).

As with  $\alpha$  IMC and NIF, the surface crystal growth on OTP glasses is disrupted by heating above  $T_g$ . The observed  $u_s$  plateaus and decreases with temperature increase (Figure 5). Also similar to the other systems, the surface crystals of OTP grow as segregated needles (Figure 4). The crystal structure of OTP (Table 1) suggests that the needle axis is the shortest unit-cell axis  $b$ . Because of its low  $T_g$ , crystal growth on OTP glasses could not be followed in real time with our AFM.

The bulk GC growth in OTP glasses is known to be halted by heating<sup>23,41</sup> and we report here that in comparison, the disruption of surface crystal growth is less abrupt. GC growth occurs steadily in OTP below  $T_t = 249$  K (onset temperature of GC growth), yielding compact spherulites. Heating above  $T_t$  halts the process and only careful examinations reveal loose, fast-growing, fiber-like crystals.<sup>24,41</sup> In contrast, surface crystal growth can persist at a steady velocity slightly above the temperature at which  $u_s$  reaches its maximum. Steady GC growth can be “poisoned” with a brief heating above  $T_t$ ; for example, steady GC growth at 243 K could not resume after heating to 253 K for 30 min and cooling back to 243 K. In contrast, the same temperature cycling did not halt surface crystal growth.

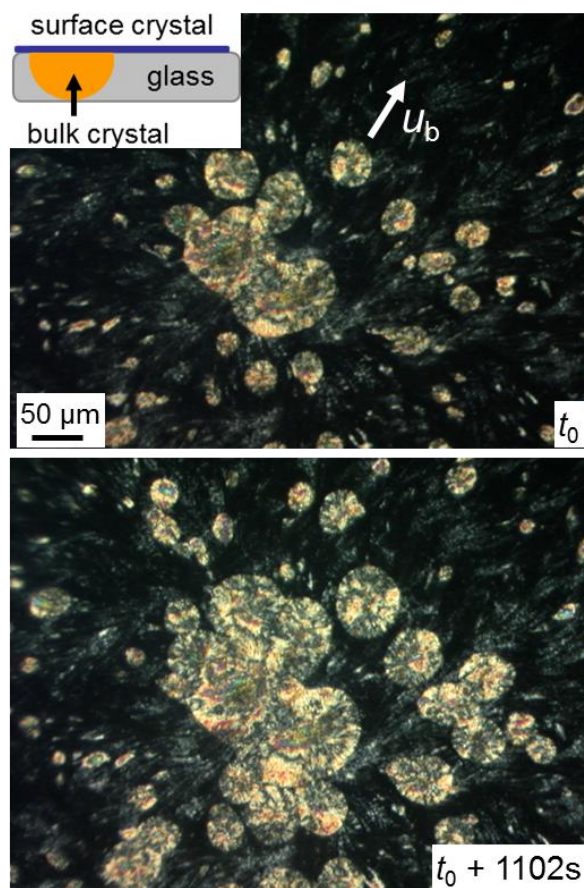


**Figure 6.** Bulk crystals of OTP growing under a layer of surface crystals at 243 K. The sample was viewed between crossed polarizers; surface crystals were too thin to be clearly visible under this condition.  $u_b$  is the growth velocity of bulk crystals.

## 2.5 Discussion

The principal finding of this work is that fast surface crystal growth on organic glasses can be disrupted as they are heated to become fluids. As summarized in Figure 7, heating above  $T_g$  disrupts the surface crystal growth in three of the four systems examined, with the observed growth becoming stagnant or *slower* with increasing temperature. Remarkably, this effect is largely absent for  $\gamma$  IMC, whose  $u_s$  continues to rise with heating. These different responses correlate with the morphologies of surface crystals: the at-risk crystals are segregated needles, whose growth fronts advance at vastly different rates relative to the glass surface, whereas the resistant crystal ( $\gamma$  IMC) grows in compact domains, whose growth front advances almost uniformly. An important feature revealed by real-time AFM is that surface crystals are surrounded by depletion zones on the surface of organic glasses. For needle-like crystals, depletion zones are along the needles; for the compact growth of  $\gamma$  IMC, they reside before the uniformly advancing growth front. In this section, we discuss the implications of these observations for understanding fast surface crystal growth on organic glasses. We argue that needle-like surface crystals are more at risk to perturbation by fluidity because their slow-advancing flanks appear stationary relative to the flowing liquid at a low temperature, allowing them to be wetted and engulfed.

### 2.5.1 Mechanism of Surface Crystal Growth on Organic Glasses.

Previous work has developed the view that surface crystals can grow rapidly on organic glasses because of fast surface diffusion. This view is supported by the proportionality of surface crystal growth rate  $u_s$  and surface diffusivity  $D_s$ ,  $u_s = D_s / (10 \text{ } \mu\text{m})$ , observed for IMC and NIF,<sup>21</sup> and by the inhibition of the process by thin surface coatings.<sup>19</sup> According to this model, the upward

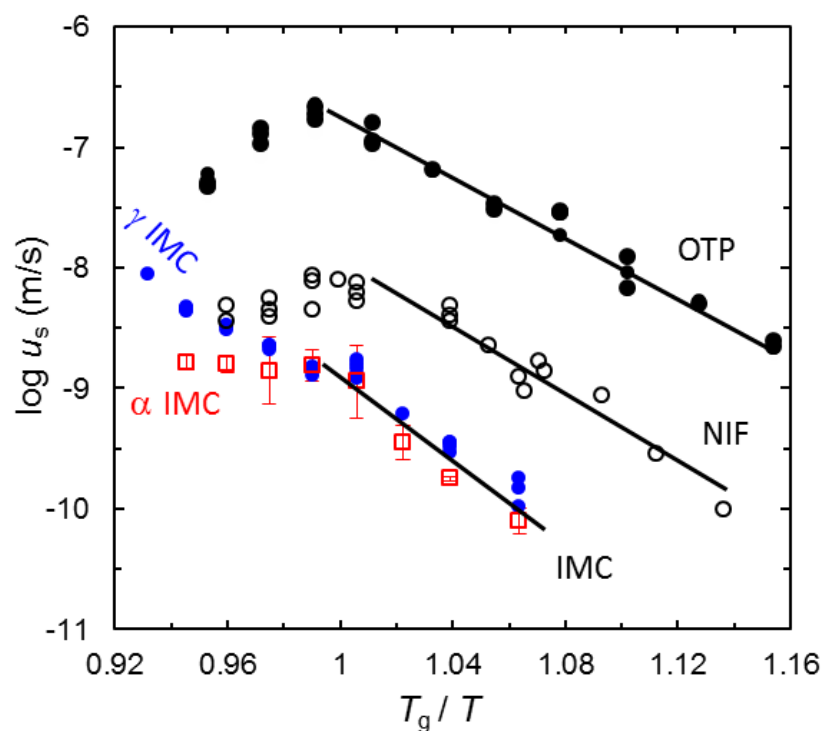


**Figure 7.** Surface crystal growth rates vs.  $T_g$  scaled temperature. For  $\alpha$  IMC, NIF, and OTP, the growth mode is disrupted by the onset of fluidity, whereas the effect is weaker for  $\gamma$  IMC. The lines indicate ranges of surface crystal growth unperturbed by fluidity.

growth of surface crystals above the glass surface<sup>6,11</sup> is a natural response of the system to slow bulk growth and fast surface diffusion.

The surface-mobility model is consistent with the new finding of this work that surface crystals are surrounded by depletion zones on the glass surface. This feature is qualitatively explained by the combined action of (i) the flux of molecules from the glass to the crystal and (ii) the diffusion of molecules on the amorphous surface. Similar depletion zones have been observed around the hemispherical surface crystals on amorphous silicon and similarly explained.<sup>13</sup> Sallèse et al. modeled the depletion zones around Si surface crystals using Mullins' theory of surface diffusion<sup>42</sup> and assuming a constant flux of atoms from the amorphous surface to the crystal.<sup>13</sup> The model explains the evolution of the depletion zone as a hemispherical crystal grows. It would be valuable to test such a model on our systems. For this purpose, it is useful to have higher-resolution images of the depletion zones than currently available. It is also necessary to take into account the differences between amorphous Si and IMC. For example, Si crystals grow hemispherical grains, but  $\alpha$  IMC grows needles. The needle growth means more time for a depletion zone to develop along the sides than before the tip. The in-plane growth of Si hemispheres is slow enough for the depletion zones to widen and deepen over time. In contrast, the depletion zone before the compact growth front of  $\gamma$  IMC is independent of time, likely a result of the limited time for the depletion zone to develop before being overrun by the crystal growth front.

The real-time AFM observations of surface crystal growth (Figure 2) suggest relevant details on the growth of surface crystals. At first glance, the needle growth of  $\alpha$  IMC (Figure 2a) might suggest direct acquisition of molecules from the glass surface *immediately before the tip*. This mechanism, however, would create a deep depletion zone before the tip, not along the sides. A

more likely mechanism is the collection of molecules by the lateral surfaces and the migration of these molecules on the crystal surface to eventual growth sites.

Had there been no surface migration, each molecule crossing the glass/crystal interface would immediately join the crystal lattice, resulting in fast lateral growth, in conflict with experimental observation. (The foregoing analysis assumes that the flux of molecules across the glass/crystal interface is the same everywhere, which is reasonable given that the flux depends mainly on surface diffusivity and the free-energy difference across the interface.) This mechanism of needle growth is consistent with Sears' model for the growth of metal whiskers from vapor, in which atoms adsorb on the lateral surface and migrate toward the tip.<sup>43</sup> We speculate that the other needle-growing surface crystals (NIF and OTP) grow in a similar mechanism as  $\alpha$  IMC. In contrast, the compact growth of  $\gamma$  IMC may occur differently, in which molecules crossing the glass/crystal interface do not travel long distances and deposit near the site of crossing.

### **2.5.2 Disruption of Surface Crystal Growth on Organic Glasses by the Onset of Fluidity.**

We hypothesize that heating above  $T_g$  activates liquid flow on the time scale of surface crystal growth, allowing the liquid to wet and embed the upward-growing surface crystals. This interaction would in turn damage the growth of surface crystals. To test this hypothesis, we compare in Figure 8 the velocities of surface crystal growth  $u_s$  and liquid flow for the systems studied. For the compact growth of  $\gamma$  IMC, the entire growth front is characterized by a single  $u_s$ . For needle-growing crystals, we distinguish the fast axial growth ( $u_{sz}$ ) and the slow lateral growth ( $u_{sx}$ ). Our measurements by light microscopy yielded  $u_{sz}$  only, a consequence of limited spatial resolution. For  $\alpha$  IMC,  $u_{sx}$  (dotted line in Figure 8) was estimated from real-time AFM to be 100 – 1000 times slower than  $u_{sz}$ . In the absence of experimental data on NIF and OTP, we apply the same factor of reduction to estimate their lateral growth rates.

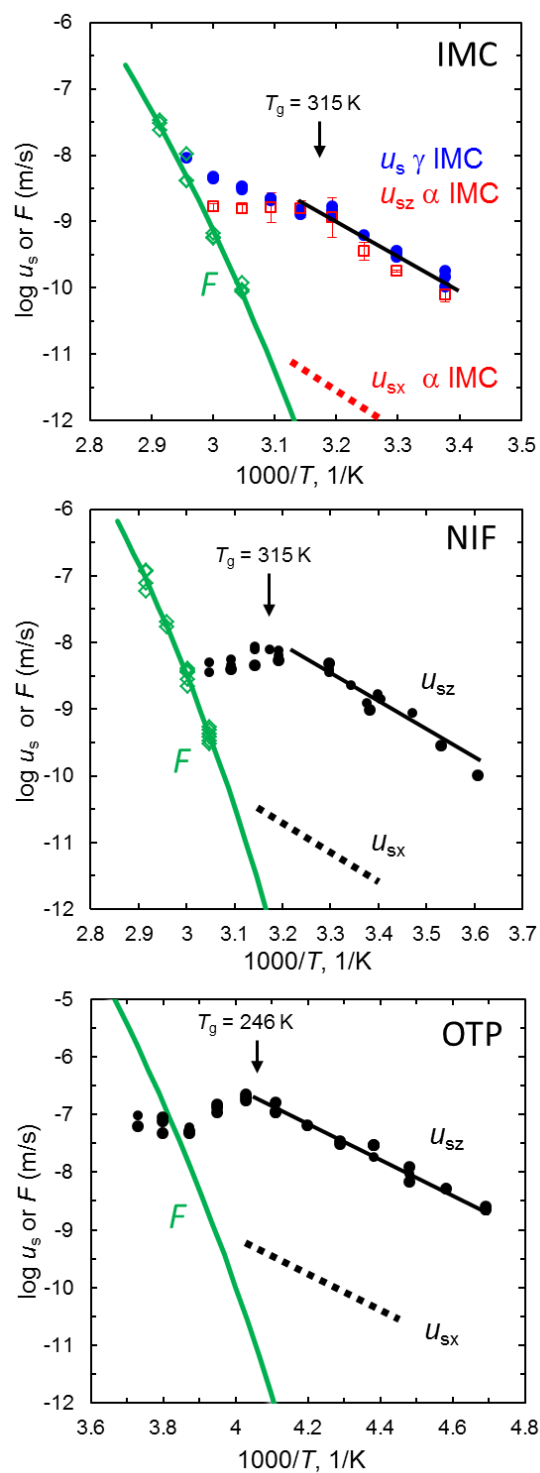


**Figure 8.** Comparison of the velocities of surface crystal growth and liquid flow. For needle-like crystals, the axial growth rates  $u_{sz}$  are experimental data and the lateral growth rates  $u_{sz}$  are estimated (dotted lines).

To estimate the velocity of liquid flow near a surface crystal, we calculate the quantity  $F = \gamma/(2\eta)$ , where  $\gamma$  is surface tension and  $\eta$  is viscosity.  $F$  approximately represents the velocity of liquid flow in many situations. For example,  $F$  is roughly the velocity at which gold spheres sink into liquid TNB.<sup>44</sup> These spheres can serve as a model for surface crystals that grow slowly relative to liquid flow. For a surface groove being flattened by viscous flow (Figure 9a), the contour velocity at the half depth is  $F$ , and the vertical velocity at the bottom is  $(y/d_w) F$ , where  $y$  is the depth of the groove and  $d_w$  its half width at the half depth.<sup>42</sup> For a sinusoidal surface grating of IMC and NIF, viscous flow decreases the amplitude  $h$  at the rate  $(2\pi h/\lambda) F$ , where  $\lambda$  is the grating's wavelength, allowing the measurement of  $F$ .<sup>20,21</sup>

We estimate the velocity of liquid flow near a surface crystal by treating the adjacent depletion zone (Figure 2a) as half of Mullins' groove (Figure 9b). The lateral velocity of the liquid relative to a slow-growing surface crystal is then  $F$ , and its vertical velocity at the bottom,  $(y/d_w) F$ . Our AFM measurements found that at the steady state of surface crystal growth, the depletion zones are approximately characterized by  $y \approx d_w$ , which leads to  $u_y \approx F$ . Thus, the velocities of liquid flow are well represented by  $F$ . Note that this calculation is only approximate given the change from Mullins' geometry. Since the liquid is expected to wet its crystal, the actual vertical velocity could exceed the prediction. Nevertheless, we regard  $F$  as a first-order estimate of the liquid velocity.

In Figure 8, we present the values of  $F$  for IMC and NIF (green diamonds) measured from the decay of surface gratings.<sup>20,21</sup> These data are further extrapolated to lower temperatures assuming viscosity is proportional to the structural relaxation time.<sup>45,46</sup> For OTP, no surface-smoothing measurements have been reported and  $F$  is calculated from its known viscosity<sup>47</sup> and surface tension.<sup>48</sup>

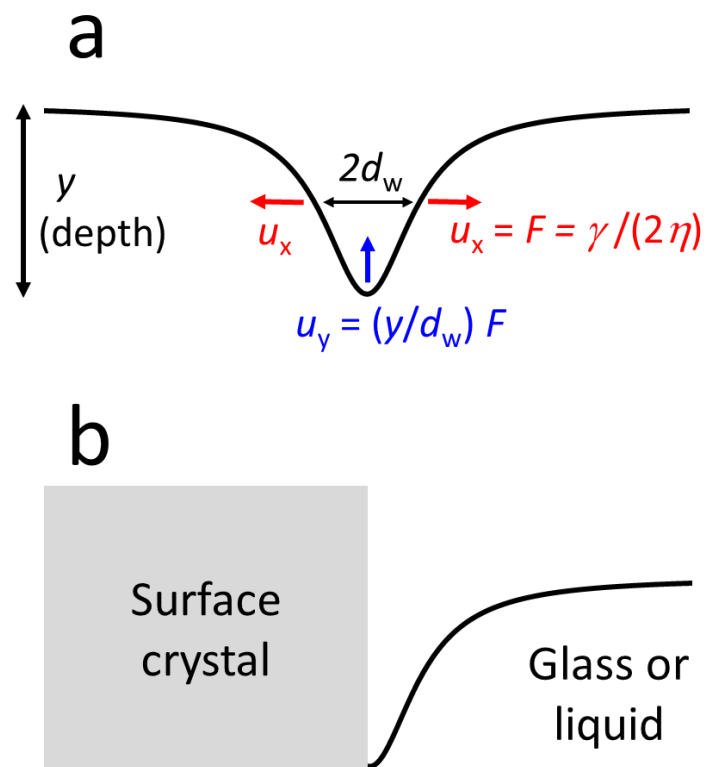


**Figure 9.** (a) Model for the smoothing of a surface groove by viscous flow.<sup>42</sup> (b) Model for the interface between a surface crystal and a glass or liquid.

Figure 8 shows that below  $T_g$ , the velocity of surface crystal growth vastly exceeds that of liquid flow,  $u_s \gg F$ .

This relation holds for  $\gamma$  IMC everywhere at the compact growth front; it holds for the needle-growing crystals both in the axial direction and in the lateral direction,  $u_{sz} > u_{sx} \gg F$ . This relation is consistent with the minor role of viscous flow in transporting materials to support surface crystal growth. For  $\gamma$  IMC, the relation  $u_s > F$  is valid up to a high temperature ( $\sim 1.2 T_g$ ). This high cross-over temperature agrees with the persistence of the surface growth of  $\gamma$  IMC at high temperatures. For the needle-growing crystals, applying the same analysis to the *axial* growth would return a similar conclusion. However, since the needles have slow *lateral* growth, the liquid velocity can reach and surpass the lateral growth rate at a lower temperature, as illustrated by the dotted lines in Figure 8. The estimated cross-over temperature is approximately  $T_g$  for each system, in good agreement with the termination temperature for surface crystal growth; this agreement is gratifying considering the errors in the estimated liquid velocities. At high enough fluidity, a slow-growing crystal will be wetted and embedded by the liquid. Such interactions will perturb the upward-growing surface crystals, to the detriment of this growth mode. Although the forgoing analysis applies to the slow-growing flanks of elongated crystals, we argue that the faster axial growth is also affected. As discussed above, the axial growth requires the lateral acquisition of molecules. Thus, disrupting the lateral mass transport in turn damages the axial growth.

### 2.5.3 Comparison of the Effects of Fluidity on Surface and Bulk Crystal Growth in Organic Glasses.

The disruption of surface crystal growth in organic glasses by fluidity is formally similar to the termination of *bulk* crystal growth under the same condition. As organic liquids are cooled to become glasses, fast crystal growth can emerge *in the bulk*.<sup>23,24</sup> This glass-to-crystal or GC mode is so fast that thousands of molecular layers join the crystal in one structural relaxation time of the liquid. Such rapid growth is in conflict with the standard view that diffusion defines the kinetic barrier for crystal growth.<sup>38,39,40</sup> GC growth is notable in its sudden activation during the cooling of liquids and disruption during the heating of glasses (see Figures 1b, 3, and 5 for the transition in IMC, NIF, and OTP). In this respect, GC growth is similar to the surface crystal growth on organic glasses in that both processes occur steadily at low temperatures and can be disrupted at sufficiently high fluidity. Both, therefore, are appropriately described as solid-state phenomena that are terminated in the liquid state.

Despite their similarity, the bulk GC growth terminates more abruptly. As a result, there exists a range of temperatures in which the bulk growth is disrupted but the surface process is still active, making possible the formation of a thin layer of surface crystals. Sun et al. argue that GC growth occurs by local oscillations at the crystal/glass interface, as in a polymorphic conversion, and is terminated if fluidity is high enough to rearrange the interface on the timescale of crystal growth.<sup>24</sup> Musumeci et al. report a quantitative condition for the existence of GC growth:  $D/u < 7$  pm, where  $D$  is bulk diffusivity and  $u$  the velocity of crystal growth.<sup>28</sup> In contrast, surface crystals grow upward on organic glasses using molecules transported by surface diffusion, and the process is disrupted at the onset of fluidity by the wetting and embedding of surface crystals.

## 1.5 Conclusion

Molecular glasses can grow crystals rapidly on their free surfaces and as we report here, the process can be disrupted as glasses are heated to become fluids. The surface crystals that grow as segregated needles ( $\alpha$  IMC, NIF, and *o*-terphenyl) are at greater risk than those that grow in compact domains ( $\gamma$  IMC). AFM showed that surface crystals rise upward as they grow laterally and produce depletion zones on the glass surface. For the needles, the depletion zones are along the slow-advancing flanks, and become wider and deeper with increasing distance from the tip. The termination of surface crystal growth on glasses is attributed to the onset of liquid flow on the timescale of crystal growth, which disrupts the upward growth of surface crystals supported by surface diffusion. Elongated growth is more endangered because the slow-advancing flanks become stationary relative to liquid flow at a low temperature. In contrast, the compact growth of  $\gamma$  IMC resists such attack, because the entire growth front advances uniformly at a speed faster than liquid flow up to a high temperature. Our results show that fast surface crystal growth on molecular glasses is inherently a solid-state phenomenon terminated in the liquid state, and that the process is sustained by surface diffusion, not viscous flow.

Further understanding of surface crystal growth will benefit from systematic studies by high-resolution microscopy, both below and above  $T_g$ , that closely follow the interaction between crystal growth and liquid flow. It would be of interest to determine the sub-surface structure of the crystals. Simulation studies would be especially valuable to understand the relationship between the velocities of surface crystal growth, the rate of surface diffusion, and the dimensions of the depletion zones. There is a remarkable similarity between the bulk GC growth and the surface crystal growth in molecular glasses, in their existence in the solid state and their

termination by fluidity, and this similarity motivates efforts to understand the two processes as a whole that differentiates under different environmental conditions.

**Acknowledgements.**

We thank the NSF (DMR-1206724) for supporting this work. EG thanks the PhRMA foundation for a postdoctoral fellowship.

**Reference:**

---

1. Debenedetti, P. G.; Stillinger, F. H. Supercooled Liquids and the Glass Transition. *Nature* **2001**, *410*, 259-267.
2. Ediger, M. D.; Harrowell, P. Perspective: Supercooled Liquids and Glasses. *J. Chem. Phys.* **2012**, *137*, 080901.
3. Yu, L. Amorphous Pharmaceutical Solids: Preparation, Characterization and Stabilization. *Adv. Drug Delivery Rev.* **2001**, *48*, 27-42.
4. Shirota, Y. Photo-and Electroactive Amorphous Molecular Materials-Molecular Design, Syntheses, Reactions, Properties, and Applications. *J. Mater. Chem.* **2005**, *15*, 75-93.
5. De Silva, A.; Felix, N. M.; Ober, C. K. Molecular Glass Resists as High-Resolution Patterning Materials. *Adv. Mater. Adv. Mater.* **2008**, *20*, 3355-61.
6. Sun, Y.; Zhu, L.; Kearns, K. L.; Ediger, M. D.; Yu, L. Glasses Crystallize Rapidly at Free Surfaces by Growing Crystals Upward. *Proc. Natl. Acad. Sci. U.S.A.* **2011**, *108*(15), 5990-5995.
7. Wu, T.; Yu, L. Surface Crystallization of Indomethacin below  $T_g$ . *Pharm. Res.* **2006**, *23*, 2350-2355.
8. Zhu, L.; Wong, L.; Yu, L. Surface-Enhanced Crystallization of Amorphous Nifedipine. *Mol. Pharm.* **2008**, *5*, 921-926.
9. Zhu, L.; Jona, J.; Nagapudi, K.; Wu, T. Fast Surface Crystallization of Amorphous Griseofulvin Below  $T_g$ . *Pharm Res* **2010**, *27*, 1558-1567.
10. Gunn, E.; Guzei, I. A.; Yu, L. Does Crystal Density Control Fast Surface Crystal Growth in Glasses? A Study with Polymorphs. *Crystal Growth & Design* **2011**, *11*, 3979-3984.
11. Cai, T.; Zhu, L.; Yu, L. Crystallization of Organic Glasses: Effects of Polymer Additives on Bulk and Surface Crystal Growth in Amorphous Nifedipine. *Pharm. Res.* **2011**, *28*, 2458-2466.
12. Stephens, R. B. Stress-Enhanced Crystallization in Amorphous Selenium Films. *J. Appl. Phys.* **1980**, *51*, 6197-6201.
13. Sallese, J. M.; Ils, A.; Bouvet, D.; Fazan, P.; Merritt, C. Modeling of the Depletion of the Amorphous-Silicon Surface during Hemispherical Grained Silicon Formation. *J. Appl. Phys.* **2000**, *88*, 5751-5755.
14. Koster, U. Surface Crystallization of Metallic Glasses. *Mat. Sci. & Eng.* **1988**, *97*, 233-239.
15. Diaz-Mora, N.; Zanutto, E. D.; Hergt, R.; Müller, R. Surface Crystallization and Texture in Cordierite Glasses. *J. Non-Crystalline Solids* **2000**, *273*, 81-93.

- 
16. Fokin, V. M.; Zanutto, E. D. Surface and Volume Nucleation and Growth in TiO<sub>2</sub>-cordierite Glasses. *J. Non-Crystalline Solids* **1999**, *246*, 115-127.
17. Wittman, E.; Zanutto, E. D. Surface Nucleation and Growth in Anorthite Glass. *J. Non-Crystalline Solids* **2000**, *271*, 94-99.
18. Schmelzer, J.; Pascova, R.; Müller, J.; Gutzow, I. Surface-Induced Devitrification of Glasses: the Influence of Elastic Strains. *J. Non-Crystalline Solids* **1993**, *162*, 23-29.
19. Wu, T.; Sun, Y.; Li, N.; de Villiers, M.; Yu, L. Inhibiting Surface Crystallization of Amorphous Indomethacin by Nanocoating. *Langmuir* **2007**, *23*, 5148-53.
20. Zhu, L.; Brian, C.; Swallen, S. F.; Straus, P. T.; Ediger, M. D.; Yu, L. Surface Diffusion of an Organic Glass. *Phys. Rev. Lett.* **2011**, *106*, 256103.
21. Brian, C. B.; Yu, L. Surface Self-Diffusion of Organic Glasses. *J. Phys. Chem. A* **2013**, *117*, 13303–13309.
22. Greet, R. J.; Turnbull, D. Glass Transition in *o*-Terphenyl. *J. Chem. Phys.* **1967**, *46*, 1243-1251.
23. Hikima, T.; Adachi, Y.; Hanaya, M.; Oguni, M. Determination of Potentially Homogeneous-Nucleation-Based Crystallization in *o*-Terphenyl and an Interpretation of the Nucleation-Enhancement Mechanism. *Phys. Rev. B* **1995**, *52*, 3900-3908.
24. Sun, Y.; Xi, H.; Chen, S.; Ediger, M. D.; Yu, L. Crystallization near Glass Transition: Transition from Diffusion-Controlled to Diffusionless Crystal Growth Studied with Seven Polymorphs. *J. Phys. Chem. B* **2008**, *112*, 5594-5601.
25. Konishi, T.; Tanaka, H. Possible Origin of Enhanced Crystal Growth in a Glass. *Phys. Rev. B* **2007**, *76*, 220201.
26. Stevenson, J. D.; Wolynes, P. G. The Ultimate Fate of Supercooled Liquids. *J. Phys. Chem. A* **2011**, *115*, 3713–3719.
27. Caroli, C.; Lemaître, A. Ultrafast Spherulitic Crystal Growth as a Stress-Induced Phenomenon Specific of Fragile Glass-Formers. *J. Chem. Phys.* **2012**, *137*, 114506.
28. Musumeci, D.; Powell, C. P.; Ediger, M. D.; Yu, L. Termination of Solid-State Crystal Growth in Molecular Glasses by Fluidity. *J. Phys. Chem. Lett.* **2014**, *5*, 1705–1710.
29. Chen, X. M.; Morris, K. R.; Griesser, U. J.; Byrn, S. R.; Stowell, J. G. Reactivity Differences of Indomethacin Solid Forms with Ammonia Gas. *J. Am. Chem. Soc.* **2002**, *124*, 15012-15019.

- 
30. Kistenmacher, T. J.; Marsh, R. E. Crystal and Molecular Structure of an Antiinflammatory Agent, Indomethacin, 1-(*p*-Chlorobenzoyl)-5-methoxy-2-methylindole-3-acetic Acid. *J. Am. Chem. Soc.* **1972**, *94*, 1340-1345.
31. Gunn, E.; Guzei, I. A.; Yu, L. Polymorphism of Nifedipine: Structure and Reversible Transformation of  $\beta$  Polymorph. *Crystal Growth and Design* **2012**, *12*, 2037–2043.
32. Aikawa, S.; Marayama, Y.; Ohashi, Y.; Sasada, Y. 1,2-Diphenylbenzene (*o*-Terphenyl). *Acta crystallogr. B*, **1978**, *34*, 2901-2904.
33. Wu, T.; Yu, L. Origin of Enhanced Crystal Growth Kinetics near  $T_g$  Probed with Indomethacin Polymorphs. *J. Phys. Chem. B* **2006**, *110*, 15694-15699.
34. Ishida, H.; Wu, T.; Yu, L. Sudden Acceleration of Crystal Growth of Nifedipine near  $T_g$  without and with Polyvinylpyrrolidone. *J. Pharm. Sci.* **2007**, *96*, 1131-1138.
35. Andrews, J. N.; Ubbelohde, A. R. Melting and Crystal Structure: The Melting Parameters of Some Polyphenyls. *Proc. R. Soc. A* **1955**, *228*, 435-447.
36. Ping, W.; Paraska, D.; Baker, R.; Harrowell, P.; Angell, C. A. Molecular Engineering of the Glass Transition: Glass-forming Ability across a Homologous Series of Cyclic Stilbenes. *J. Phys. Chem. B*, **2011**, *115*, 4696-4702.
37. Magill, J. H.; Li, H. M. Physical Properties of Aromatic Hydrocarbons V. The Solidification Behavior of 1:2 Diphenylbenzene. *J. Cryst. Growth* **1973**, *20*, 135-144.
38. Ngai, K. L.; Magill, J. H.; Plazek, D. J. Flow, Diffusion and Crystallization of Supercooled Liquids: Revisited. *J. Chem. Phys.* **2000**, *112*, 1887-1892.
39. Mapes, M. K.; Swallen, S. F.; Ediger, M. D. Self-diffusion of Supercooled *o*-Terphenyl near the Glass Transition Temperature. *J. Phys. Chem. B* **2006**, *110*, 507-511.
40. Ediger, M. D.; Harrowell, P.; Yu, L. Crystal Growth Kinetics Exhibit a Fragility-Dependent Decoupling from Viscosity. *J. Chem. Phys.* **2008**, *128*, 034709.
41. Xi, H.; Sun, Y.; Yu, L. Diffusion-controlled and Diffusionless Crystal Growth in Liquid *o*-Terphenyl near Its Glass Transition Temperature. *J. Chem. Phys.* **2009**, *130*, 094508.
42. Mullins, W. Flattening of a Nearly Plane Solid Surface due to Capillarity. *J. App. Phys.* **1959**, *30*, 77-83.
43. Sears, G. W. A Growth Mechanism for Mercury Whiskers. *Acta Metallurgica* **1955**, *3*, 361-366

---

44. Daley, C. R.; Fakhraai, M. D.; Ediger, M. D.; Forrest, J. A. Comparing Surface and Bulk Flow of a Molecular Glass Former. *Soft Matter* **2012**, *8*, 2206-2212.

45. Wojnarowska, Z.; Adrjanowicz, K.; Włodarczyk, P.; Kaminska, E.; Kaminski, K.; Grzybowska, K.; Wrzalik, R.; Paluch, M.; Ngai, K. L. Broadband Dielectric Relaxation Study at Ambient and Elevated Pressure of Molecular Dynamics of Pharmaceutical: Indomethacin. *J. Phys. Chem. B* **2009**, *113*, 12536-12545.

46. Goresy, T. E.; Böhmer, R. Dielectric Relaxation Processes in Solid and Supercooled Liquid Solutions of Acetaminophen and Nifedipine. *J. Phys.: Condens. Matter* **2007**, *19*, 205134.

47. Plazek, D. J.; Bero, C. A.; Chay, I.-C. The Recoverable Compliance of Amorphous Materials. *J. Non-Cryst. Solids* **1994**, *172-174*, 181 – 190.

48. Friz, G.; Vossen, H. Density and Surface-Tension Measurements of Pure Polyphenyls and Some Polyphenyl Mixtures. *European Atomic Energy Community - Euratom* **1963**. EUR165.e

## **Chapter 3**

# **Fast Surface Crystallization of Molecular Glasses: Creation of Depletion Zones by Surface Diffusion and Crystallization Flux**

Mariko Hasebe, Daniele Musumeci, and Lian Yu

Department of Chemistry and School of Pharmacy

University of Wisconsin – Madison, Madison, WI, 53705

As published in

Journal of Physical Chemistry B, Volume 119 (7), Pages 3304-3311, 2015

### 3.1 Abstract

Molecular glasses can grow crystals much faster at the free surface than in the interior. A property of this process is the creation of depressed grooves or depletion zones around the crystals on the initially flat amorphous surface. With scanning electron microscopy and atomic force microscopy, we studied this phenomenon in indomethacin, which crystallizes in two polymorphs ( $\alpha$  and  $\gamma$ ) of different morphologies. The observed depletion zones are well reproduced by the known coefficients of surface diffusion and the velocities of crystal growth. At the slow-growing flanks of needle-like  $\alpha$  IMC crystals, depletion zones widen and deepen over time according to the expected kinetics for surface diffusion responding to a crystallization flux. Before fast-advancing growth fronts, depletion zones have less time to develop; their steady-state dimensions agree with the same model revised for a moving phase boundary. These results support the view that surface diffusion enables fast surface crystal growth on molecular glasses. Our finding helps understand crystal growth in thin films in which the formation of deep depletion zones can cause de-wetting and alter growth kinetics.

### 3.2 Introduction

Glasses are remarkable materials that combine the mechanical strength of crystals and the spatial uniformity of liquids, making them useful in many areas of science and technology.<sup>1,2</sup> Although familiar glasses are inorganic and polymeric, there has been growing interest in the glasses of small organic molecules for bio-preservation, drug delivery, and electronics.<sup>3,4,5</sup> In these applications, an amorphous material must resist crystallization since crystallization negates its advantages.

Recent work has observed surprising features of crystallization in molecular glasses. For example, as molecular liquids are cooled to become glasses, the velocity of crystal growth can abruptly increase from being limited by bulk diffusion to vastly exceeding such limit.<sup>6,7,8,9,10,11</sup> This fast growth mode has been called the glass-to-crystal or GC mode. In the presence of a free surface, even faster crystal growth can occur,<sup>12,13,14,15,16,17</sup> causing crystals to grow much faster along the surface than into the interior. At present, GC growth is known only for molecular glasses, and while fast surface crystal growth is reported for amorphous Se<sup>18</sup> and Si,<sup>19</sup> the phenomenon is apparently absent in metallic glasses<sup>20</sup> and the reports differ on silicate glasses.<sup>21,22,23,24,25</sup>

Several features of surface crystal growth on molecular glasses are worth noting. Surface crystals rise upward as they grow laterally<sup>12</sup> and are surrounded by depressed grooves or depletion zones that form on the initially flat amorphous surface.<sup>17</sup> The process of surface crystal growth is halted by a thin coating (e.g., 10 nm of gold or a few nm of polymer).<sup>26</sup> For the glasses of indomethacin and nifedipine, the velocity of surface crystal growth is proportional to the diffusivity of surface molecules independently measured through the decay of surface gratings.<sup>27,28</sup> Furthermore, the active growth of surface crystals in the glassy state is disrupted if the glasses are heated to become fluids.<sup>17</sup> Fast surface crystal growth has been attributed to the high mobility of surface molecules.<sup>12</sup> In this model, surface molecules diffuse to join upward-growing crystals layer-by-layer. Surface crystallization has also been attributed to the easier release of crystallization-induced tension at the free surface.<sup>29</sup>

This study concerns a key feature of surface crystal growth on molecular glasses – the depletion zones around surface crystals created on the initially flat glass surface. This feature is diagnostic of the mechanism of molecular transport that grows surface crystals. We used

scanning electron microscopy (SEM) and real-time atomic force microscopy (AFM) to study the phenomenon in the system indomethacin (IMC). This system is especially rich because two polymorphs ( $\alpha$  and  $\gamma$ ) can produce surface crystals of different morphologies, with depletion zones developing around them on different timescales and to different dimensions. We report that the observed depletion zones agree well with those expected for the combined action of surface diffusion and crystal growth. For the slow-growing flanks of needle-like  $\alpha$  IMC crystals, the depletion zone widens and deepens over time, in a manner consistent with surface diffusion responding to a crystallization flux. On the other hand, the depletion zone has limited time to develop before a fast-advancing growth front, and its steady-state dimension agrees well with the same model adapted for a moving phase boundary. We obtain self-consistent crystallization fluxes from the evolution of depletion zones and the growth velocities of surface crystals. These results argue that surface crystal growth on molecular glasses is enabled by surface diffusion. The phenomena studied here have much in common with the formation of surface grooves in other processes: the growth of hemispherical crystals on amorphous silicon,<sup>19</sup> the development of grain boundaries in polycrystals,<sup>30,31</sup> and the evolution of polymer surfaces.<sup>32</sup>

### 3.3 Materials and methods

Indomethacin (1-(*p*-chlorobenzoyl)-5-methoxy-2-methylindole-3-acetic acid, 99+%,  $\gamma$  polymorph) was purchased from Sigma-Aldrich. To prepare a sample for studying surface crystal growth, indomethacin was melted on a clean coverslip at 15 K above the melting point and covered with a smaller coverslip (typically round, 15 mm in diameter). The assembly was cooled to below  $T_g$  by contact with a metal block pre-equilibrated at room temperature. The sample was confirmed to be free of crystals by polarized light microscopy. The larger coverslip

was detached by bending its edges away from the sample, which creates a glass film with a free surface. The films were 10 – 100  $\mu\text{m}$  thick. Surface crystals were nucleated at 313 K in approximately two days and if necessary, the sample was transferred to a chosen temperature to follow further growth. To favor a particular polymorph ( $\alpha$  or  $\gamma$ ), seeding was sometimes used. Polymorphs were identified by x-ray diffraction (Bruker D8 Advance diffractometer with Cu  $K\alpha$  radiation) and Raman microscopy (Thermo DXR, excitation wavelength 532 nm).

SEM analysis was performed with a field-emission LEO 1530 low-voltage and high-resolution SEM operated at 6 KV and 12-14 mm working distance using an in lens secondary electron detector. Prior to SEM analysis, the sample was coated with a gold film 10 nm thick (Denton Vacuum Desk II, Denton Vacuum, Moorestown, NJ; 50 mTorr pressure, 45 mA current, and 30 s deposition). The gold film stopped surface crystal growth and prevented charging during SEM analysis. To further prevent charging, the sample was attached to a metal stub with a carbon tape. For the cross-sectional view of a sample, the substrate coverslip was previously scored with a carbide knife and just before analysis, the sample was snapped in half and coated with gold. The IMC glass had clean brittle fractures.

Real-time AFM was performed with a Veeco Multimode IV Scanning Probe Microscope in the tapping mode under  $\text{N}_2$  purge. An AFM hostage was used to control temperature; it was calibrated against the melting point of *o*-terphenyl (329 K). According to the manufacturer, the AFM tip (300Al-G10, BudgetSensors) had a tip radius of 10 nm and half-cone angle of 20-25° (10° at apex).

### 3.4 Results

Two polymorphs can grow on the surface of an IMC glass:  $\alpha$  and  $\gamma$ . These polymorphs have different structures<sup>33,34</sup> and growth morphologies, enabling observations of different depletion zones that develop at growth fronts that are nearly stationary or fast moving.

#### 3.4.1 $\alpha$ IMC

Figure 1 shows SEM and real-time AFM images of  $\alpha$  IMC crystals on the surface of IMC glasses. At the temperatures of this study (300 – 317 K), these crystals grow steadily as needles that rise above the glass surface.<sup>12</sup> The side view of surface crystals (Figure 1b) shows that the tip of an  $\alpha$  IMC needle is raised above the glass surface, a feature invisible to the AFM tip scanning from above. In cross sections (Figure 1c and 1d), we see that the crystals do not grow significantly into the interior of the glass and are surrounded by depressed grooves or depletion zones.

Real-time AFM obtained the velocities of crystal growth; for the crystal in Figure 1e,  $u_z = 0.9$  nm/s in the axial direction. As implied by the needle morphology, axial growth is much faster than lateral growth,  $u_z \gg u_x$ . The axial growth velocities from AFM agree with the reported growth velocities measured by optical microscopy.<sup>12,13,17</sup>

Figure 2 shows the typical width  $w$  and height  $H$  of  $\alpha$  IMC needles. Both are several hundred nanometers and both increase slightly with the distance to the tip. The  $H$  reported here is relative to the flat glass surface far from the crystal; its value would be greater if measured from the depressed glass surface immediately next to the crystal. In determining the width of a needle-like crystal, SEM is more accurate than AFM, since the crystal can rise sharply above the glass surface (Figure 1), causing the AFM tip, with its finite cone angle, to overestimate the crystal

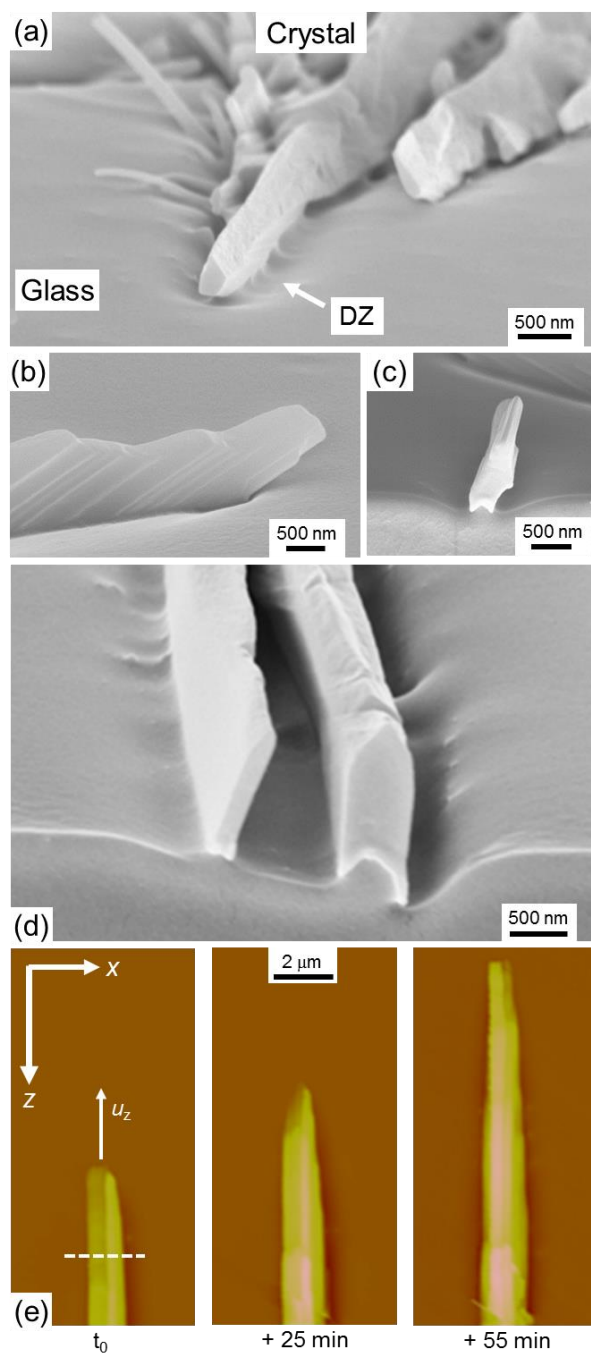


**Figure 1.** (a-d) SEM images of  $\alpha$  IMC surface crystals grown at 300 – 317 K. “DZ”: depletion zone. (e) Real-time AFM images at 317 K. Color scale = 1200 nm in height. The dotted line illustrates the measurement of depletion zone profiles (Figure 3a).

width. On the other hand, AFM is more accurate than SEM for measuring the height of crystals, since SEM relies on side-view observations at uncertain angles.

Consistent with the previous finding,<sup>17</sup> we observed depletion zones around  $\alpha$  IMC surface crystals on the initially flat glass surface. In cross-sectional views (Figure 1d), SEM shows that the depletion zone descends as it approaches the flank of an  $\alpha$  IMC needle, approximately reaching a local minimum at the intersection. Figure 3a shows the typical profiles of depletion zones from AFM, measured normal to the needle axis at different distances  $z$  to the tip (see the dotted line in Figure 1e). These profiles are truncated near the crystal edge ( $x = 0$ ). We see that the depletion zone becomes wider and deeper with increasing distance to the tip. This enlargement of the depletion zone is also observable at the same position on the glass surface upon comparing the AFM images recorded at different times. As we discuss later, the evolution of the depletion zone is well explained by surface diffusion responding to a crystallization flux.

Because the crystal can rise sharply over the glass surface (Figure 1), the AFM tip, with its finite cone angle, cannot always find the exact location of a crystal/glass boundary ( $x = 0$ ). To locate this boundary, SEM images were a valuable aid and independent check on the AFM data. SEM reports the accurate width of a needle-like crystal (Figure 2a), as well as the widths of depletion zones. Meanwhile, an AFM scan across the needle accurately determines the height profile and the total width of the perturbed glass surface (the two depletion zones flanking the needle). From these two techniques, we obtain the crystal/glass boundary for an AFM depletion-zone profile.

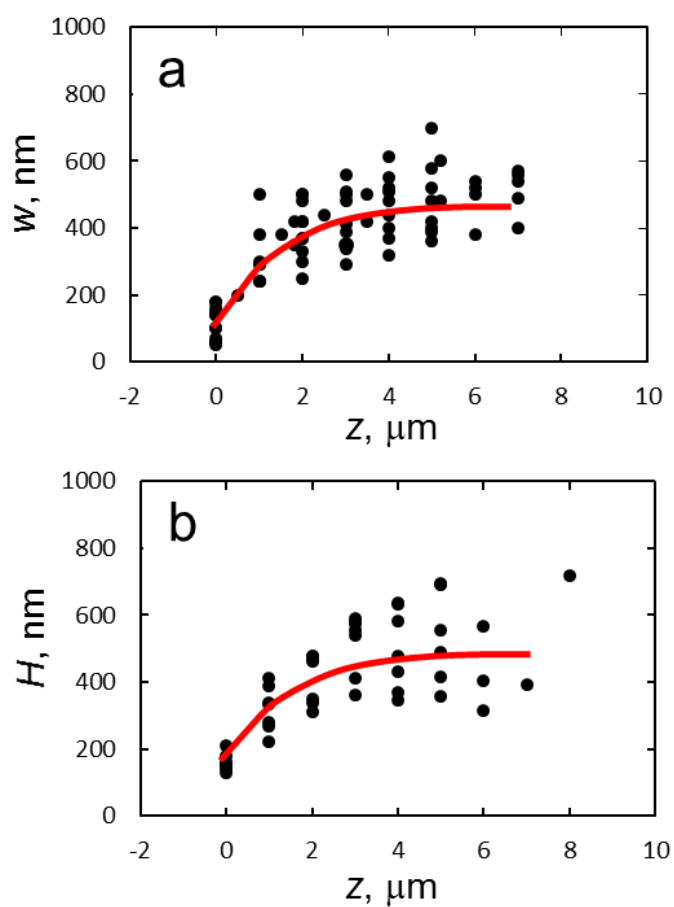


**Figure 2.** Typical width (a) and height (b) of  $\alpha$  IMC surface crystals versus distance  $z$  to the tip, measured by SEM and AFM, respectively. The temperature range was 300 – 317 K, with no strong dependence on temperature noted.

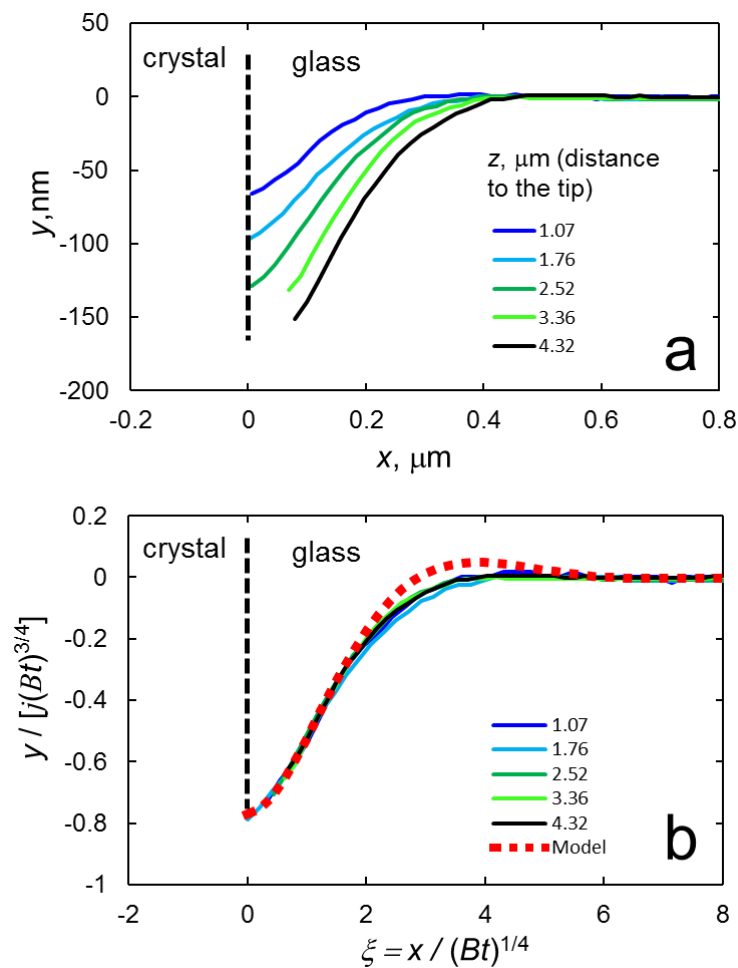


**Figure 3.** (a) Depletion zone profiles at 317 K near an  $\alpha$  IMC crystal along  $x$  (direction of slow growth) at different distances  $z$  to the tip. The actual crystal is in Figure 1e. (b) Scaling the depletion-zone profiles according to eq. (6) [ $x$  by  $(Bt)^{1/4}$  and  $y$  by  $j(Bt)^{3/4}$ ] yields a master curve, which agrees reasonably well with the model (red dotted line).

### 3.4.2 $\gamma$ IMC

This polymorph grows in compact domains, in contrast to the segregated needles of  $\alpha$  IMC. Surface crystals of  $\gamma$  IMC also rise above the glass surface as they grow laterally, but not as high as those of  $\alpha$  IMC. Consistent with the previous report,<sup>17</sup> SEM in cross sections found a small depletion zone before the  $\gamma$  IMC growth front (Figures 4a/b). The depletion zone approximately reaches a minimum at the intersection with the crystal. Real-time AFM measurements (Figure 4c) also detected this feature before steadily advancing growth fronts. Figure 5 shows the typical profiles of the depletion zone in the direction of crystal growth (dotted lines in Figure 4c). The dimensions of the depletion zone are independent of time. In the case of  $\gamma$  IMC, the “tall crystal” problem encountered in the AFM analysis of  $\alpha$  IMC is less severe, allowing the AFM tip to locate the crystal/glass interface. Real-time AFM also yielded the growth velocities of  $\gamma$  IMC surface crystals, which agree with those from optical microscopy;<sup>17</sup> for the crystal in Figure 4c,  $u = 0.9$  nm/s at 317 K. As we discuss later, the depletion zones are well explained by surface diffusion near a moving interface responding to crystal growth.

In cross-sectional views, SEM revealed significant subsurface growth of  $\gamma$  IMC concurrent with surface growth. This bulk growth is faster for  $\gamma$  IMC than for  $\alpha$  IMC, and has been called the glass-to-crystal (GC) growth mode.<sup>11</sup> Despite the more active bulk growth, however, the surface growth of  $\gamma$  IMC still well outpaces the bulk process.

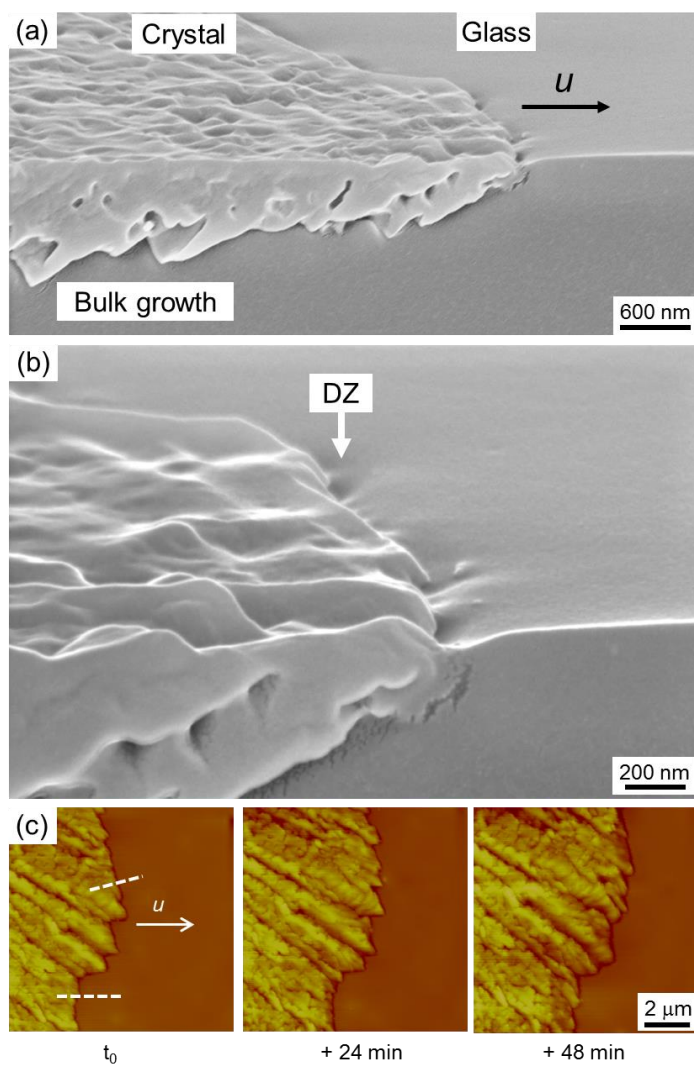


**Figure 4.** (a, b) SEM images of  $\gamma$  IMC surface crystals (313 K). “DZ”: depletion zone. (c) Real-time AFM images vs time at 317 K. Color scale = 300 nm in height. The dotted lines illustrate the measurement of depletion-zone profiles.

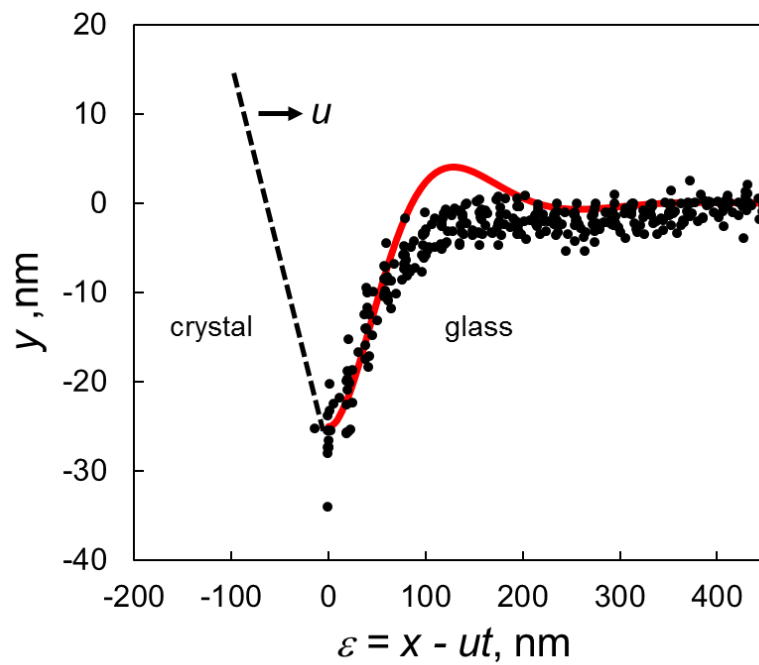


**Figure 5.** Depletion zone profiles before  $\gamma$  IMC growth front at 317 K (solid circles) and the profile predicted by a model (eq. (14); red line). The profiles refer to the advancing growth front.

### 3.5 Discussion

This work has characterized the surface crystals growing on the molecular glass IMC by high-resolution microscopy and the surrounding depletion zones. Surface crystals rise above the local amorphous surface and are surrounded by depletion zones whose dimensions depend on the velocities of crystal growth. Before slow-advancing growth fronts, depletion zones enlarge over time; before fast-advancing growth fronts, our experiments observed depletion zones of constant dimensions. We show below that these observations are well explained by the known coefficients of surface diffusion and kinetics of crystal growth.

#### 3.5.1 Depletion zones along slow-advancing flanks of $\alpha$ IMC needles.

We first consider the depletion zones along the slow-growing flanks of an  $\alpha$  IMC needle. The depletion zone around the fast-advancing tip will be discussed later, because a different analysis is required. We model each depletion-zone profile measured normal to the needle axis (Figure 6) as a one-dimensional problem and as the result of surface diffusion in response to a crystallization flux. We assume the side wall of the crystal is stationary, a reasonable assumption given the slow lateral growth. If the cross-section is distance  $z$  to the tip, the depletion zone has the time  $t = z/u_z$  to develop, where  $u_z$  is the velocity of crystal growth *in the needle direction*.

The equation for the evolution of a one-dimensional surface profile,  $y(x,t)$ , by surface diffusion is:<sup>35</sup>

$$\frac{\partial y}{\partial t} + B y'''' = 0 \quad (1)$$

where  $B = \frac{D_s \gamma \Omega^2 \nu}{kT}$ ,  $D_s$  is the surface diffusion coefficient,  $\gamma$  the surface tension,  $\Omega$  the molecular volume, and  $\nu$  the number of molecules per unit area. Eq. (1) holds under the small-slope

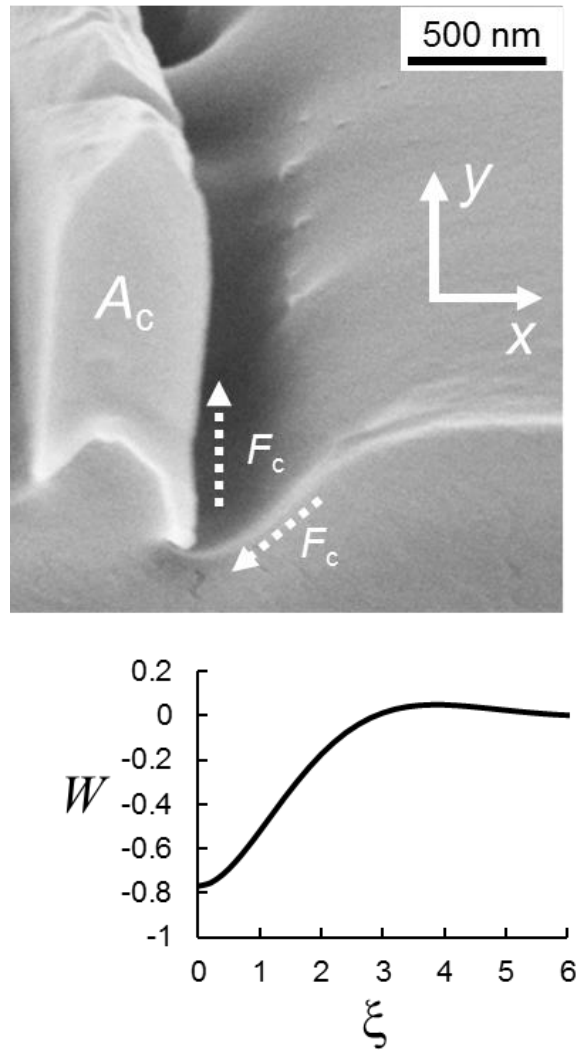


**Figure 6.** Model for the depletion zone along the side of an  $\alpha$  IMC needle.  $F_c$  is crystallization flux.  $A_c$  is the area of the needle's cross section.

assumption ( $y' \sim 0$ ). Zhu et al. have measured the values of  $B$  for IMC glasses using the method of surface-grating decay.<sup>27</sup>

For the evolution of the glass surface along the side of an  $\alpha$  IMC needle, we introduce the following boundary conditions:

$$y(x, 0) = 0 \quad (2)$$

$$y(\infty, t) = 0 \quad (3)$$

$$y'(0, t) = 0 \quad (4)$$

$$y'''(0, t) = j = \frac{F_c \Omega}{B} \quad (5)$$

Condition (2) states that the glass surface is initially flat. Condition (3) states that the glass surface is flat far away from a surface crystal. Condition (4) sets the slope of the glass surface to zero at the boundary with the crystal, to be consistent with experimentally observed surface profiles. Condition (5) specifies the flux of molecules that leave the glass surface to join the crystal;  $F_c$  is the number flux in the unit of molecules/m/s and  $F_c \Omega$  is the volume flux in  $\text{m}^3/(\text{m}\cdot\text{s})$ . The “scaled flux”  $j$  is introduced for mathematical convenience. Sallese et al. defined a similar model for the depletion zone near a hemispherical surface crystal on amorphous silicon.<sup>19</sup> Their model differs from ours in that in place of our Condition (4), they write  $y(0, t) = 0$ ; that is, they assume that the base of the hemispherical crystal remains at the level of the original amorphous surface (this condition is somewhat at odds with their TEM images of the crystals.)

The problem defined by eqs. (1-5) has been solved by Genin et al. in a different context.<sup>30</sup> In that solution, the process under study is the formation of grain-boundary (GB) grooves by surface diffusion in the presence of a matter flux into or out of the GB. Mathematically, that problem is defined in the same way as our crystal growth problem, and the solution is:

$$y(x, t) = j(Bt)^{3/4}W(\xi) \quad (6)$$

where  $\xi = \frac{x}{(Bt)^{1/4}}$  is a scaled distance and the function  $W(\xi)$  is plotted in Figure 6.

Eq. (6) implies that the depletion-zone profiles reduce to the curve  $W(\xi)$  if  $x$  is scaled by  $(Bt)^{1/4}$  and  $y$  by  $[j(Bt)^{3/4}]$ . This self-similarity is indeed observed in our system. For a series of depletion-zone profiles at  $z = 1 - 4 \mu\text{m}$  from the tip (Figure 3), the scaling collapses them to a single master curve that agrees reasonably well with  $W(\xi)$ . Note that for this scaling, we use the experimental value of  $B$  from surface-grating decay ( $10^{-31.4} \text{ m}^4/\text{s}$ ),<sup>27</sup> and the experimental value of  $u_z$  from real-time AFM (0.9 nm/s). This consistency argues that surface diffusion responding to a crystallization flux quantitatively explains the evolution of the depletion zones near surface crystals. From this analysis, the volume flux of crystallization is estimated to be  $F_c \Omega = 6 \text{ nm}^3/(\text{nm}\cdot\text{s})$ .

There is a disagreement in Figure 3b between the scaled experimental profiles and the function  $W(\xi)$  at the “overshoot”. The model predicts a profile of damped oscillations, which is not observed experimentally. In the surface crystal growth on amorphous silicon, Sallese et al. noted a similar discrepancy between the observed and predicted depletion-zone profiles.<sup>19</sup> The oscillatory profile, however, was observed in the evolution of grain-boundary grooves and polymer surfaces.<sup>32</sup>

The foregoing analysis applies only to the region  $1 \mu\text{m}$  behind the tip of an  $\alpha$  IMC needle. This is necessary because the tip of the crystal is raised over the glass surface, with the overhang being approximately  $1 \mu\text{m}$ . The tip advances more rapidly, requiring a different treatment than the one described above but similar to that for  $\gamma$  IMC (see below).

The crystallization flux just obtained from the evolution of the depletion zone,  $6 \text{ nm}^3/(\text{nm}\cdot\text{s})$ , can be tested against the flux estimated from crystal growth rates. If each flank of an  $\alpha$  IMC

needle receives the volume flux  $F_c \Omega$ , the area of the needle's cross section  $A_c$  (Figure 6) should increase with its distance to the tip as

$$F_c \Omega = \frac{u_z}{2} \frac{dA_c}{dz} \quad (7)$$

To see eq. (7), consider two vertical slices of an  $\alpha$  IMC needle of width  $h$  and distance  $dz$  apart. The slice further from the tip has the additional time  $dz/u_z$  to receive the flux, collecting  $2hF_c dz/u_z$  more molecules, where the factor 2 reflects the two flanks of the needle. The volume difference between the two slices is then  $h dA_c = 2\Omega h F_c dz/u_z$ , from which eq. (7) follows. We evaluate  $dA_c/dz$  from the AFM height profiles of surface crystals (Figure 1e) and obtain  $F_c \Omega = 12 \text{ nm}^3/(\text{nm}\cdot\text{s})$  at 317 K, which is in fair agreement with the value from the evolution of depletion zones.

### 3.5.2 Depletion zones near $\gamma$ IMC surface crystals.

In contrast to the slow-growing flanks of  $\alpha$  IMC needles, the growth front of  $\gamma$  IMC surface crystals advances uniformly and rapidly. Before a fast-advancing growth front, a depletion zone has less time to develop, before being overrun by the crystal. Experimentally, we observe a steady-state profile of the depletion zone before the growth front (Figure 4). To model this depletion zone, we seek a steady-state solution of Mullins's equation of surface diffusion (eq. 1) for a moving phase boundary subject to a crystallization flux. For this problem, eq. (1) is rewritten in the moving reference frame  $\varepsilon = x - ut$ , where  $u$  is the velocity of crystal growth, to read:<sup>36</sup>

$$By'''' - uy' + \frac{\partial y}{\partial t} = 0 \quad (9)$$

At the steady-state,  $\frac{\partial y}{\partial t} = 0$  and Eq. (9) becomes an ordinary differential equation for  $y(\varepsilon)$ :

$$y'''' - \alpha^3 y' = 0 \quad (10)$$

where  $\alpha^3 = u/B$ .

We subject Eq. (10) to the following the boundary conditions:

$$y(\infty) = 0 \quad (11)$$

$$y'(0) = 0 \quad (12)$$

$$y'''(0) = j = \frac{F_c \Omega}{B} \quad (13)$$

Condition (11) states that the glass surface is flat far away from the crystal. Condition (12) sets the slope of the glass surface to zero where it meets the crystal, which is consistent with the experimental profile. Condition (13) specifies the flux of crystallization.

The solution of (10) subject to (11)-(13) is

$$y = \frac{2}{\sqrt{3}} \frac{j}{\alpha^3} \exp(-\alpha \varepsilon / 2) \cos\left(\frac{\sqrt{3}}{2} \alpha \varepsilon - \frac{\pi}{6}\right) \quad (14)$$

The shape of the predicted depletion-zone profile is shown in Figure 7 as a plot of  $y/[-2j/(\sqrt{3} \alpha^3)]$  vs  $\alpha \varepsilon$ . Note that eq. (10) has been solved by Genin<sup>37</sup> and by Sekerka et al.<sup>30</sup> under other boundary conditions in their treatment of traveling grain-boundary grooves in the presence of a matter flux. Their problems are mathematically similar to our crystal growth problem, but the solutions differ owing to different boundary conditions.

To apply eq. (14) to model the surface growth of  $\gamma$  IMC, we again use the experimental data  $B = 10^{-31.4} \text{ m}^4/\text{s}$ ,<sup>27</sup> and  $u = 0.9 \text{ nm/s}$ . The predicted depletion-zone profile is overlain in Figure 5 with the observed. The prediction agrees reasonably well with the experimental data. From this analysis, we obtain  $F_c \Omega = 27 \text{ nm}^3/(\text{nm}\cdot\text{s})$  for the volume flux of crystallization. The latter value is larger than that for the flanks of an  $\alpha$  IMC needle ( $6 \text{ nm}^3/\text{nm}\cdot\text{s}$ ), a difference we shall discuss

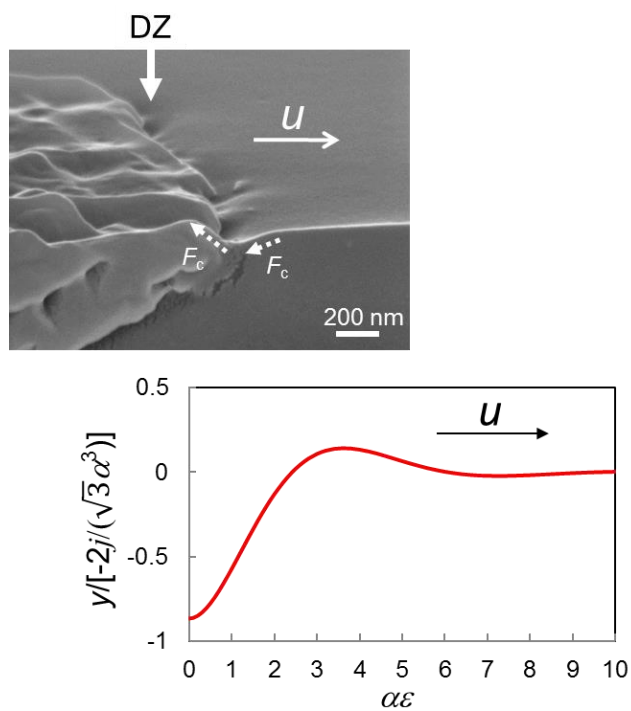


**Figure 7.** A model for the steady-state depletion zone before the growth front of  $\gamma$  IMC.  $F_c$  is crystallization flux;  $u$  is growth-front velocity. The negative sign before  $2j$  corresponds to removing molecules from the glass surface, creating a depressed groove.

later. Note that as in the case of  $\alpha$  IMC, there is a disagreement at the “overshoot” for  $\gamma$  IMC as well.

The crystallization flux just obtained from the depletion zone ( $27 \text{ nm}^3/\text{nm}\cdot\text{s}$ ) can be tested against the flux implied by the velocity of crystal growth. For a section of the growth front of length  $L$  and height  $H$  advancing at velocity  $u$ , the crystal volume increases at the rate  $uHL$ , implying the volume flux of crystallization is

$$F_c \Omega = uH \quad (15)$$

At 317 K,  $u = 0.9 \text{ nm/s}$ ,  $H \approx 40 \text{ nm}$  (average height of the  $\gamma$  IMC growth front), we obtain  $F_c \Omega = 36 \text{ nm}^3/(\text{nm}\cdot\text{s})$ , in reasonable agreement with the crystallization flux for  $\gamma$  IMC from the depletion zone.

### 3.5.3 Depletion zones around the fast-growing tips of $\alpha$ IMC needles.

The depletion zone before the tip of an  $\alpha$  IMC needle must be treated separately from that along its sides. The fast tip growth suggests a similar treatment to that just described for  $\gamma$  IMC. The present situation, however, is less well characterized experimentally, since the raised tip of an  $\alpha$  IMC needle blocks the access of an AFM tip to the region of the expected depletion zone. The limited data from SEM suggest that the depletion zone before the tip has roughly the same dimensions as that before the growth front of  $\gamma$  IMC. We speculate that the similarity exists because the two situations are characterized by similar growth-front velocities and crystallization fluxes. That the two polymorphs should have similar crystallization fluxes (in their fast growing directions) is reasonable because across the crystal/glass interface, there should be similar chemical-potential gradients and similar molecular mobilities. The two situations differ slightly

in that the tip of an  $\alpha$  IMC needle probably grows by collecting molecules from the glass surface around the tip, not just in front of it.

Our study finds that the crystallization flux at the side of an  $\alpha$  IMC needle is significantly lower than that at the growth front of  $\gamma$  IMC and probably at the tip of  $\alpha$  IMC. We attribute this difference to the different growth velocities of crystal faces. The flank of an  $\alpha$  IMC needle advances more slowly than the tip because of its lower surface energy. We imagine that both the tip and the flank receive the same flux of molecules, but only at the tip can the molecules quickly join the crystal. The side surface of an  $\alpha$  IMC needle is slower to incorporate incoming molecules into its lattice and may return some of them to the amorphous surface, leading to lower net fluxes.

The upward growth of surface crystals on molecular glasses is superficially similar to the growth of whiskers off a solid material, but is in fact quite different. Metal whiskers can grow from a vapor phase, which deposits atoms to the side surface of a whisker,<sup>38</sup> tin whiskers can be extruded from a solid material as a mechanism of stress release.<sup>39</sup> These processes differ from surface crystal growth on molecular glasses, in which molecules join the crystals by surface diffusion, creating characteristic depletion zones on the amorphous surface. It is also noteworthy that not all surface crystals on molecular glasses resemble whiskers; for example,  $\gamma$  IMC grows compact domains.

It seems possible to develop an alternative explanation for the depletion zones around surface crystals reported here, in which surface viscous flow, as opposed to surface diffusion, supplies molecules to growing crystals. Assuming that there exists a low-viscosity surface layer that obeys Stokes equations in the lubrication approximation with no slip from the underlying bulk material, Chai et al. derived an equation for surface evolution that is mathematically equivalent

with Mullins' equation for surface diffusion (eq. 1).<sup>32</sup> While Mullins' model defines surface diffusion as involving only the top layer of molecules, Chai et al.'s model invokes a fluid surface layer of unspecified thickness. Further studies, perhaps by simulations, are warranted to determine which model better describes the surface evolution of molecular glasses, including surface crystal growth and the decay of surface gratings.

### 3.6 Conclusions

Molecular glasses can grow crystals much faster at the free surface than in the interior, a phenomenon uncommon for other glasses. A key property of this process is the formation of depressed grooves or depletion zones near the crystals on the initially flat amorphous surface. With scanning electron microscopy and real-time atomic force microscopy, we studied this phenomenon in indomethacin, which crystallizes in two polymorphs ( $\alpha$  and  $\gamma$ ) of different morphologies. The observed depletion zones are quantitatively reproduced by the combined action of surface diffusion and crystal growth. Near the slow-advancing growth fronts, depletion zones widen and deepen over time, and their evolution follows the expected kinetics for surface diffusion responding to crystallization fluxes. Before fast-advancing growth fronts, depletion zones attain steady-state dimensions, which are predicted by the same model adapted for a moving phase boundary. These results strongly support the view that fast surface crystal growth on molecular glasses occurs by surface diffusion.

Better understanding of mass transport responsible for surface crystal growth will benefit from studying other systems and testing the generality of the conclusions reached here. Of the molecular glasses capable of fast surface crystal growth, indomethacin has relatively slow growth and exhibits polymorphism. The slow growth enables observations at high resolution,

while the polymorphism gives access to different growth morphologies and growth-front velocities. Surface crystals grow faster on the glasses of nifedipine and *o*-terphenyl,<sup>17</sup> and the study of these systems will require faster microscopy and can provide a fuller test of the models proposed here. It is also of interest to apply high-resolution microscopy to examine the disruption of surface crystal growth at the onset of liquid flow<sup>17</sup> to understand the mechanism by which solid-state crystal growth terminates in the liquid state.

Although our experiments were performed with bulk glass films (ca. 100  $\mu\text{m}$  thick), our results are relevant for understanding crystal growth in thin glass films, where the formation of depletion zones could lead to de-wetting and altered growth kinetics. Sun et al. reported that with decreasing thickness, surface crystal growth can slow down in a glass film of indomethacin.<sup>12</sup> The effect is more pronounced for  $\alpha$  IMC than for  $\gamma$  IMC; in films thinner than 100 nm, the growth of needle-like  $\alpha$  IMC crystals exposes regions of bare substrate. It is noteworthy that slower growth is observed even in films a few hundred nanometers thick, despite the expectation that fast surface diffusion occurs in a mobile layer a few nanometers thick. This effect can be explained by the creation of depletion zones around surface crystals. With increasing distance to the tip, the depletion zones flanking an  $\alpha$  IMC needle can become several hundred nanometers deep. Once a depletion zone is deep enough to reach the substrate, de-wetting can occur, and the exposed region can expand with further crystal growth. If the de-wetted region reaches the growth tip, its fast growth could be halted. The shallower depletion zones before  $\gamma$  IMC surface crystals explain their relative immunity to the decrease of film thickness. It would be of interest to test these ideas by real-time AFM.

We have studied the formation of depletion zones in the context of understanding surface crystal growth on molecular glasses. This phenomenon has much in common with other

processes that create surface grooves by a combined action of surface diffusion and matter flux; for example, the growth of hemispherical crystals on amorphous silicon<sup>19</sup> and the evolution of grain boundaries in polycrystals.<sup>30,31</sup> Having received similar treatments, these phenomena can collectively report the success and shortcomings of current models. For example, while the models predict mildly oscillating surface contours as a consequence of crystal growth supported by surface diffusion, such features are not observed for the process on amorphous silicon<sup>19</sup> and indomethacin, though they are sometimes observed in grain-boundary grooves. There is room for future work to achieve a better agreement between theory and experiment.

**Acknowledgements.**

We thank the NSF (DMR-1206724) for supporting this work and M.D. Ediger for helpful discussion.

**References:**

- 
1. Debenedetti, P. G.; Stillinger, F. H. Supercooled Liquids and the Glass Transition. *Nature* **2001**, *410*, 259-267.
  2. Ediger, M. D.; Harrowell, P. Perspective: Supercooled Liquids and Glasses. *J. Chem. Phys.* **2012**, *137*, 080901.
  3. Yu, L. Amorphous Pharmaceutical Solids: Preparation, Characterization and Stabilization. *Adv. Drug Deliv. Rev.* **2001**, *48*, 27-42.
  4. Shirota, Y. Photo-and Electroactive Amorphous Molecular Materials-Molecular Design, Syntheses, Reactions, Properties, and Applications. *J. Mater. Chem.* **2005**, *15*, 75-93.
  5. De Silva, A.; Felix, N. M.; Ober, C. K. Molecular Glass Resists as High-Resolution Patterning Materials. *Adv. Mater.* **2008**, *20*, 3355-3361.
  6. Hikima, T.; Adachi, Y.; Hanaya, M.; Oguni, M. Determination of Potentially Homogeneous-Nucleation-Based Crystallization in *o*-Terphenyl and an Interpretation of the Nucleation-Enhancement Mechanism. *Phys. Rev. B* **1995**, *52*, 3900-3908.
  7. Sun, Y.; Xi, H.; Chen, S.; Ediger, M. D.; Yu, L. Crystallization near Glass Transition: Transition from Diffusion-Controlled to Diffusionless Crystal Growth Studied with Seven Polymorphs. *J. Phys. Chem. B* **2008**, *112*, 5594-5601.
  8. Konishi, T.; Tanaka, H. Possible Origin of Enhanced Crystal Growth in a Glass. *Phys. Rev. B* **2007**, *76*, 220201.
  9. Stevenson, J. D.; Wolynes, P. G. The Ultimate Fate of Supercooled Liquids. *J. Phys. Chem. A.* **2011**, *115*, 3713-3719.
  10. Caroli, C.; Lemaître, A. Ultrafast Spherulitic Crystal Growth as a Stress-Induced Phenomenon Specific of Fragile Glass-Formers. *J. Chem. Phys.* **2012**, *137*, 114506-114506.
  11. Musumeci, D.; Powell, C. P.; Ediger, M. D.; Yu, L. Termination of Solid-State Crystal Growth in Molecular Glasses by Fluidity. *J. Phys. Chem. Lett.* **2014**, *5*, 1705-1710.
  12. Sun, Y.; Zhu, L.; Kearns, K. L.; Ediger, M. D.; Yu, L. Glasses Crystallize Rapidly at Free Surfaces by Growing Crystals Upward. *Proc. Natl. Acad. Sci. U.S.A.* **2011**, *108*, 5990-5995.
  13. Wu, T.; Yu, L. Surface Crystallization of Indomethacin below  $T_g$ . *Pharm. Res.* **2006**, *23*, 2350-2355.
  14. Zhu, L.; Wong, L.; Yu, L. Surface-Enhanced Crystallization of Amorphous Nifedipine. *Mol. Pharm.* **2008**, *5*, 921-926.
  15. Zhu, L.; Jona, J.; Nagapudi, K.; Wu, T. Fast Surface Crystallization of Amorphous Griseofulvin below  $T_g$ . *Pharm Res* **2010**, *27*, 1558-1567.

- 
16. Gunn, E.; Guzei, I. A.; Yu, L. Does Crystal Density Control Fast Surface Crystal Growth in Glasses? A Study with Polymorphs. *Crystal Growth & Design* **2011**, *11*, 3979-3984.
  17. Hasebe, M.; Musumeci, D.; Powell, C.T.; Cai, T.; Gunn, E.; Zhu, L.; Yu, L. Fast Surface Crystal Growth on Molecular Glasses and Its Termination by the Onset of Fluidity. *J. Phys. Chem. B* **2014**, *118*, 7638-7646.
  18. Stephens, R. B. Stress-Enhanced Crystallization in Amorphous Selenium Films. *J. Appl. Phys.* **1980**, *51*, 6197-6201.
  19. Sallese, J. M.; Ils, A.; Bouvet, D.; Fazan, P.; Merritt, C. Modeling of the Depletion of the Amorphous-Silicon Surface during Hemispherical Grained Silicon Formation. *J. Appl. Phys.* **2000**, *88*, 5751-5755.
  20. Koster, U. Surface Crystallization of Metallic Glasses. *Mat. Sci. & Eng.* **1988**, *97*, 233-239.
  21. Diaz-Mora, N.; Zanotto, E. D.; Hergt, R.; Müller, R. Surface Crystallization and Texture in Cordierite Glasses. *J. Non-Crystalline Solids* **2000**, *273*, 81-93.
  22. Fokin, V. M.; Zanotto, E. D. Surface and Volume Nucleation and Growth in TiO<sub>2</sub>-cordierite Glasses. *J. Non-Crystalline Solids* **1999**, *246*, 115-127.
  23. Wittman, E.; Zanotto, E. D. Surface Nucleation and Growth in Anorthite Glass. *J. Non-Crystalline Solids* **2000**, *271*, 94-99.
  24. Yuritsyn, N. S. Crystal growth on the surface and in the bulk of Na<sub>2</sub>O·2CaO·3SiO<sub>2</sub>-glass. In *Nucleation Theory and Applications*, Editors: J.W.R.Schmelzer, G.Roepke, V.B.Priezzhev. Dubna, JINR, **2005**, p.22-42.
  25. Wisniewski, W.; Bocker, C.; Kouli M.; Nagel M.; Rüssel, C. Surface Crystallization of Fresnoite from a Glass Studied by Hot Stage Scanning Electron Microscopy and Electron Backscatter Diffraction. *Cryst. Growth Des.* **2013**, *13*, 3794-3800.
  26. Wu, T.; Sun, Y.; Li, N.; de Villiers, M.; Yu, L. Inhibiting Surface Crystallization of Amorphous Indomethacin by Nanocoating. *Langmuir* **2007**, *23*, 5148-5153.
  27. Zhu, L.; Brian, C.; Swallen, S. F.; Straus, P. T.; Ediger, M. D.; Yu, L. Surface Diffusion of an Organic Glass. *Phys. Rev. Lett.* **2011**, *106*, 256103.
  28. Brian, C. B.; Yu, L. Surface Self-Diffusion of Organic Glasses. *J. Phys. Chem. A* **2013**, *117*, 13303-13309.
  29. Schmelzer, J.; Pascova, R.; Müller, J.; Gutzow, I. Surface-Induced Devitrification of Glasses: the Influence of Elastic Strains. *J. Non-Crystalline Solids* **1993**, *162*, 23-29.
  30. Genin, F.Y.; Mullins, W.W.; Wynblatt, P. The Effect of Stress on Grain Boundary Grooving. *Acta metall. mater* **1993**, *41*, 3541-3547.
  31. Sekerka, R.F.; Boettinger, W.J.; McFadden, G.B. Surface Morphologies due to Grooves at Moving Grain Boundaries Having Stress-Driving Fluxes. *Acta Materialia* **2013**, *61*, 7216-7226.

- 
32. Chai, Y.; Salez, T.; McGraw, J. D.; Benzaquen, M.; Dalnoki-Veress, K.; Raphaël, E.; Forrest, J.A. A Direct Quantitative Measure of Surface Mobility in a Glassy Polymer. *Science* **2014**, *343*, 994-999.
33. Chen, X.; Morris, K. R.; Griesser, U. J.; Byrn, S. R.; Stowell, J. G. Reactivity differences of indomethacin solid forms with ammonia gas. *J. Am. Chem. Soc.* **2002**, *124*, 15012-15019.
34. Kistenmacher, T. J.; Marsh, R. E. Crystal and molecular structure of an anti-inflammatory agent, indomethacin, 1-(p-chlorobenzoyl)-5-methoxy-2-methylindole-3-acetic acid. *J. Am. Chem. Soc.* **1972**, *94*, 1340-1345.
35. Mullins, W. Flattening of a Nearly Plane Solid Surface due to Capillarity. *J. Appl. Phys.* **1959**, *30*, 77-83.
36. Mullins, W. The effect of Thermal Grooving on Grain Boundary Motion. *Acta Metall.* **1958**, *6*, 414-427.
37. Genin, F.Y. Effect of Stress on Grain Boundary Motion in Thin Films. *J. Appl. Phys.* **1995**, *77*, 5130-7.
38. Sears, G. W. A Growth Mechanism for Mercury Whiskers. *Acta Metall.* **1955**, *3*, 361-366.
39. Tu, K.N.; Li, J.C.M. Spontaneous whisker growth on lead-free solder finishes. *Mater Sci Eng* **2005**, *409*, 131-139.

## **Chapter 4**

### **Effect of Spatial Confinement on Fast Surface Crystal Growth on Molecular Glasses**

Mariko Hasebe, and Lian Yu

Department of Chemistry and School of Pharmacy

University of Wisconsin – Madison, Madison, WI, 53705

Draft of a paper to be submitted in the future

## 4.1 Abstract

Recent studies have shown that organic glasses can grow crystals substantially faster at the free surface than in the interior. Previous studies were performed with glass films essentially infinitely thick and wide. This study examines the effect of spatial confinement on the process using glass films of limited width and thickness and with the supporting substrate being more to less adhesive. The major finding is that surface crystal growth on molecular glasses is disrupted by spatial confinement on length scales that greatly exceed several molecular layers – the length scale expected for surface diffusion. For a thick glass film of nifedipine (NIF) or *o*-terphenyl (OTP), the process is disrupted if the width is reduced to below several micrometers. This critical width is approximately the lateral “footprint” for surface crystal growth, composed of the single-crystal domain in steady development and the distance over which the amorphous surface is perturbed. Similarly, the process in indomethacin (IMC) is disrupted if the glass film is thinner than the vertical “footprint”, which is defined by the depth of the depletion zones around growing crystals. We also report a more subtle confinement effect observed with glass films approximately 10  $\mu\text{m}$  thick supported by strongly adhesive substrates. Surface crystal growth in these films has the expected initial velocity, but the velocity decreases over time, approximately on the timescale at which the surface crystal layer grows to the bottom of the substrate. All these effects reflect the environmental perturbation to the growth of surface crystals. These effects are significant because organic glasses of technological importance have finite dimensions, may be attached to substrates, and the resulting confinement can affect the kinetics of surface crystallization.

## 4.2 Introduction

Glasses or amorphous solids can be formed by cooling liquids, drying solutions or condensing vapor without crystallization. Amorphous solids are advantageous over their crystalline

counterparts for many applications<sup>1</sup>. Although the more familiar amorphous solids are inorganic (e.g., window glass) and polymeric, there has been an increased attention to organic or molecular glasses as vehicles for delivering poorly soluble drugs<sup>2</sup>, and as photo- and electro-active materials<sup>3,4</sup>. An amorphous solid is generally more soluble than the corresponding crystal, and this property is useful for delivering drugs whose bioavailability is limited by their poor solubility. For all amorphous materials, stability against crystallization is important. Recent studies discovered that crystal growth at the free surface can be orders of magnitude faster than crystal growth in the interior<sup>5,6,7,8,9</sup>. It is worth noting that surface-enhanced crystallization is observed for molecular glasses and amorphous Se<sup>10</sup> and Si<sup>11</sup>, but the phenomenon is apparently absent in metallic glasses<sup>12</sup> and silicate glasses<sup>13,14,15,16,17</sup>. Understanding fast surface crystal growth on molecular glasses is important for developing amorphous materials that are stable against crystallization.

Previous studies have reported many interesting features of surface crystal growth on molecular glasses. Surface crystals rise above the glass surface, and are surrounded by depletion zones,<sup>5,9</sup> as a result of the combined action of surface diffusion and crystallization flux<sup>18</sup>. The growth of surface crystals can be inhibited by a nanocoating (e.g. 10 nm of gold or a few nanometers of polymers)<sup>19</sup>. Surface crystal growth is active on molecular glasses, but is terminated by the onset of fluidity.<sup>9</sup> Surface diffusion and surface crystal growth have similar kinetics, described by  $u_s = D_s / (3 \mu\text{m})$ <sup>20,21,22</sup>. This relation suggests that surface mobility is responsible for fast surface crystal growth.

In this work, we investigate the effect of spatial confinement on surface crystal growth. Previous studies were performed with glass films essentially infinitely thick and wide. Previous work also observed that the growth of surface crystals has characteristic length scales.<sup>9,18</sup> The lateral “footprint” of the process is on the order of several micrometers, consisting of the size of single-crystal domains that steadily develop and the size of the surrounding depletion zones on the

amorphous surface; the vertical footprint is on the order of hundreds of nanometers defined by the depth of the depletion zone. We hypothesize that if the available space for surface crystal growth is reduced to the size of its footprints, the process will be disrupted.

Apart from understanding surface crystal growth, this work is motivated by the recent proposal<sup>23</sup> that crystal growth in the interior of molecular glasses is related to that on the free surface. Powell et al. propose that bulk crystal growth in mechanically fragile organic glasses might involve continuous fracture and surface mobility. This model in essence treats bulk crystal growth as a spatially confined form of surface crystal growth. Thus, understanding how surface crystal growth responds to spatial confinement could help understand bulk crystal growth.

This work is also motivated by the work of Rades and coworkers<sup>24</sup>, who performed crystallization experiments in open micro-containers. They observed slower crystallization of indomethacin glasses in containers that are tens of micrometers in diameter. This observation is unexpected given that the length scale of this effect is vastly larger than the estimated thickness of the mobile surface layer (the thickness of several molecules).

We performed several preliminary experiments to learn how spatial confinement affects surface crystal growth. First, we varied the width of the channel into which surface crystals can grow. Crystal growth was monitored at the edge of a glass film sandwiched between two cover slips. In this experiment, the material feeding crystal growth is unlimited in depth but limited in width. Second, we performed experiments with glass films of different thicknesses and supported on different substrates.

We find that spatial confinement on the length scale of micrometers can disrupt the growth of surface crystals. For a thick glass film of NIF or OTP, the process is disrupted if the width is reduced to below several micrometers. This critical width is approximately the lateral “footprint”

of surface crystal growth (the size of a single-crystal domain plus the distance over which the amorphous surface is perturbed). Similarly, the process in IMC is disrupted if the glass film is thinner than the vertical “footprint”, which is defined by the depth of the depletion zones around a growing crystal. We also report a more subtle confinement effect observed with glass films approximately 10  $\mu\text{m}$  thick supported by strongly adhesive substrates. Surface crystal growth in these films has the expected velocity *initially*, but the velocity decreases over time, approximately on the timescale at which the surface crystal layer grows through the film to touch the substrate. These effects are explained on the basis of the environmental perturbation on the growth of surface crystals.

### 4.3 Materials and Methods

Indomethacin (1-(p-chlorobenzoyl)-5-methoxy-2-methylindole-3-acetic acid; IMC;  $\gamma$  polymorph), nifedipine (1,4-dihydro-2,6-dimethyl-4-(2-nitophenyl)-3,5-pyridinedicarboxylate;NIF), and o-terphenyl (OTP) were purchased from Sigma-Aldrich. As described in previous chapters, glass films were prepared between silicate coverslips and film thickness was controlled by adjusting the sample mass. One coverslip was detached to create a glass film with a free surface to study the effect of glass thickness on surface crystal growth. Some experiments were performed in which the silicate substrate was replaced by a Kapton film and a gold-coated Kapton film (the gold layer was 20 nm thick and deposited by sputtering).

For a “perimeter surface experiment”, a glass film was prepared between two coverslips in such a way that the edge of the film was recessed from the edges of the coverslips to allow easy observation. The edge of the glass film was a ribbon of exposed free surface whose width is the

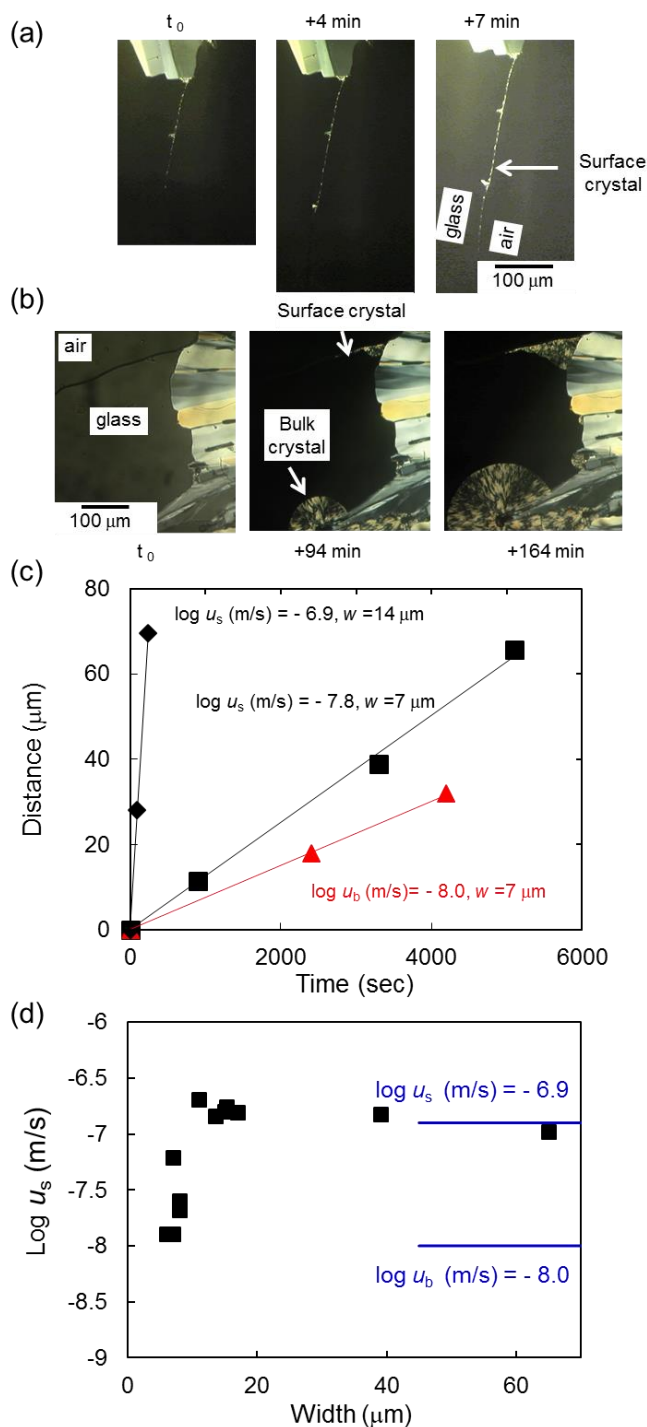
thickness of the film. In this geometry, it was possible to observe both surface crystal growths along the edge and bulk growth into the interior.

Surface crystallization was observed real-time with the aid of the temperature-controlled Linkam microscope stage under a N<sub>2</sub> purge (Olympus BH2 – UMA). Real-time AFM was performed with a Veeco Multimode IV Scanning Probe Microscope in the tapping mode under N<sub>2</sub> purge. An AFM hostage was used to control temperature; it was calibrated against the melting point of *o*-terphenyl (329 K). According to the manufacturer, the AFM tip (300Al-G10, BudgetSensors) had a tip radius of 10 nm and half-cone angle of 20-25° (10° at apex).

## 4.4 Results

### 4.4.1 Effect of glass width on surface crystal growth

Figure 1 shows the effect of glass width on surface crystal growth on an OTP glass at 243 K ( $T_g - 3$  K;  $T_g$  is the glass transition temperature). In this experiment, the edge of a glass film was observed to allow simultaneous measurements of surface crystal growth along the edge and bulk crystal growth into the interior. The depth for bulk growth was essentially infinite, whereas the width  $w$  for surface growth was limited. At  $w = 14$   $\mu\text{m}$  (Figure 1a), the velocity of surface crystal growth  $u_s$  matches that for growth without any width limitation:  $\log u_s$  (m/s) = -6.9.<sup>9</sup> The bulk crystal growth rate  $u_b$  is also consistent with the previous report:  $\log u_b$  (m/s) = -8.0.<sup>25,26</sup> At  $w = 7$   $\mu\text{m}$  (Figure 1b), however, surface crystal growth along the edge is significantly slower, while the bulk crystal growth is unaffected. Figure 1c shows the data used to measure these growth rates.



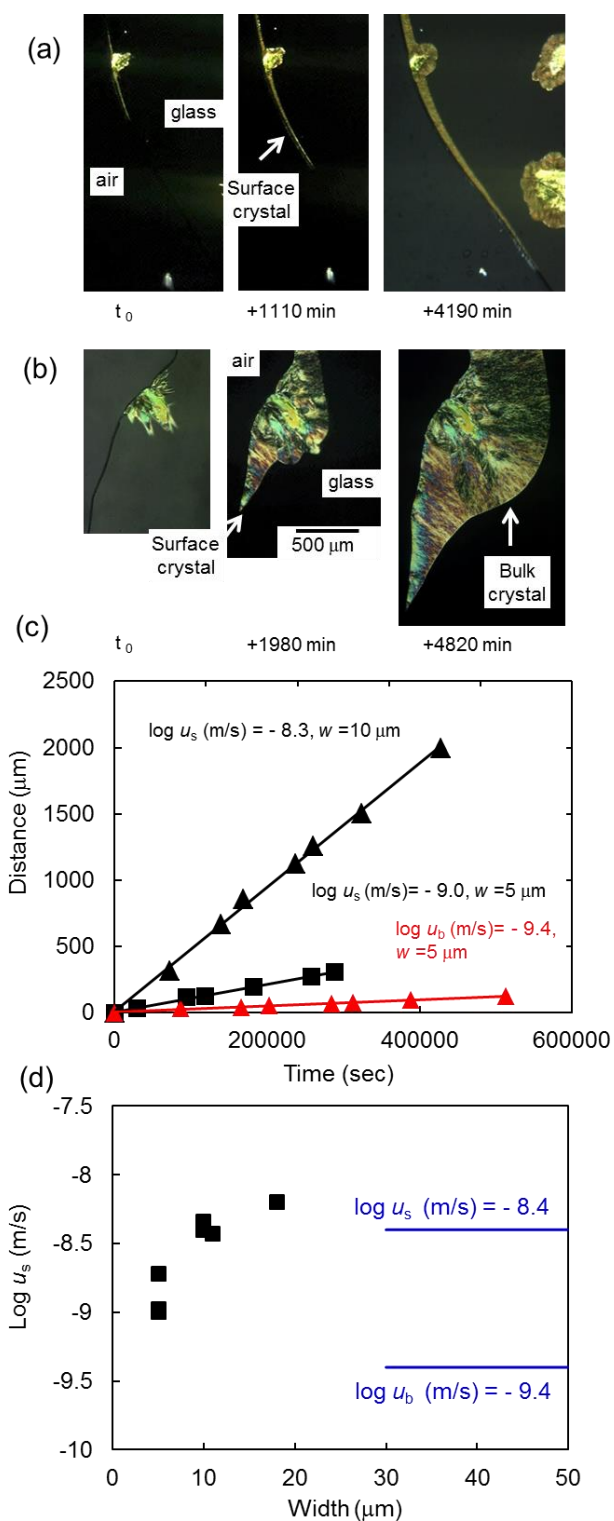
**Figure 1.** OTP surface crystals growing at 243 K ( $T_g - 3$  K) in glass films 14  $\mu\text{m}$  (a) and 7  $\mu\text{m}$  (b) thick. (c) Kinetics of surface (black) and bulk (red) crystal growth in the two films. (d)  $u_s$  as a function of glass width.  $u_s$  and  $u_b$ : previously reported velocities of surface and bulk crystal growth.<sup>9,25,26</sup>

Figure 1d shows the velocity of surface crystal growth as a function of glass width. Notice a drop of  $u_s$  as the glass width decreases to several micrometers. Above this width,  $u_s$  is consistent with the reported value for unlimited width. Below this width,  $u_s$  approaches the bulk crystal growth rate  $u_b$ .<sup>9,25,26</sup>

Similar results were observed with NIF glasses crystallizing at 303 K ( $T_g - 12$  K) (Figure 2). At  $w = 10$   $\mu\text{m}$ , the observed  $u_s$  and  $u_b$  agree with the previous reports:  $\log u_s$  (m/s) = -8.4,  $\log u_b$  (m/s) = -9.4.<sup>7,9,26</sup> However, at  $w = 5$   $\mu\text{m}$ , the observed  $u_s$  is significantly slower, while the  $u_b$  is unaffected. The plot of  $u_s$  vs.  $w$  (Figure 2d) shows a drop of  $u_s$  as the glass width decreases to several micrometers. Above this width,  $u_s$  is approximately the reported value for unlimited width; below this width,  $u_s$  approaches the bulk crystal growth rate  $u_b$ .<sup>9,29</sup> Notice that for both OTP and NIF glasses, the critical glass width below which surface crystal growth is disrupted is comparable (several micrometers).

#### 4.4.2 Effects of glass thickness and substrate materials on surface crystal growth

Sun et al. systematically studied the effect of glass thickness  $h$  on the surface crystal growth on IMC glasses, using  $h$  that is on the order of the depth of the depletion zones around surface crystals.<sup>5</sup> They observed that as  $h$  approaches the depth of the depletion zone, surface crystal growth is disrupted. In this study, we used thicker films to study a more subtle confinement effect. Figure 3a shows the kinetics of surface crystal growth of  $\gamma$  IMC at 303 K ( $T_g - 12$  K) in films 14 and 170  $\mu\text{m}$  thick, both supported by a silicate coverslip. The crystal growth rate  $u_s$  was measured by AFM under nitrogen purge. In this experiment, the sample was initiated to crystallize at 313 K and transferred to 303 K for further crystal growth; because bulk crystal growth is slow at 313 K



**Figure 2.** NIF surface crystals growing at 303 K ( $T_g - 12$  K) in glass films 10  $\mu\text{m}$  (a) and 5  $\mu\text{m}$  (b) thick. (c) Kinetics of surface (black) and bulk (red) crystal growth in the two films. (d)  $u_s$  as a function of glass width.  $u_s$  and  $u_b$ : previously reported velocities of surface and bulk crystal growth.<sup>9,29</sup>

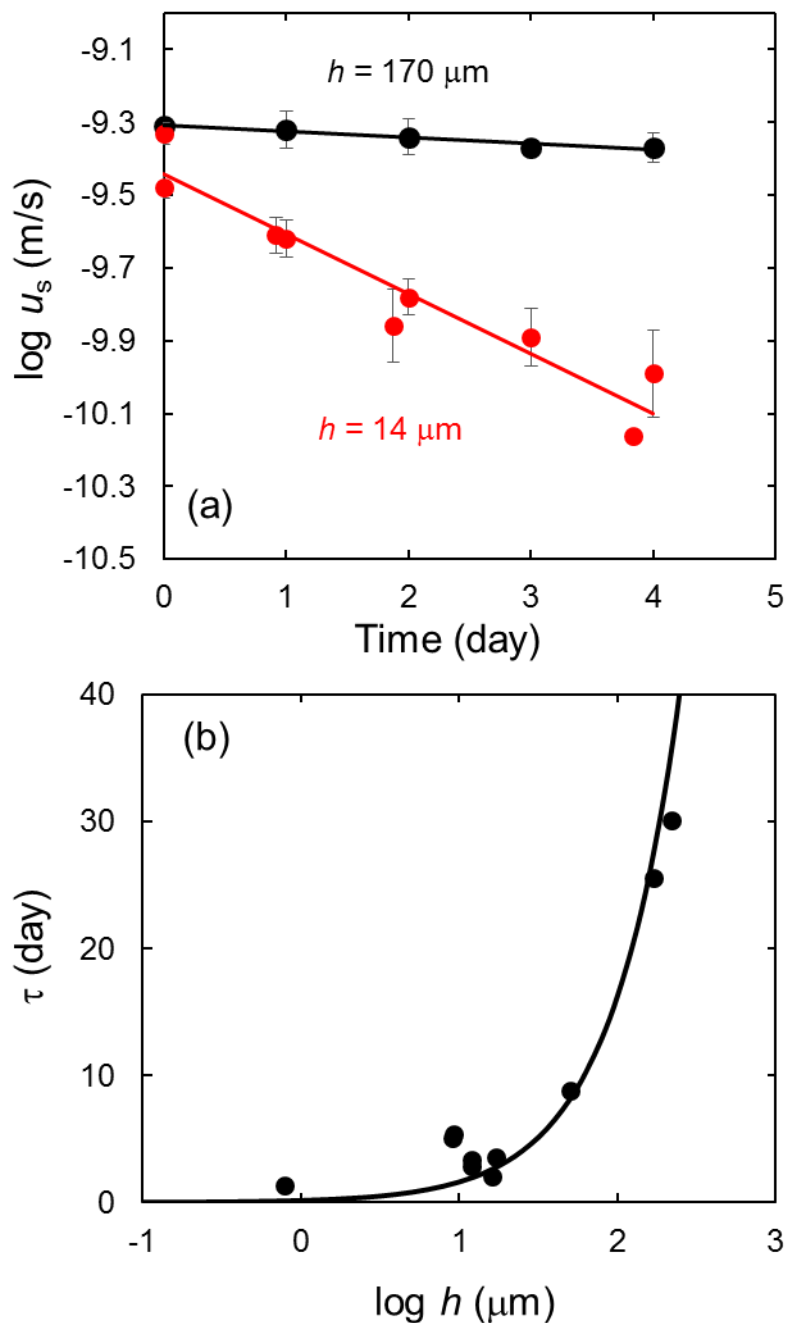


**Figure 3.** (a) Crystal growth rates  $u_s$  of  $\gamma$  IMC in glass films 170 and 14  $\mu\text{m}$  thick at 303 K, observed by real-time AFM.  $u_s$  decreases over time approximately exponentially. The decay time  $\tau$  is shown in (b) as a function of glass thickness. The trend is approximately captured by the calculated curve  $\tau_{\text{calc}} = k h / u_b$ , where  $k = 0.5$  is a fitting parameter,  $h$  is glass thickness, and  $u_b$  is bulk crystal growth.

(the onset temperature for bulk GC growth is 306 K),<sup>27</sup> the 303 K observation began with only a surface crystal layer.

Notice that in both films,  $u_s$  decreases over time, with the effect being much stronger in the thinner film. Initially, the two films have similar  $u_s$ , but at the end of the measurements,  $u_s$  for the thinner film is nearly 10 times slower. The initial velocity of surface crystal growth is consistent with previous reports for thick films during the early stage of crystal growth.<sup>5,6,9</sup> Notice also that the decrease of  $u_s$  over time is approximately exponential ( $\log u_s$  roughly linear in  $t$ ). Figure 3b plots the characteristic time  $\tau$  for the exponential decay vs. the glass thickness  $h$ . The data have considerable scatter; the overall trend is that  $u_s$  slows down at a faster rate in thinner films than in thicker films. The curve passing through the data points is the time for bulk crystal growth to descend halfway through the film toward the substrate (see later).

We next present three other observations that help understand the thickness-dependent slowdown of the surface crystal growth of  $\gamma$  IMC. First, the effect is temperature dependent. If the temperature is raised from 303 K to 313 K ( $T_g - 2$  K), the effect largely vanishes. This result indicates that the solidity of the matrix is important for observing the phenomenon. Second, the effect depends on the surface of the substrate. Figure 4 compares the kinetics of surface crystal growth on an IMC glass 12  $\mu\text{m}$  thick supported on a silicate coverslip, a Kapton film, or a Kapton film coated with a layer of gold (20 nm thick). Notice that by replacing the silicate substrate with the Kapton substrate,  $u_s$  becomes nearly independent of time. In contrast, on a gold-coated Kapton substrate,  $u_s$  decreases over time as on a silicate substrate. In this comparison, these three substrates differ in the strength of adhesion to the IMC glass: IMC adheres weakly to the Kapton surface and more strongly to the silicate or gold-coated Kapton surface. This difference in adhesion was readily seen in a peel test. A Kapton film is easily and cleanly peeled off the IMC glass, whereas a silicate coverslip or

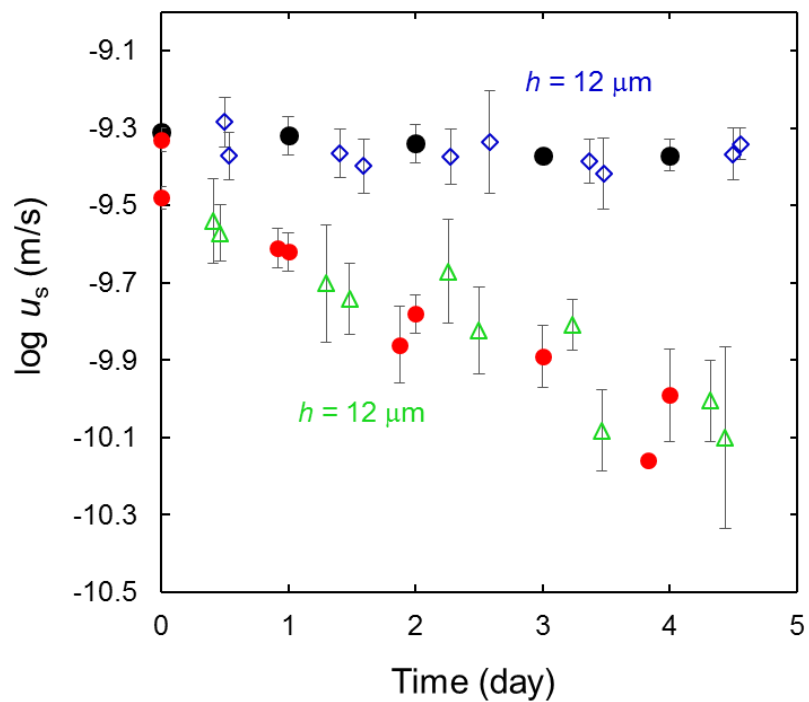


**Figure 4.** Substrate effect on the surface crystal growth of  $\gamma$  IMC at 303 K. In addition to the data in Figure 3a, data are shown for Kapton (blue) and gold-coated Kapton (green) as substrates. In both cases, the IMC glass film was  $12 \mu\text{m}$  thick.

a gold-coated Kapton film is not. This finding indicates that the slowdown of surface crystal growth is related to the interaction between the IMC glass and the substrate.

A third observation relevant for understanding the thickness-dependent slowdown of surface crystal growth is that in contrast to  $\gamma$  IMC, the surface crystal growth of  $\alpha$  IMC *does not* slow down significantly at the same film thickness. Figure 5 shows the growth kinetics for  $\alpha$  IMC growing in a glass film 14  $\mu\text{m}$  thick. Within experimental error, the growth rate is constant. As we discuss later, we attribute the difference between the two IMC polymorphs to their different bulk crystal growth rates  $u_b$ : in the bulk,  $\gamma$  IMC grows 10 times faster than  $\alpha$  IMC.<sup>27</sup>

#### 4.5 Discussion

In this preliminary study, experiments were performed to learn how spatial confinement affects the growth of surface crystals on molecular glasses. We find that for a thick glass film of nifedipine (NIF) or *o*-terphenyl (OTP), surface crystal growth is disrupted if the width is reduced to below several micrometers. It was reported previously that surface crystal growth in the glass films of indomethacin (IMC) is disrupted if the thickness is reduced to several hundred nanometers<sup>18</sup>. Below we will discuss these confinement effects on the basis of the “footprints” of surface crystal growth and the space available for growth. This study has also observed a more subtle confinement effect with IMC films approximately 10  $\mu\text{m}$  thick. On strongly adhesive substrates, surface crystal growth has the expected *initial* velocity, but the velocity decreases over time. This effect disappears on the less adhesive Kapton substrate. We will discuss this effect on the basis of simultaneous bulk growth under surface crystals and its interaction with the substrate.

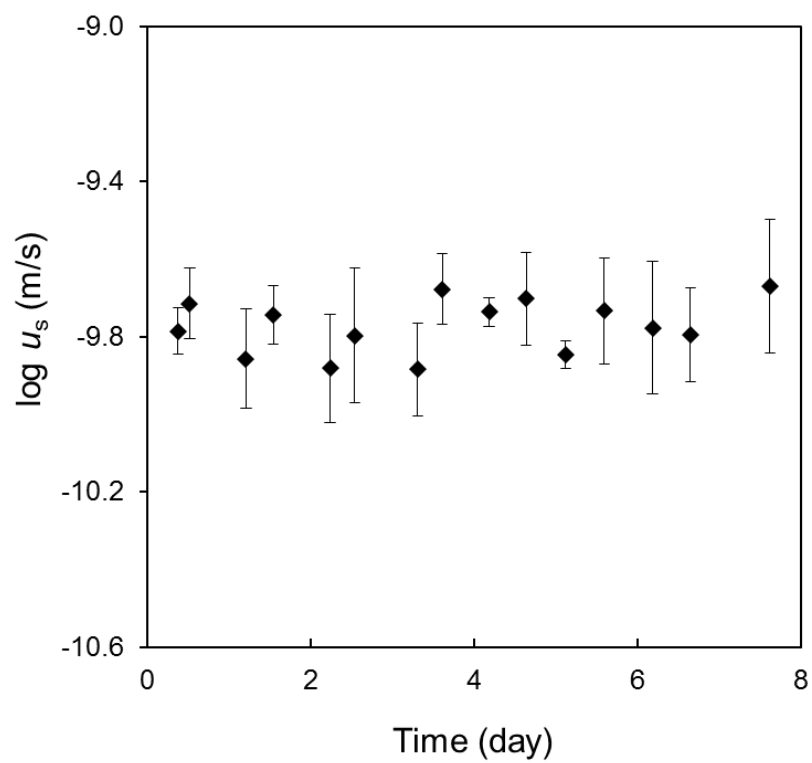


**Figure 5.** Crystal growth kinetics of  $\alpha$  IMC in 10  $\mu\text{m}$  thick films at 303 K. In contrast of  $\gamma$  IMC, the surface growth of  $\alpha$  IMC has constant rate.

#### 4.5.1 Critical width and depth for disrupting surface crystal growth on molecular glasses

Surface crystal growth on molecular glasses has characteristic dimensions or “footprints”. We hypothesize that if these footprints exceed the space available for crystal growth, the process will be disrupted. This hypothesis is consistent with known morphologies of surface crystals summarized in Figure 6.<sup>9,18,29</sup> The best quality images were obtained for IMC surface crystals because of their slower growth and the possibility to characterize them at room temperature (as opposed to sub-ambient temperatures for OTP glasses).  $\alpha$  IMC grows segregated needles that rise above the glass surface and are surrounded by depletion zones (Figure 6a). The width of an  $\alpha$  IMC needle is  $10^2 - 10^3$  nm; the distance over which the crystal perturbs the surrounding amorphous surface (Chapter 3) is also  $10^2 - 10^3$  nm. We estimate the “footprint” for the steady-state growth of  $\alpha$  IMC surface crystals to be several micrometers (the sum of the crystal width and the width of the depletion zones on both sides). In comparison,  $\gamma$  IMC surface crystals are more compact (Figure 6b), with each single-crystal domain estimated to be several micrometers in size. NIF surface crystals are bundles of fibers or plates that advance together (Figure 6c).<sup>9</sup> The lateral footprint of this growth process is probably on the order of several micrometers. For OTP (Figure 6d), surface crystals have been characterized only with the relatively low-resolution light microscopy, a result of its sub-ambient  $T_g$ . The lateral dimension of independently advancing domains is estimated to be several micrometers. For all these systems, surface crystal growth is roughly described as having a lateral footprint of several micrometers, and this dimension agrees with the critical glass width below which the process is disrupted (Figures 1d and 2d).

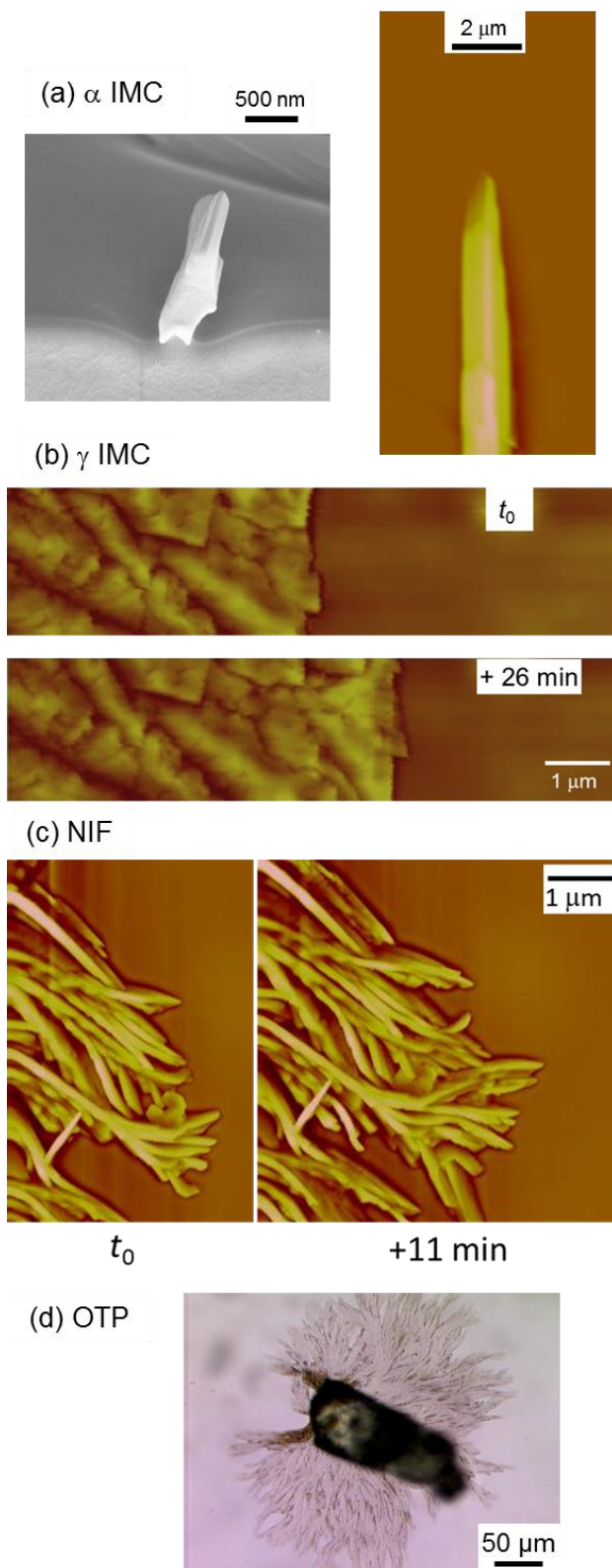


**Figure 6.** Surface crystals on molecular glasses:  $\alpha$  IMC (a),  $\gamma$  IMC (b), NIF<sup>29</sup> (c), and OTP (d).

To further test this understanding, it would be valuable to compare the growth of the two IMC polymorphs in the same experiment that has been performed for OTP and NIF glasses. Because they grow as segregated needles, the surface crystals of  $\alpha$  IMC could enter channels slightly narrower than those of  $\gamma$  IMC. Such polymorphic selectivity would have practical utility.

The vertical footprint for surface crystal growth is expected to be comparable to the depth of depletion zones around surface crystals. For  $\alpha$  IMC, the depletion zones around the needle-like crystals are  $10^2 - 10^3$  nm, increasing with the distance to the tip.<sup>18</sup> For  $\gamma$  IMC, the depletion zone before the steadily advancing growth front is  $10 - 10^2$  nm deep.<sup>18</sup> These depths roughly agree with the thicknesses below which the surface growth of these polymorphs is disrupted: 300 nm for  $\alpha$  IMC, and 180 nm for  $\gamma$  IMC.<sup>5</sup> It would be of interest to test this correlation with additional systems, such as NIF.<sup>9, 29</sup>

#### 4.5.2 Slowdown of surface crystal growth over time

Concerning the gradual slowdown of the surface growth of  $\gamma$  IMC over time (Figure 3), the experimental facts suggest a role for the simultaneous bulk crystal growth under surface crystals and the interaction between the organic glass and the substrate. Paeng et al. report that as a crystal growth front advances through the bulk of an *o*-terphenyl glass, a modest stress field is present near the growth front over a distance of 10  $\mu\text{m}$ , with the maximal tension reached being 8 MPa<sup>28</sup>. Powell et al. argue that bulk crystal growth in molecular glasses continuously fractures the glass matrix, which limits the buildup of crystallization-induced tension to a modest level (8 MPa for *o*-terphenyl).<sup>23</sup> Consistent with these ideas, we imagine that as surface crystals grow laterally atop a glass film, a bulk growth front is initiated and moves towards the substrate. As the bulk front approaches a strongly adhering substrate, the kinetics of fracture changes. This effect might arise

because the substrate has a different elastic modulus and because it is more difficult to delaminate the organic glass off the strongly adhering substrate than to fracture the organic glass. This effect could cause stress to increase and to spread. The stress field could propagate to the glass surface, causing local separations between crystalline and amorphous domains and slowing surface crystal growth. This model can explain the existence of the phenomenon with the faster bulk-growing  $\gamma$  polymorph but not with the slower growing  $\alpha$  polymorph and the disappearance of the effect on replacing the silicate substrate with the less adherent Kapton substrate. The model also explains the disappearance of the phenomenon at the onset of fluidity by invoking the efficient stress relaxation through liquid flow.

For an empirical test of this model, we assume the characteristic time for the slowdown of surface crystal growth is proportional to the time for the bulk growth front to arrive at the substrate:

$$\tau_{\text{calc}} = k h/u_b \quad (1)$$

Where  $h$  is film thickness,  $u_b$  is bulk crystal growth rate, and  $k$  is a factor on the order of unity. Figure 3b shows that with a reasonable value  $k = 0.5$ , eq. 1 approximately reproduces the trend of the experimental data. Thus, the characteristic time for the slowdown of surface crystal growth is approximately the time for the bulk growth front to descend halfway through the film toward the substrate.

At present, the model is highly speculative and future work is needed. A test of this model could be performed with the aid of polymer additives, which slows down bulk crystal growth effectively, but has a smaller effect on surface crystal growth.<sup>29</sup> The model predicts that the slowdown of surface crystal growth over time becomes less pronounced in the presence of a polymer dopant. It would be valuable to examine the process of crystal growth by SEM for evidence of fracture and propagation of the stress field.

## 4.6 Conclusions

We performed preliminary studies of the effect of spatial confinement on surface crystal growth in indomethacin, nifedipine, and *o*-terphenyl glasses. The major finding is that surface crystal growth on molecular glasses can be disrupted by spatial confinement on length scales that greatly exceed several molecular layers – the length scale envisioned for surface diffusion. For a thick glass film of nifedipine (NIF) or *o*-terphenyl (OTP), the process is disrupted if the width is reduced to below several micrometers. This critical width is approximately the lateral “footprint” for surface crystal growth, composed of the single-crystal domain and the distance over which the amorphous surface is perturbed. Similarly, the process in indomethacin (IMC) is disrupted if the glass film is thinner than its vertical “footprint”, defined as the depth of the depletion zones around a growing crystal. We also report a more subtle confinement effect observed with glass films approximately 10  $\mu\text{m}$  thick on strongly adhesive substrates. Surface crystal growth in these films has the expected initial velocity, but the velocity decreases over time, approximately on the timescale at which the surface crystal layer grows to the bottom of the substrate. All these effects reflect the environmental perturbation of the growth of surface crystals.

Further understanding these effects is significant because organic glasses of technological importance have finite thickness and may be attached to substrates, and the resulting confinement effect on surface crystallization is relevant for predicting and controlling their physical stability. Future work could systematically examine the phenomenon in different glass formers and with different techniques of spatial confinement. Microfluidic channels could be a useful tool for controlling the space available for crystal growth.

**References:**

1. Zallen, R. *The Physics of Amorphous Solids*, Wiley, New York, **1983**.
2. Yu, L. Amorphous Pharmaceutical Solids: Preparation, Characterization and Stabilization. *Adv. Drug Delivery Rev.* **2001**, *48*, 27-42.
3. Shirota, Y. Photo- and Electroactive Amorphous Molecular Materials-Molecular Design, Syntheses, Reactions, Properties, and Applications. *J. Mater Chem.* **2005**, *15*, 75-93.
4. De Silva, A.; Felix, N.M.; Ober, C.K. Molecular Glass Resists as High-Resolution Patterning Materials. *Adv Mater.* **2008**, *20*, 3355-3361.
5. Sun, Y.; Zhu, L.; Kearns, K.L.; Ediger, M. D.; Yu, L. Glasses Crystallize Rapidly at Free Surfaces by Growing Crystals Upward. *Proc. Natl. Acad. Sci U.S. A.* **2011**, *108*, 5990-5995.
6. Wu, T.; Yu, L. Surface Crystallization of Indomethacin below  $T_g$ . *Pharm Res.* **2006**, *23*, 2350-2355.
7. Zhu, L.; Wong, L.; Yu, L. Surface-Enhanced Crystallization of Amorphous Nifedipine. *Mol. Pharm.* **2008**, *5*, 921-926.
8. Gunn, E.; Guzei, I. A.; Yu, L. Does Crystal Density Control Fast Surface Crystal Growth in Glasses? A Study with Polymorphs. *Cryst. Growth Des.* **2011**, *11*, 3979-3984.
9. Hasebe, M.; Musumeci, D.; Powell, C. T.; Cai, T.; Gunn, E.; Zhu, L.; Yu, L. Fast Surface Crystal Growth on Molecular Glasses and Its Termination by the Onset of Fluidity. *J. Phys. Chem. B* **2014**, *118*, 7638-7646.
10. Stephens, R. B. Stress-Enhanced Crystallization in Amorphous Selenium Films. *J. Appl. Phys.* **1980**, *51*, 6197-6201.
11. Sallese, J. M.; Ils, A.; Bouvet, D.; Fazan, P.; Merritt, C. Modeling of the Depletion of the Amorphous-Silicon Surface during Hemi- spherical Grained Silicon Formation. *J. Appl. Phys.* **2000**, *88*, 5751- 5755.
12. Koster, U. Surface Crystallization of Metallic Glasses. *Mater. Sci. Eng.* **1988**, *97*, 233-239.
13. Diaz-Mora, N.; Zanutto, E. D.; Hergt, R.; Muller, R. Surface Crystallization and Texture in Cordierite Glasses. *J. Non-Cryst. Solids* **2000**, *273*, 81-93.
14. Fokin, V. M.; Zanutto, E. D. Surface and Volume Nucleation and Growth in TiO<sub>2</sub>-cordierite Glasses. *J. Non-Cryst. Solids* **1999**, *246*, 115-127.
15. Wittman, E.; Zanutto, E. D. Surface Nucleation and Growth in Anorthite Glass. *J. Non-Cryst. Solids* **2000**, *271*, 94-99.

- 
16. Yuritsyn, N. S. Crystal Growth on the Surface and in the Bulk of Na<sub>2</sub>O 2CaO 3SiO<sub>2</sub>-Glass. In Nucleation Theory and Applications; Schmelzer, J. W. R., Roepke, G., Priezhev, V. B., Eds.; JINR: Dubna, **2005**; pp 22-42.
17. Wisniewski, W.; Bocker, C.; Kouli, M.; Nagel, M.; Russel, C. Surface Crystallization of Fresnoite from a Glass Studied by Hot Stage Scanning Electron Microscopy and Electron Backscatter Diffraction. *Cryst. Growth Des.* **2013**, *13*, 3794-3800.
18. Hasebe, M.; Musumeci, D.; and Yu, L. Fast Surface Crystallization of Molecular Glasses: Creation of Depletion Zones by Surface Diffusion and Crystallization Flux. *J. Phys. Chem. B* **2015**, *119*, 3304-3311.
19. Wu, T.; Sun, Y.; Li, N.; de Villiers, M.; Yu, L. Inhibiting Surface Crystallization of Amorphous Indomethacin by Nanocoating. *Langmuir* **2007**, *23*, 5148-5153.
20. Zhu, L.; Brian, C.; Swallen, S. F.; Straus, P. T.; Ediger, M. D.; Yu, L. Surface Diffusion of an Organic Glass. *Phys. Rev. Lett.* **2011**, *106*, 256103.
21. Brian, C. B.; Yu, L. Surface Self-Diffusion of Organic Glasses. *J. Phys. Chem. A* **2013**, *117*, 13303-13309.
22. Zhang, W.; Brian, C.; Yu, L. Fast Surface Diffusion of Amorphous *o*-Terphenyl and Its Competition with Viscous Flow in Surface Evolution. *J. Phys. Chem. B* **2015**, *119*, 5071-5078.
23. Powell, C. T.; Xi, H.; Sun, Y.; Gunn, E.; Chen, Y.; Ediger, M. D.; Yu, L. Fast Crystal Growth in *o*-Terphenyl Glasses: A Possible Role for Fracture and Surface Mobility. *J. Phys. Chem. B* **2015**, in review.
24. Nielsen, L.H.; Keller, S.S.; Gordon, K.C.; Boisen, A.; Rades, T.; Mullertz, A. Spatial Confinement can Lead to Increased Stability of Amorphous Indomethacin. *Eur. J. Pharm. Biopharm.* **2012**, *81*, 418-425.
25. Hikima, T.; Adachi, Y.; Hanaya, M.; Oguni, M. Determination of Potentially Homogeneous-Nucleation-Based Crystallization in *o*-Terphenyl and an Interpretation of the Nucleation-Enhancement Mechanism. *Phys. Rev. B* **1995**, *52*, 3900-3908.
26. Xi, H.; Sun, Y.; Yu, L. Diffusion-controlled and Diffusionless Crystal Growth in Liquid *o*-Terphenyl near Its Glass Transition Temperature. *J. Chem. Phys.* **2009**, *130*, 094508.
27. Musumeci, D.; Powell, C. P.; Ediger, M. D.; Yu, L. Termination of Solid-State Crystal Growth in Molecular Glasses by Fluidity. *J. Phys. Chem. Lett.* **2014**, *5*, 1705-1710.
28. Paeng, K.; Powell, C. T.; Yu, L.; Ediger, M. D. Fast Crystal Growth Induces Mobility and Tension in Supercooled *o*-Terphenyl. *J. Phys. Chem. Lett.* **2012**, *3*, 2562-2567.

---

29. Cai, T.; Zhu, L.; Yu, L. Crystallization of Organic Glasses: Effects of Polymer Additives on Bulk and Surface Crystal Growth in Amorphous Nifedipine. *Pharm. Res.* **2011**, *28*, 2458-2466.

## Chapter 5

### Future Work

The work described in this thesis investigates the mechanism of fast surface crystal growth on molecular glasses. Recent literature and subsequent research presented in this thesis have established that fast surface crystallization on molecular glasses is enabled by surface diffusion. These studies have been conducted mainly using indomethacin. Many other systems can be examined for future studies. In this final chapter, I will propose some future studies that would advance our understanding of surface crystallization on molecular glasses, and consequently, contribute towards our understanding of the stabilization of amorphous solids.

#### 5.1 The effect of heating above $T_g$ on the growth of surface crystal

Using optical microscopy, we observed that fast surface crystal growth is active below  $T_g$ , but is terminated by the onset of fluidity above  $T_g$ .<sup>1</sup> However, the effect is not consistent across different crystals. While heating leads to the termination of surface crystal growth in *o*-terphenyl (OTP), nifedipine (NIF) and indomethacin ( $\alpha$  IMC), its effect on  $\gamma$  IMC is comparatively less.

I propose to study the competition between surface diffusion and viscous flow using scanning electron microscopy (SEM) and atomic force microscopy (AFM). With the help of high-resolution microscopy, it should be interesting to observe how the activated liquid interacts with and terminates surface crystal growth. Do surface crystals still grow upward upon heating? Do we observe depletion zones around a growing crystal? Do depletion zones persist upon heating? If not, does the velocity of viscous flow explain the filling of depletion zones? How different is the

interface between  $\alpha$  and  $\gamma$  IMC? In addition to IMC system, it might be interesting to further investigate the effect of heating on surface crystallization in NIF.

In addition to surface grating decay experiments, observations with nanoparticles embedded in both native and doped in an IMC glass will help understand the mechanism of surface transformation. These particles can represent slow-growing crystals. For preliminary experiments, we deposited 500 nm diameter PS spheres on the surface of IMC upon heating. Figure 1a shows a series of AFM images that track the height of PS spheres over time at 327 K. The initial velocity of sinking of PS spheres (the slope of the red line) is plotted in figure 1b along with the characteristic rate of viscous relaxation,  $F = \gamma/2\eta$ , where  $\gamma$  is surface tension, and  $\eta$  is viscosity. A reasonable agreement between  $F$  and the sinking rates of PS particles was observed, suggesting that PS particles sink by viscous relaxation (Figure 1c).

It would be beneficial to measure the velocity of sinking as a function of the size of particles. Systematic studies (at many temperatures) might provide a better estimate of sinking rate and consequently, a better estimate of viscosity. The analysis of sinking rate should be extended to understand whether the exposed particle size affects the sinking velocity.

It would be of additional benefit to study particle deposition on other systems such as NIF. Previous studies demonstrate that NIF shows surface enhanced crystallization<sup>1,2</sup> and diffusion.<sup>3,4</sup> Also, NIF has the same glass transition temperature as IMC ( $T_g = 315$  K). A test of the generality of our findings on systems other than IMC would be helpful to understand the transformation of main mechanism between surface diffusion and viscous flow as a function of temperature.

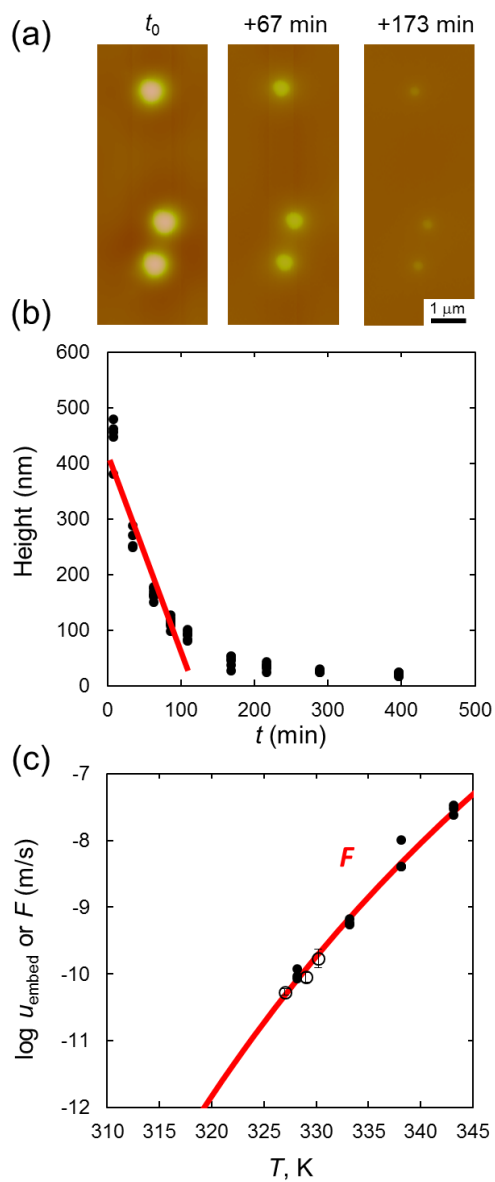


**Figure 1.** Real-time AFM images (a) and height vs. time plot of 500 nm PS spheres embedding into liquid IMC at 327 K (b). (c) The sinking velocities of PS particles (open symbols) overlaid with the values of  $F$  measured from the decay of surface grating (closed symbols). Color scale = 1000nm

## 5.2 Creation of depletion zones

A key feature of surface crystal growth on IMC glasses is the creation of a depletion zone around a growing crystal. In this thesis, we focused our work on IMC. In Chapter 3, we presented a physical model to describe the evolution of surface for two different polymorphs of surface crystals,  $\alpha$  and  $\gamma$  IMC<sup>5</sup>. We concluded that the depletion zones near the crystals of both polymorphs are explained by surface diffusion and crystallization flux.

It would be a better argument to examine if other mechanisms such as viscous flow or bulk diffusion are also responsible for the development of depletion zones. Further studies are warranted to extend Mullin's mathematical model to determine if the surface evolution of depletion zones around a growing crystal can be explained by bulk diffusion or viscous flow.<sup>6</sup>

It will be also useful to examine the evolution of depletion zones in other systems such as NIF glasses. AFM observations of NIF surface crystals indicate the presence of a segregated needle-like surface morphology. As mentioned in Chapter 3, for the slow-growing flanks of needle-like  $\alpha$  IMC crystals, the interface between a crystal and a glass surface is considered to be stationary. On the other hand, the depletion zone has limited time to develop before a fast-advancing growth front for a compact domain of  $\gamma$  IMC. The crystal morphology of NIF is between needles and compact domains, which may necessitate a new physical model for NIF crystals.

Another system to study could be the felodipine system. Kester and Taylor studied the surface and bulk crystal growth of felodipine, a hydrophobic calcium channel blocker.<sup>7</sup> They reported that of the two polymorphs, Form I exhibits faster surface crystal growth rate compared to the bulk crystal growth rate. The other polymorph, Form II, shows only bulk crystal growth. The surface crystal growth rate of Form I below  $T_g$  (316 K) is approximately six times faster than the bulk growth rate. The surface crystal morphology of Form I is spherulitic, with a compact, dense and

smooth interface with the glass. The morphology of Form I might be similar to  $\gamma$  IMC. To date, no experiments have been conducted to characterize the depletion zones around the surface crystals on felodipine glass by high-resolution microscopy. If depletion zones are observed, further characterization would be necessary to see if a physical model used for  $\gamma$  IMC can describe the evolution of surface on felodipine glasses.

Another possible system for these studies is cabamazepine (CBZ), an anticonvulsant drug. Gunn and Yu reported three polymorphs of CBZ that exhibit enhanced surface crystallization.<sup>8</sup> They demonstrated that the crystal morphology of Form I is needle-like, while that of Form IV is spherulitic, as shown in Figure 2. The rate of crystal growth for Form I and IV makes these polymorphs amenable to AFM analysis of their surface morphology at 303K (Form I:  $\log u_s$  (m/s) = -9.35, Form IV:  $\log u_s$  (m/s) = -8.62). Since the crystal morphology of Form I and IV are similar to  $\alpha$  and  $\gamma$  IMC, respectively, these experiments would be valuable to examine the generality of the physical model we used to explain the relationship between surface diffusion and fast surface crystal growth.

The work in this thesis has focused on pure compounds. However, multi component glasses are often used for commercial formulations. Polymer additives are used to stabilize amorphous drugs. Polymer dopants<sup>9,10,7</sup> can inhibit the bulk crystal growth more strongly than they affect the surface crystal growth. The exact mechanisms underlying the effect of polymer additives on surface crystal growth is still unclear. Thus, characterizing the surface evolution with LM (Light microscopy), SEM and AFM may provide better explanation for understanding the interaction between drugs and polymers at the surface.

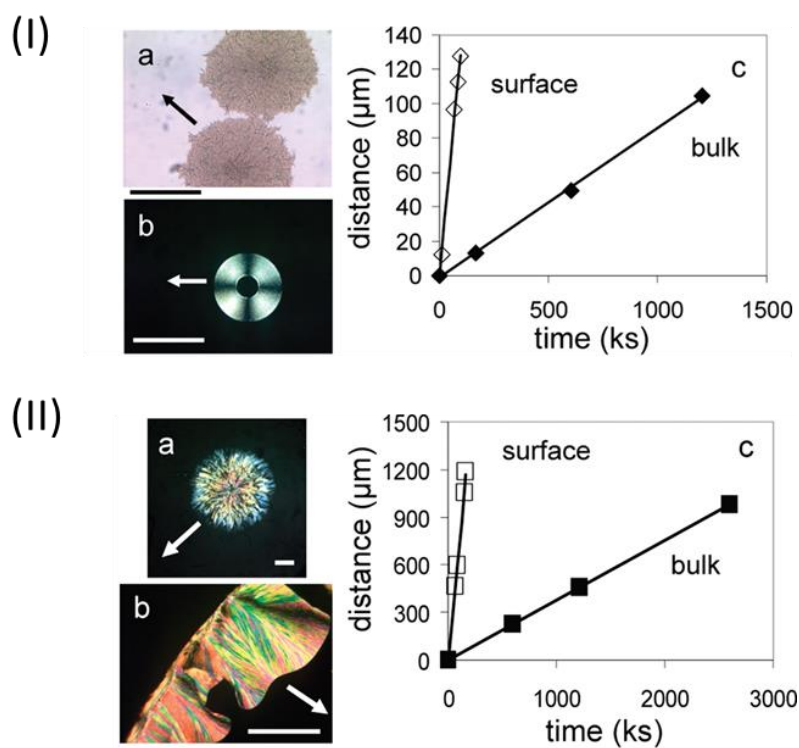


**Figure 2.** (I) Optical images show the crystal growth of Form I at the surface (a) and in the bulk (b). Crystallization kinetics for surface and bulk crystal growth is shown in (c). (II) Optical images show the crystal growth of Form IV at the surface (a) and in the bulk (b). Crystallization kinetics for surface and bulk crystal growth is shown in (c) <sup>8</sup>.

Surface morphology of pure NIF has been examined by AFM.<sup>1,9</sup> For future studies, polyvinylpyrrolidone (PVP) or polystyrene (PS) doped in NIF glass or IMC glass can be tested by real-time AFM observations. In addition, polyethylene oxide (PEO) could be investigated as Powell et al observed the acceleration of surface crystal growth for PEO doped NIF.<sup>10</sup> I am interested in pure compounds. I expect to see the width and depth of depletion zones become larger in multi-component glasses because the crystal growth rate becomes slower for the polymer additives in observing the differences in how the surface evolves in multiple component glasses compared to drugs. If depletion zones are observed, we will test if they are reproduced by an experimental coefficient of surface diffusion. With help of high resolution microscopy, I anticipate that this study could also help explain the mechanism of surface crystal growth for multi-component glasses.

Overall, understanding the properties of depletion zones around a growing surface crystal on a broad range of organic glasses will aid in the development of better models to explain the mechanism of surface crystallization.

### **5.3 Confinement effect on surface crystal growth**

#### **5.3.1 Critical width on inhibition of surface crystallization in molecular glasses**

The spatial confinement effect has been generating great interest in practical applications. Much work has been devoted to study finite size effects on glass transition temperature for polymer molecules.<sup>11,12,13,14,15,16</sup> The study of polymer thin film may have a tremendous impact on the application of electronics, lubrication. For instance, Keddie et al. discussed that glass thickness was a function of  $T_g$ . As the glass thickness decreased,  $T_g$  was slightly increased because of the

interaction with substrate, which resulted in slower mobility for thin films of poly(methyl methacrylate) (PMMA).<sup>11</sup>

Note that the length scale of glass thickness for studying polymer glass is angstrom or nanometer scale, while the dimensions in our case are hundreds of nanometers. Another example of spatial confinement is porous matrices such as controlled pore glass (CPG) to test the spatial confinement effect on stabilizing amorphous solids or selection of polymorphs.<sup>17,18,19,20,21,22</sup>

We show in this thesis that glass width, glass depth and glass thickness alter surface crystallization kinetics. As a test of confinement effect, in addition to the experiments discussed in chapter 4, I propose to grow surface crystal of IMC in a channel. In preliminary work, an IMC glass was prepared by quenching of a melt, and a 10 nm gold was coated through a copper grid sitting on the IMC glass, producing channels 35 microns wide Figure 3(b-d) show SEM images of  $\gamma$  IMC surface crystals growing at 313 K in the channels. The rate of surface crystal measured by optical microscopy agreed reasonably with previous studies ( $\log u_s$  (m/s) = -8.9).<sup>1,23,24</sup> Although this experiment was successful for growing crystals in a channel, the main concern was that the interface between the glass and gold coating was not distinguishable. Knowing the exact length scale of the system is critical for studying the confinement effect.

For future work, we can use microfluidic approaches as an alternative to better understand the confinement effect. Figure 4 shows the proposed microfluidic crystallization channel for organic material system. The width is between 2- 4  $\mu\text{m}$ , and the thickness has to be above 10  $\mu\text{m}$ . As discussed in Chapter 4, the smallest width of “perimeter surface experiments” is approximately 5  $\mu\text{m}$ . Thus, microfluidics technique will be useful to allow precise control over a few microns scale. However, there are two disadvantages of using microfluidics techniques for our systems. The conventional microfluidics channel is usually not surface, but bulk system. Thus, it is necessary

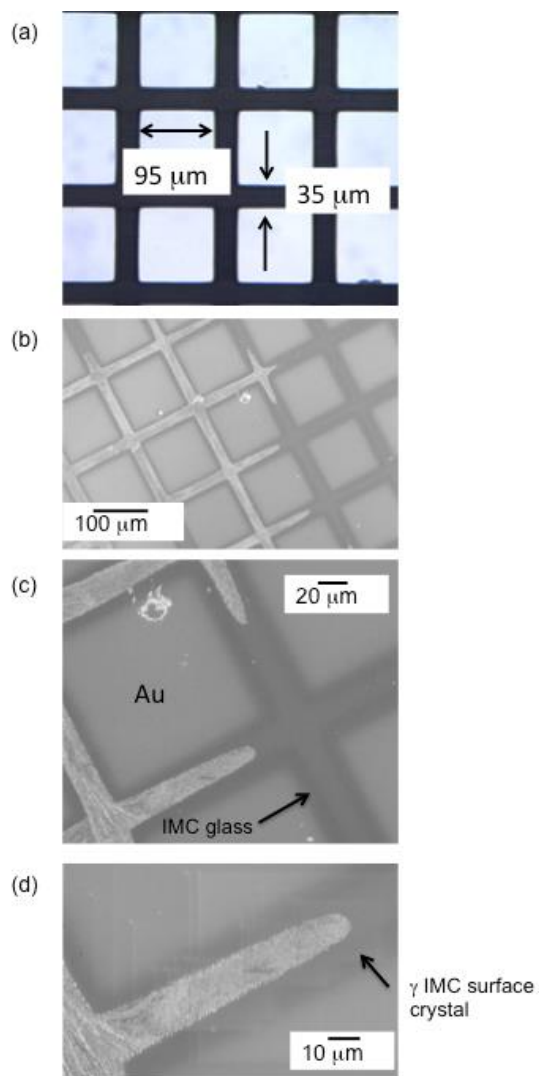


**Figure 3.** The dimensions of a copper grid (a). SEM images of  $\gamma$  IMC surface crystal growing in a glass confined by 10 nm gold coating of a copper grid at 313 K (b-d).

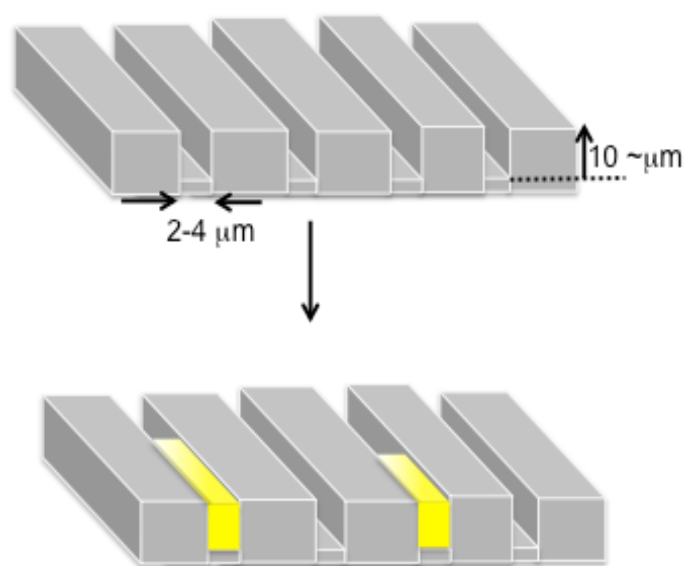


**Figure 4.** Scheme of a microfluidic crystallization channel (top). Yellow color surface crystallization fabricated in a channel below  $T_g$ .

that the top layer of polydimethylsiloxane (PDMS) has to be removed gently without any damage to a sample or mold. Secondly, the microfluidic platform comprises a thin multilayer PDMS cannot endure a high temperature above 353K, which indicates that cooling of a melt method for preparing IMC glass is impossible because the melting point of  $\gamma$  or  $\alpha$  IMC, for example, is respectively 433-438 K<sup>25,26</sup>, 425-427K.<sup>26</sup> In order to grow crystals in a channel prepared by microfluidic technique, solvent has to be used to prepare a glass. It is important to confirm the solvent is completely evaporated before measuring the rate of surface crystal growth. Real time measurement of surface crystal growth rate will be monitored by an optical microscopy plus hot-stage with nitrogen purged to reduce the effect of moisture. Raman microscopy will be used for identification of polymorphism. We will use AFM and SEM to study the surface morphology of crystals growing in the channel.

### **5.3.2 The effect of glass thickness on surface crystal growth**

In Chapter 4, we report that surface crystallization kinetics is affected by glass thickness and material substrate. Surface crystal growth in thinner films supported by silicates has the expected initial velocity. However, the velocity decreases over time, approximately on the timescale of the surface crystal layer grows to the bottom of the substrate.

It would be beneficial to observe, in real-time, the subsurface of both, thin (10  $\mu\text{m}$ ) and thick (more than 100  $\mu\text{m}$ ) glass films of  $\alpha$  and  $\gamma$  IMC glasses. This may allow the observation of voids that are created in the bulk. SEM is a useful technique to study subsurface of glass. However, real time observation of subsurface using SEM is not currently possible because the sputter gold coating that is used to study IMC glasses using SEM inhibits further surface crystal growth.<sup>27</sup> Preparing samples at each day to observe crystal growth rate at the surface and in the bulk can be

a useful experiment. SEM can also help us understand how the interaction between a substrate and a glass can affect crystal growth rate at the surface. We hypothesize that when the bulk crystal growth reaches a substrate, the interaction between them creates tension. Subsurface SEM experiments could be beneficial to test this hypothesis.

Our current analysis investigates surface crystallization kinetics  $\gamma$  IMC at 303 K. In the future, we will examine this phenomenon at different temperatures. For  $\gamma$  IMC, the onset of temperature for terminating GC growth (glass-to-crystal;  $T_t$ ) is 306 K.<sup>28</sup> We anticipate that at temperatures above 306 K, the slowdown of surface crystallization will not occur because GC growth is terminated. Additionally, we will perform similar analysis with the NIF system around 316 K ( $T_t$  for NIF) to gather additional support for this hypothesis.

According to the observation in  $\alpha$  and  $\gamma$  IMC, the bulk crystal growth rate of  $\gamma$  IMC is an order of magnitude faster than that of  $\alpha$  IMC, but surface crystal growth rate of  $\alpha$  and  $\gamma$  IMC are similar.<sup>1,28</sup> We found that the surface crystal growth rate of  $\gamma$  IMC slows over time, while  $\alpha$  IMC does not. As mentioned, the hypothesis is that the time for surface crystal growth to slow down correlates with the time for bulk crystal to grow. In other words, at early stage the surface crystal growth is fast, but surface crystallization kinetics is dependent on how much the crystal grows in the bulk at late stage. We will apply this idea on CBZ. Form III shows surface crystal growth rate is a factor of 3 faster than bulk crystal growth rate. For Form I and IV, surface crystal growth rate is more than ten times faster than bulk crystal growth rate. Thus, we expect that Form III show the stronger effect on the slowdown of crystallization over times, but Form I and IV may show less effect. Testing the crystal growth rate of three polymorphs might help further understanding of correlation between surface and bulk crystal growth rate.

## 5.4 Conclusions

This thesis has demonstrated that fast surface crystal growth on molecular glasses is explained by surface diffusion. This phenomenon is new area of research because all of the studies have been published in the last 10 years. All observations are surprising features to be addressed in order to understand and develop for stabilizing the amorphous solids. This chapter suggests a wide range of experiments that can be conducted to better understand surface crystallization on molecular glasses. This will have many practical application in stabilization of systems used in pharmaceutical, food and electronic industries.

Molecular glasses in confined systems should be explored further because this could be one of useful strategies to stabilize amorphous solids, selecting polymorphism and controlling nucleation. At the current experimental set up, it might be difficult to pursue the confinement effect on surface crystallization because it usually requires studying from micrometer to the nanometer scale. Therefore, multiple additional techniques should be certainly tried to employ studying crystallization process at the nano scale in a confined system in the future.

**References:**

---

1. Hasebe, M.; Musumeci, D.; Powell, C. T.; Cai, T.; Gunn, E.; Zhu, L.; Yu, L. Fast Surface Crystal Growth on Molecular Glasses and Its Termination by the Onset of Fluidity. *J. Phys. Chem. B* **2014**, *118*, 7638-7646.
2. Zhu, L.; Wong, L.; Yu, L. Surface-Enhanced Crystallization of Amorphous Nifedipine. *Mol. Pharm.* **2008**, *5*, 921-926
3. Brian, C. B.; Yu, L. Surface Self-Diffusion of Organic Glasses. *J. Phys. Chem. A* **2013**, *117*, 13303-13309.
4. Zhang, W.; Brian, C.; Yu, L. Fast Surface Diffusion of Amorphous *o*-Terphenyl and Its Competition with Viscous Flow in Surface Evolution. *J. Phys. Chem. B* **2015**, *119*, 5071-5078.
5. Hasebe, M.; Musumeci, D.; Yu, L. Fast Surface Crystallization of Molecular Glasses: Creation of Depletion Zones by Surface Diffusion and Crystallization Flux. *J. Phys. Chem. B* **2015**, *119*, 3304-3311.
6. Mullins, W. Flattening of a Nearly Plane Solid Surface due to Capillarity. *J. App. Phys.* **1959**, *30*, 77-83.
7. Kestur, U.S.; Lee, H.; Santiago, D. Rinaldi, C.; Won, Y-Y.; Taylor, L.S. Effects of the Molecular Weight and Concentration of Polymer Additives, and Temperature on the Melt Crystallization Kinetics of a Small Drug Molecule. *Cryst Growth Des.* **2010**, *10*, 3585-3595.
8. Gunn, E.; Guzei, I. A.; Yu, L. Does Crystal Density Control Fast Surface Crystal Growth in Glasses? A Study with Polymorphs. *Cryst. Growth Des.* **2011**, *11*, 3979-3984.
9. Cai, T.; Zhu, L.; Yu, L. Crystallization of Organic Glasses: Effects of Polymer Additives on Bulk and Surface Crystal Growth in Amorphous Nifedipine. *Pharm. Res.* **2011**, *28*, 2458-2466.
10. Powell, C. T.; Cai, T.; Hasebe, M.; Gunn, E. M.; Gao, P.; Zhang, G.; Gong, Y.; Yu, L. Low-Concentration Polymers Inhibit and Accelerate Crystal Growth in Organic Glasses in Correlation with Segmental Mobility. *J. Phys. Chem. B* **2013**, *117*, 10334-10341.
11. Keddie, J. L.; Jones, R. A. L.; Cory, R.A. Interface and Surface Effects on the Glass Transition Temperature in Thin Polymer Films. *Faraday Discuss.* **1994**, *98*, 219-230.
12. Keddie, J. L.; Jones, R. A. L.; Cory, R. A. Size-Dependent Depression of the Glass Transition Temperature in Polymer Films. *Europhys. Lett.* **1994**, *27*, 59-64.
13. Forrest, J. A.; Dalnoki-Veress, K.; Stevens, J. R.; Dutcher, J. R. Effect of Free Surfaces on the Glass Transition Temperature of Thin Polymer Films. *Phys. Rev. Lett.* **1996**, *77*, 2002-2005.

- 
14. Forrest, J. A.; Dalnoki-Veress, K.; Dutcher, J. R. Interface and Chain Confinement Effects on the Glass Transition Temperature of Thin Polymer Films. *Phys. Rev.E* **1997**, *56*, 5705-5716.
15. Dalnoki-Veress, K.; Forrest, J. A.; Murray, C.; Gigault, C.; Dutcher, J. R. Molecular Weight Dependence of Reductions in the Glass Transition Temperature of Thin Freely Standing Polymer Films. *Phys. Rev.E* **2001**, *63*, 031801.
16. Varnik, F.; Baschnagel, J.; Binder, K. Reduction of the Glass Transition Temperature in Polymer Films: a Molecular-Dynamics Study *Phys. Rev. E* **2002**, *65*, 021507.
17. Beiner, M.; Rengarajan, G.T.; Pankaj, S.; Enke, D.; Steinhart, M. Manipulating the Crystalline State of Pharmaceuticals by Nanococonfinement. *Nano Lett*, **2007**, *7*, 1381-1385.
18. Rengarajan, G. T.; Enke, D.; Steinhart, M.; Beiner, M. Stabilization of the Amorphous State of Pharmaceuticals in Nanopores. *J. Mater. Chem.* **2008**, *18*, 2537-2539.
19. Ha, J. M.; Wolf, J. H.; Hillmyer, M. A.; Ward, M. D. Polymorph Selectivity under Nanoscopic Confinement. *J. Am. Chem. Soc.* **2004**, *126*, 3382-3383.
20. Rengarajan, G. T.; Enke, D.; Beiner, M. Crystallization Behavior of Acetaminophen in Nanopores. *Open Phys. Chem. J.* **2007**, *1*, 18-24.
21. Hamilton, B. D.; Hillmyer, M. A.; Ward, M. D. Glycine Polymorphism in Nanoscale Crystallization Chambers. *Cryst. Growth Des.* **2008**, *8*, 3368-3375.
22. Hamilton, B.D.; Ha, J.M.; Hillmyer, M.A.; Ward, M.D. Manipulating Crystal Growth and Polymorphism by Confinement in Nanoscale Crystallization Chambers. *Acc.Chem.Res.* **2012**, *45*, 414-423.
23. Sun, Y.; Zhu, L.; Kearns, K.L.; Ediger, M. D.; Yu, L. Glasses Crystallize Rapidly at Free Surfaces by Growing Crystals Upward. *Proc. Natl. Acad. Sci U.S. A.* **2011**, *108*, 5990-5995.
24. Wu, T.; Yu, L. Surface Crystallization of Indomethacin below  $T_g$ . *Pharm Res.* **2006**, *23*, 2350-2355.
25. Hancock, B. C.; Shamblin, S. L.; Zografi, G. Molecular Mobility of Amorphous Pharmaceutical Solids below Their Glass Transition Temperatures. *Pharm. Res.* **1995**, *12*, 799-806.
26. Hancock, B.C.; Zografi, G. Characteristics and Significance of the Amorphous State in Pharmaceutical Systems *J. Pharm. Sci.* **1997**, *86*, 1-12.
27. Wu, T.; Sun, Y.; Li, N.; de Villiers, M.; Yu, L. Inhibiting Surface Crystallization of Amorphous Indomethacin by Nanocoating. *Langmuir* **2007**, *23*, 5148-5153.

---

28. Musumeci, D.; Powell, C. P.; Ediger, M. D.; Yu, L. Termination of Solid-State Crystal Growth in Molecular Glasses by Fluidity. *J. Phys. Chem. Lett.* **2014**, *5*, 1705-1710.